DOI: 10.1002/((please add manuscript number))
Article type: Review

Cyber-Physiochemical Interfaces

Ting Wang, Ming Wang, Le Yang, Zhuyun Li, Xian Jun Loh, and Xiaodong Chen**

Dr. T. Wang, Dr. M. Wang, Dr. Z. Li, Prof. X. Chen
Innovative Center for Flexible Devices (iFLEX), Max Planck – NTU Joint Lab for Artificial Senses, School of Materials Science and Engineering, Nanyang Technological University, 50 Nanyang Avenue, 639798, Singapore
E-mail: chenxd@ntu.edu.sg

Dr. L. Yang, Prof. X. J. Loh
Institute of Materials Research and Engineering, Agency for Science Technology and Research (A*STAR), 2 Fusionopolis Way, 138634, Singapore
E-mail: lohxj@imre.a-star.edu.sg

Keywords: Physiochemical interfaces, cyber information, stretchable sensors, healthcare, artificial intelligence

Abstract:

Living things rely on various physical, chemical, and biological interfaces which constitute somatosensation, olfactory / gustatory perception, and nervous system etc. They help the organisms to perceive the world, adapt to surroundings, and maintain internal and external balance. Interfacial information exchanges are complicated but efficient, delicate but precise, multimodal but unisonous, which have driven researchers to clarify the interfacial scientific issues and develop techniques with potential application in health monitoring, smart robotics, increasingly complex future wearable devices, and cyber physical/human system. To elucidate these interfacial issues, we propose the concept of cyber-physiolochemical interface (CPI) that is

capable of extracting biophysical and biochemical signals, and closely relating them to electronic, communication, and computing technology, to provide the core for aforementioned applications. This review summarizes the scientific and technical progress in CPI, and highlights the challenges and strategies in building stable interfaces, including material basis, sensor development, system integration, data processing techniques. We hope to put forward an unprecedented multi-disciplinary network of scientific collaboration in CPI to explore much uncharted territory for progress, providing technical inspiration - to the development of the next-generation personal healthcare technology, adaptive prosthetics and augmentation of human capability, smart sports-technology, health and dietary care, etc.

1. Introduction

Living things of any scale, from cells and microorganisms, to plants and animals, rely on the continuous internal and external information exchange, such as trans-membrane ion transport, viral infection, photosynthesis, and respiration.[1-3] The mammalian skin is a typical example of a multifunctional interface to illustrate signal exchange, including temperature, humidity and various mechanical signals.[4-5] To enable such information exchange interfaces, many elements interact in tandem, including stimuli-receptor cells as sensing units, neuron cells as signal processing units, and muscle cells as feedback units, which contribute to build up a system with adaptation, precise regulation, and durability.[6] The significances of these interfaces

drive researchers to clarify the interfacial scientific issues for potential applications in healthcare, rehabilitation, prosthetics, and human-machine interactions. Sensing technology and computing technology, two research branches closely related to signal transduction and processing, thrives in recent decades. Their fusion brought great convenience to our lives and even revolutionized human lifestyles.

Sensing technology transfers the target information to readable output providing technical inspiration for signal monitoring. The earliest sensor dated back to 1880s, a thermostat based on structural change principles (**Figure** 1).[7] To meet a broad range of sensing targets, various sensors emerged, such as the strain gauge based on Wheatstone bridge design, silicon pressure sensors based on the piezoelectric principle, and glucose meter based on enzyme-catalyzed electrochemical reactions. The rapid development of microfabrication technology further impels the emergence of microelectromechanical systems (MEMS) with merits of facile integration, miniaturization, and multifunction, which is a promising candidate for portable biomarker detection.[8-9] These devices depend on blood-sampling, a painful and impractical process for continuous testing to capture the dynamic variations of health indicators. Herein, minimally / non-invasive and real-time sensing methods have garnered increasing attention.

In 2000s, epidermal sensors appeared, as the epidermis contains huge volumes of health-related information to be detected with minimal or no invasivity. Typical demonstration was the skin-like pressure sensors based on pyramidal structures,[10] the sensing principle of which is similar to pulse diagnosis in traditional Chinese

medicine. To further fully utilize all the information for health indicators, various epidermal electrophysiological and biochemical sensors have appeared, such as electrocardiogram (ECG), electromyography (EMG), and glucose, lactate, and ionic biosensors.[11-13] Therefore, epidermal biosensor opens a chemosensory window to monitor human internal status. And interfacial matching issues between soft tissues and sensors attracted increasing attention considering data fidelity, signal reliability, system compatibility, user experience, etc.

In parallel with sensing technology, information technology (Although this terminology is first appeared in 1958, but device-assistant computation has been used to analyze sensory data for thousands of years) can be traced back to the first invention of mechanical computer based on punch-card machines in 1800s (Figure 1). In 1945, Z4 appears as the world's first electromechanical programmable-based commercial digital computer, designed by Konrad Zuse.[14] With the advent of electronic vacuum tube, Electronic Numerical Integrator and Computer (ENIAC) was developed which is the first purely electronic programmable, general-purpose digital computer, weighing 30 tons partly due to its more than 17,000 vacuum tubes.[15] Thereafter, the wide application of transistors have been completely revolutionized computer to more compact machines, which became a commercial success as seen in IBM.[16] It eventually led to an era of integrated circuits, with a surge in high performance computers and functional electronics.

Wearable electronics started with electronic accessories in fashion technology such as watch. The high performance electronics repel the rapid development of

wearable activity tracker. The wearable production chains bring about challenges to conventional silicon-based electronics which appeared to be increasingly mechanically incompatible with humans.[17-18] Considering the specific applications on soft creatures, mechanical properties such as flexibility, stretchability, and Young's modulus propelled the emergence of soft electronics.[19-23] To overcome the mechanical mismatch of rigid silicon-based electronics, researchers have turned to bottom-up strategies in molecular and geometry design, and hybrid systems to fabricate flexible, stretchable, and biocompatible electronic systems.[24-27]

To manage sensory data acquisition and analysis efficiently and smartly, sensors and computers converge which gave rise to the concept of cyber physical systems (CPS).[28-29] Cyber is derived from "cybernetic", which originated from the Greek word "κυβερνητικός" meaning "skilled in steering or governing". In CPS, multiple and distinct information is monitored in real time by physical sensors and synchronously analyzed through cyber computational sources, where the physical world and cyber space (computational and communication resources)[30] are highly connected and deeply intertwined.[29, 31-32] CPS involves interdisciplinary research fields, including control, mechatronics, sensing, communication, and computation science.[33] Humans have been playing a more prominent and decisive role in CPS, gearing towards a user-centric system which is named as cyber human system (CHS).

In the human-centric CHS, there are many complicated and dynamic signal transduction, exchanging and computing procedures among the human, physical sensors and cyber space, which causes a mass of interfacial issues, especially

involving soft tissues. Moreover, these biosignals from human are usually irregular, sophisticated, multimodal and constantly changing, which is difficult to collection *in-situ* and understand. To clarify these challenges, we herein propose cyber physiochemical interfaces (CPI) that focuses on the device-tissue interfacial issues from the sensing to computing of physiochemical signals (Figure 1). Cyber in CPI has similar meaning with that in CPS which comprises processing, communication, and active feedback with aims of understanding or even governing of biosignals.

1.1 Cyber Human System

As a human-centric smart system, CHS focuses on studying the increasingly coupled relationship between humans and computing to enhance the human capabilities.[34-35] It is important to accurately acquire the reliable data from humans and their surroundings, and further analyze them by advanced computing to deeply understand the role of human in dynamic scenarios, which are relevant to the interface between humans and information technology.

CHS comprises five invisible levels, I) smart connection, II) data-to-information conversion, III) cyber, IV) cognition, and V) configuration.[34] Level I establishes methods for acquiring accurate and reliable data from humans and their surroundings, forming the basis and initial input for other levels. Level II focuses on preprocessing human-generated data including amplifying, filtering, averaging, and eventually transferring the raw data to useful digital signals or relevant features to be used as input for computation. Levels III to V characterize the process from data

aggregation from individual human information streams, do data analysis based on higher-level understanding of the system, and generate feedback at each level under supervisory control to eventually ensure adaptive implementation of decisions. These five parts are interconnected and indispensable. The invisible signal exchanges or communication between biosystems and cyber space constitute the basis of CHS and play a decisive role in constructing a reliable CHS hierarchy. All this process is really complicated by the subtle structure and complexity of biosystems. Therefore, reliable interfaces are highly desired to adapt to such complex circumstances for promoting CHS to work efficiently and effectively.

1.2 Cyber-Physiochemical Interfaces

There are micro/nano biomechanical signals from cell mechanisms, weak electrophysiological signals from (de)polarization of membrane potential, and biochemical signals produced during complex metabolism. Recent years have witnessed the rapid development in wearable technologies and bioanalysis such as body wireless sensor networks, which attempt to extract real-time physiochemical information of context-dependent human signals via a minimally/non-invasive way.[36] However, the specific on-skin application poses many challenges, such as significant inferences, specific designed soft and flexible materials, and dynamic uncertainty. In addition, computing interface to extract meaningful information from biosignals is also challenging due to the inherent complexity of sensor data, as well as current computing capabilities and infrastructures. Such interfacial issues are significant as

the result fidelity and accuracy are highly dependent on the signal exchange, processing and computing at the interface between device and human body (details given in section 1.3). To address these physiochemical interface problems, we propose the concept of CPI that is capable of reliably acquiring and analyzing these biophysical/biochemical signals for constructing CHS.

CPI accounts for this signal exchange process which includes (1) converting biophysical/chemical clues (electrophysiological, (e.g. electroencephalogram (EEG), electrooculography (EOG), EMG and ECG) and biochemical signals (e.g. metabolites, ions, proteins, and nucleotide)) to quantifiable (electrical or colorimetric) signals, and (2) transforming these quantifiable signals to digital output for computing and further providing active response. To realize this goal, CPI comprises a pyramidal hierarchy structure: (1) biochemical/biophysical sensing interface, (2) signal processing and transmission interface, and (3) intelligent computing interface. To make sure the interfaces function well, sensors and systems can be exquisite designed via materials and geometrical design to endow the interfaces with stretchable, conformable and adhesive, biorecognitive, and stable features in both device and system levels. Furthermore, advanced computing and communication technologies/architectures, e.g. machine learning, edge computing and low power data transmission, will also benefit the construction of CPI platform.

Taking the epidermal CPI as an example, to achieve aforementioned signal extraction, CPI generally comprises four basic layers: a buffer layer, a biorecognition or transduction layer, a signal processing and transmission layer and a computing

layer (**Figure 2**). For the buffer layer, it can act as the adhesive, insulation, and/or anti-inference layer depending on the application. For the biorecognition or transduction layer, biosignals such as blood pressure, heart pulse, ECG, EMG, or metabolite concentrations will be transformed to quantifiable electrical, colorimetric, or other identifiable signals. The detection of biochemical signals relies on the specific biorecognition function of biomolecules such as ion-specific ligands and metabolite-specific proteins. The detection of biophysical signals relies on microstructured or patterned electrodes that can identify the biomechanical or electrophysiological signals, for instance electrode with optimal size for monitoring of local muscle activity. For the signal processing layer, it then transfers these electrical, colorimetric, or other identifiable signals to digital signals, through peripheral circuits designed with functions of amplifying, filtering, compensation, and then eventually converting the raw data to recognizable digital output. Finally, all these signals will be transmitted to the computing layer which conducts intelligent data analysis and provides active feedback to users.

In brief, CPI should possess three identifiable features: (1) matched mechanical properties to tissues; (2) reliable biophysical and biochemical signal extraction ability; and (3) active feedback via electronic and computing technology (cyber). Based on these features, CPI enables the simultaneously monitor the multiple biophysical/biochemical markers and merges these biosignals together for thoroughly interpreting their correlation and dynamics, which will benefit the comprehensive description of human activity for smart CHS construction.

1.3 Interfacial mismatch and incompatibility

Extracting biosignals from human bodies relies on the information flow from human body to devices which involves signal multiple exchanges at different interfaces, e.g. between the epidermis and functional layers, and between different functional layers. These interfaces play a vital role in acquiring reliable data, realizing real-time monitoring and decreasing signal attenuation.

The skin can be approximately regarded as a bilayer, namely, the epidermis and the dermis (former with modulus of 140-600 kPa; thickness of 0.05-1.5 mm and later with modulus of 2-80 kPa; thickness of 0.3-3 mm).[37-38] The skin surface shows lots of wrinkles, creases, and pits with feature sizes of 40 to 1000 μm and feature height of 15 to 100 μm.[37] As the skin interacts with physical devices at macro (bulky tissues) and micro levels (cells),[39] there are macro/micro-mismatch issues in terms of mechanical, electrical, optical, magnetic, biocompatible properties, and data modality. They have a large impact on the aforementioned processes by affecting the signal transmission pathway, behavior of interfacial cells, and signal transduction efficiency.[29, 40-42] And the mismatching issue eventual leads to sensing inaccuracy, instability, and even device breakdown manifesting itself in strain-induced cracks, interfacial gap, and peeling off of devices from tissues (**Figure 3**a).[43]

Mechanical mismatching issue is most pronounced, as the majority of well-developed sensing and data processing components are based on silicon-technologies, which are stable but rigid (several GPa and stretchability less

than 5%). Human tissues show Young's modulus from tens of KPa to several MPa and stretchability from 10% to 100%, for example 0.1-2 MPa and 30-70% strain for the epidermis, 0.5-2.5 KPa and 10% strain for the brain, and tens of KPa and 20–35% strain for the heart.[44-46] For on-skin applications, these rigid sensing units failed to realize conformable contacts to the arbitrarily shaped skin with dynamic deformations.[47] The strains exposed to the device can cause user discomfort and device breakdown or peel-off to release the strain, inevitably inducing instability in sensing performance.[48] Moreover, for implant applications, they require devices to be conformal and non-invasive contact with tissues to avoid secondary tissue damage and inner inflammation, and decrease external repulsion reactions. Hence, it is highly desirable to develop materials with inherent mechanical properties resembling human tissues or devices with adaptive structure to endure mechanical deformations.

The second issue is interfacial adhesion which affects the sensing stability and results fidelity. Current solutions include fixing electrodes onto the skin via mechanical clamps, adhesive tapes, or conductive gels. And their terminal is connected to boxes that include rigid circuit boards, power sources and communication modules. These methods allow the passive attachment of devices onto tissues, but neglect the interfacial interactions (e.g. hydrophobic–hydrophilic phenomenon and cellular repulsion/attraction), which has significantly effect on signal transduction efficiency.[41] Besides the epidermis/device adhesion issue, adhesion between the conductive layers (mostly based on rigid metal electrodes) and stretchable elastomer also greatly affects the sensing reliability. When devices are

exposed to strain, conductive or sensing layer is readily separated from the elastomer due to weak adhesion, which causes noise augmentation and sensing instability problems.

The third issue relates to incompatibility in performance. Epidermal signals are generally weaker than that in human bodies (signal source) due to signal attenuation (biomechanical and electrophysiological signals) and complicated metabolites processes. Surface electrophysiological signals generally show a potential of mV or μV level and these signals are rather complicated by neighbouring active cells. For example, surface EMG (sEMG) is influenced by adipose tissue and limited by muscle cross talk issues, which has difficulty in detecting deep muscles activities, calling for high sensitivity and fidelity sEMG sensors.[49] As for biochemical signals, the concentration of biomarkers in perspiration or saliva is generally one order of magnitude lower than that in blood, e.g. glucose is found at 0.06–0.11 mM in sweat, 0.23–0.38 mM in saliva, 2.78–5.55 mM in urine, 3.9–6.6 mM in interstitial fluid and 4.9–6.9 mM in blood.[50] This poses a great challenge for biosensing techniques without using lab-confined sensing techniques. Apart from sensing performance, issues on the signal processing, transmission, system integration, and data analysis also require further efforts.

CPI refers to a platform that integrates interfaces at different functional levels with properties compatible to tissues, including the biochemical or biophysical sensing layer, signal transmission layer, and computing layer. With carefully controlled interfaces between different components, novel physical phenomena and

functionalities can be exhibited which cannot realized by either of the constituent component alone such as high efficiency and fidelity in data transmission. In this review, efforts and strategies on biophysical/biochemical signal acquisition and processing for CPI are summarized, including approaches to achieve high stretchability, adhesion, biorecognition, and durability via utilizing bottom-up molecular, geometry design, system integration and optimization, and data computing. Based on signals modality and detection methods, we first discuss materials development strategies, then the stretchable and conformal sensors for cyber biophysical interfaces as well as flexible and patchable biosensors for cyber biochemical interfaces, followed by system-level integration and data computing for CPI. With the vital role of CPI in CHS in mind, we intend to draw more attention to the physiochemical interfaces for utilizing and understanding these significant biosignals via a real-time, non-invasive, reliable, durable, and intelligent way.

2. Materials development for CPI

Materials are the basis for constructing CPI system with multilayer stretchable functional units.[51-52] Researchers have turned to designing materials with compatible mechanical properties via various approaches such as molecular and geometry design, nanomaterial network manipulation, and hydrogel based electrodes.[53-55] Molecular design is a bottom-up approach, where both elastic and rigid units are rationally designed to dynamically tune the mechanical properties (Figure 3b).[56-61] When exposed to strains, the non-covalent 2,6-pyridine

dicarboxamide (PDCA) moieties with hydrogen bonding dissipate energy via bond breakage and the conjugated backbones in the polymer maintain the high charge transport abilities. Supramolecular provides even more rich molecular combination choices.[61] One typical example is combining soft polytetramethylene glycol and tetraethylene glycol chains, as well as strong reversible quadruple hydrogen-bonding cross-linkers with molar ratio from 0 to 30%.[62] The polymer could withstand a strain of up to 17 000% and show fracture energy of ~30 000 J/m^2, which acts as a satisfactory stretchable substrate with high interfacial adhesion for gold electrodes. Molecular design provides self-programmable stretchability but is generally applicable to polymeric materials and highly dependent on careful molecular design and extensive synthesis experience.

Liquid metals such as Gallium and its alloys exhibit intrinsic flexible, soft, stretchable, and reconfigurable features which allow them as good candidates for stretchable wires and interconnects, conformal electrodes, soft sensors, shape-reconfigurable antennas, and self-healing circuits.[63-65] Despite being a liquid, a surface oxide outer layer with several nm scale is very helpful for facile pattern processes including non-spherical shapes by using fluidic injection or 3D printing techniques.[66] Due to the fluidity and electrochemical activity, encapsulation is necessary and also not applicable for extracting electrophysiological or biochemical signals which requires direct a conductive path with electrodes.

Besides design strategies on the molecular level, nano or micro-materials, including particles,[67] nanowires,[68-70] two-dimensional materials[71-72] and their

composites,[73-74] are able to dynamically tune the strain distribution via conductive nano/micro networks. For example, based on silver nanoparticles (Ag NPs), a printable elastic conductor was reported to exhibit conductivity higher than 4000 S cm^{-1} at 0% strain and 935 S cm^{-1} when exposed to 400% strain (Figure 3c). The decent conductivity upon stretching is attributed to uniformly dispersed Ag NPs which improve the electrically connection between micrometer-sized Ag flakes and suppress crack propagation from the reinforcement effect of Ag NPs.[75] Nanowire (NW) conductive materials e.g. carbon nanotubes (CNTs),[76] Ag and Cu NWs,[68, 77-79] and conductive polymers[80] are also promising candidates for stretchable and foldable electronics by sliding and/or changing the network shapes. Despite the achievements in conductivity and stretchability, there is still much room for improvement for stability due to potential delamination and inherent instability of these materials.

Geometric design for fabricating stretchable electronics has been proven successful as it is a general way to transfer traditional rigid materials (Silicon, metals) to stretchable devices. This strategy is based on mechanical stretchability, where the strains are dispersed by the pre-designed shapes, such as the “island–bridge” structure with serpentine geometry, origami and kirigami, and spontaneously formed mesh networks, waves, wrinkles and cracks (Figure 3d).[81-87] The “island–bridge” structure can achieve high stretchability by providing mechanical isolation on the islands which protects the functional components. This strategy is widely used for system level integration which will be discussed in Section 5.[88-89] Precisely

engineered buckling geometry can produce various self-programmable semiconductor nanoribbons without being limited by the intrinsic rigidity of materials. Typically, the preparation of nanoribbons of GaAs and Si uses lithography and surface chemistry to control the adhesion sites on elastic supporting substrate. When the elastomer deforms, these adhesion sites enable the local displacement of nanoribbons with controlled geometry.[89] Modification or evaporation of conductive layer on prestretched elastic substrates randomly produces wrinkles which also contribute to stretchability.[90] Using this prestretching method, stretchable polymeric microelectrodes such as the polypyrrole (PPy) electrode was produced with high stretchability (≈100%).[45] Similar to ancient paper folding art, the origami and kirigami approach was proposed for stretchable electronics with advantages such as high throughput, large deformability, and comparable performance to rigid electronic.[91] Unlike the island–bridge design, the origami and kirigami approach does not use elastomers and is compatible with well-established manufacturing processes.

Cracks generally refer to material defects which lead to decreased homogeneity, increased resistance, performance decay or even device failure. However, regarding stretchable electronics, cracks are a powerful strategy for forming stretchable conductive network.[92] The randomly formed cracks distribute the strains, which benefits the formation of continuous conductive paths of Au films.[93] Similarly, nanomesh is also a conductive network that is resistant to mechanical deformation. For instance, based on grain boundary lithography technologies, Au nanomesh

electrodes exhibits highly stretchbility with sheet resistance in the range from ~21 Ω per square to ~67 Ω per square upon 160% of strain.[94] Besides, nanomesh can also allow gas-permeable, ultrathin, lightweight properties which could be laminated onto skin for long term monitoring applications (Figure 3d).[95]

Compared with electronic conduction widely used in current electronics, ionic conduction is a prevailing mechanism in nature. It is advantageous in terms of its inherent stretchability, biocompatibility, and conformability at macro- (tissues), micro- (cells), and molecular scale.[38, 96] By combining ionically and covalently cross-linked networks, supramolecular polymeric hydrogel exhibits stretchability up to tensile strain ~2000% and fracture energy of ~9000 J/m^2.[97] Besides, the ionic conductors are fully transparent, and capable of operation at high frequency (>10 kHz) and high voltage (10 kV) (Figure 3e).[96] One shortcoming is dehydration in hydrogels, inevitably altering the hydrogen bonds and ion transmission that lead to adverse changes in stretchability, adhesion and conductivity.

3. Stretchable and conformal sensors for cyber biophysical interface

Based on aforementioned stretchable strategies, various functional physiochemical interfaces are constructed for monitoring biophysical signals. Biophysical signals can be classified into biomechanical and electrophysioloical ones. The former includes body movement such as acceleration, angular rate of rotation, blood pressure, heart rate, and body temperature, while the latter includes ballistocardiography, electroencephalography (EEG), electrocardiography (ECG), and

electromyography (EMG). Based on the difference in sensing principle, strategies for biomechanical and electrophysioloical sensors construction are discussed separately.

3.1 Biomechanical signals sensing interface

The monitoring of biomechanical signals generally relies on sensing the epidermal mechanical deformations.[98] There are two challenges: 1) achieving high sensitivity and accuracy upon receiving subtle or weak signals from human bodies, and 2) enhancing interfacial adhesion for high stability during continuous dynamic testing (**Figure 4**).

3.1.1 Deformation regulation for high sensitivity

Deformation regulation is a main strategy for enhancing device sensitivity (Figure 4a-d). The human finger has numerous grooves and furrows contributing to our sensitive tactile perception. Inspired by these microstructures, microstructured pressure sensor was proposed. Elastomers with pyramidal structures were exploited as the functional layer for flexible, capacitive/piezoresistive pressure sensors which exhibit high sensitivity (several Pa) and response times at millisecond range.[10, 99] The high sensitivity toward very low pressures was explained by the finite element analysis showing von Mises stress distribution, indicating rapidly changing shapes when exposed to a relatively small pressure.[100] Their pressure sensitivity is tunable by changing the sidewall angle and the separation of pyramidal microstructures which far surpassed that of unstructured elastomeric films with similar thickness (Figure 4a).[101] The flexible and sensitive sensors capable of perceiving interfacial pressure

signals are widely applied in pulse monitoring, blood pressure testing and human-machine interface.[102-103]

Tuning strain distribution via deformation regulation is also proven to be a powerful strategy to obtain high sensitive strain sensors.[104-106] For example, in terms of fiber-shaped strain sensors, a surface strain redistribution strategy based on microbeads on fibers is proposed for increasing sensitivity (Figure 4b).[107] Microbeads rearrange the strain along the fibers leading to the strain concentrated at the end of beads. The local strain results in longer microcracks formation in conductive films. In this way, the sensitivity is significantly enhanced by microbeads compared to fibers without microbeads.

Besides the one-dimensional strain distribution, there are also methods aimed to two-dimensional film, such as auxetic mechanical metamaterials. For tradition elastic film, it expands longitudinally but compresses in the transverse direction. Expansion separates the conductive materials while Poisson compression squeezes the conductive materials.[108] Hence, the former contributes to sensitivity but the latter intrinsically limits the sensitivity. The interesting feature of auxetic mechanical metamaterials is their two-dimensional expansion due to their negative structural Poisson's ratio. Their bidirectional expansion promotes the separation of conductive materials and enhances the sensitivity of strain sensors by 24-fold (Figure 4c).[108] These stretchable strain sensors can be attached on neck muscles (Figure 4d), which is useful for the diagnosis of damaged vocal cords, respiratory disorders, and throat cancers. These sensors laminated on wrists can assist in diagnosis of Parkinson's

disease, hyperactivity, and tremor in epilepsy.[109-110]

3.1.2 Enhancing interfacial adhesion for high stability

Besides matching sensor sensitivity to human biomechanical signals, enhancing interfacial adhesion also greatly benefits the sensing of biomechanical signals, especially in terms of transmission stability and data fidelity. Due to the existence of nonflat surfaces and fine topology on tissues, non-conformal contact between devices and tissues commonly exist. Air gaps at the device-object interface would reduce the contact area which potentially induce noise and artifacts, thus compromising signal fidelity.[88] Furthermore, due to low interfacial adhesion, strain-induced peeling off of sensing film from skin can even lead to device breakdown. Hence, enhancing interfacial adhesion is necessary for ensuring biomechanical signals are transmitted to the device with high stability and fidelity.

Geckos show extraordinary adhesive capabilities based on millions of adhesive setae on their toes, each made up of hundreds of 200 nm spatular tips to enable the intimate contact with both rough and smooth surfaces. Inspired by these, adhesive microstructures were introduced for enhancing the interfacial skin-adhesion. Microhair sensors display signal-to-noise ratio (SNR) enhancement of 12 folds by maximizing interfacial contact of sensors to the irregular epidermal surface (Figure 4e).[111] Apart from microstructure design, surface modification is also a powerful strategy to increase interfacial adhesion. For example, the mushroom-shaped vinylsiloxane tips on microfibers further improves skin adhesion (adhesion strength of 18 kPa) at cellular lever, which further enhances the SNR to 59.7 (Figure 4f).[112] It

is noted that introducing a transient layer helps to increase data fidelity by enhancing adhesion, but may slightly impair sensing sensitivity due to the buffer effect of transient elastic microstructured layer towards mechanical deformation.

Meanwhile, the interfacial adhesion between conductive materials (e.g., metals and CNTs) and elastomer (e.g., polydimethylsiloxane (PDMS) and styrene ethylene butylene styrene (SEBS)) inside the device also matters, especially for thin metal film electrodes on elastomer.[113] Their huge difference in physical and chemical properties influences the inherent device stability (e.g. Young's modulus of tens of GPa for gold while several MPa for PDMS). To solve this electrode and elastomer interfacial adhesion problem, a nanopile interlocking strategy by biomimetic roots was developed, which contributes to the high interfacial adhesion.[114] In the meantime, the roots embedded in the elastomer alleviate strain concentration in the conductive film, restraining the cracks formation, which contributes to high stretchability (Figure 4g).[114] Enhancing interfacial adhesion eventually contributes to the stable collection of weak epidermal biomechanical signals. Applying conformability to an ultrasonic device allows the capture of blood pressure waveforms with long-term stability at embedded arterial and venous sites with depth of ~4 cm.[115] These signals contain important diagnostic information such as deep-lying internal jugular venous pulses which are helpful for real-time monitoring of the user's state of health (Figure 4h).[111]

3.2 Electrophysiological signals sensing interface

Electrophysiological signals refer to the electrical fluctuations of human body that

originate from the ions movement. The electrical fluctuations occur across many different scales, including single ion channel proteins, neurons, and whole organs such as heart. Based on testing electrophysiological signals, techniques such as electroencephalography (EEG), ECG, EOG, and EMG are proven as effective methods for monitoring neurological disorders, cardiovascular diseases, cancers and stroke.[116-117] Typically, EEG signals show signal frequency bandwidth between 1 and 50 Hz, amplitudes of about 100 μV on the scalp and 1–2 mV on the brain surface containing much information related to brain activities.[118] The equivalent circuit model assumes that there are a lead resistance and a parallel RC circuit at the contact, and capacitive impedance (**Figure 5**).[119] Current technologies use bulky electrodes with complex electronic auxiliaries which is unsuitable for out-of-lab testing and unpractical for long-term testing due to skin irritation problems.[37] Moreover, there is pronounced mechanical discrepancy in cell–electrode interface such as ~6 orders of magnitude difference in Young's moduli. This is adverse for the interfacial conformal contact and thus the smooth signal flow pathways. [120-121] Implantation of nanoelectronics have proven that the intimate contact between electrode and cells via 3D organogenesis allows us to observe the synchronically bursting dynamics in human cardiac organoids.[122] Hence, researchers hope to search for a soft electrophysiological interface capable of transducing weak electrical signals from cells to epidermal devices with high fidelity.

3.2.1 Enhancing conformability for sensitivity

Enhancing conformability has been proven to increase the electrophysiological

signals sensing sensitivity.[123-124] The conformal contact of device on epidermis helps the formation of the conductive signals transduction pathway.[125-128] Apart from the aforementioned conformable contact in the biomechanical signal testing, conformal functional elements should also exhibit ionic or electrical conductivity to transduce electrophysiological signals. Hence, researchers need to (re)discover conductive materials or composites with inherent conformability.

Size modulation such as decreasing diameter and material thicknesses is commonly used to achieve conformability enabled by strain engineering.[125, 129] In neuron activity recording, electrodes with the neuron-like dimensions shows reduced mechanical stiffness by 5–20 times compared to reported flexible probes, which allows the probing and modulation of electrical and chemical signals at subcellular scale (Figure 5b).[130-131] Decreasing thickness is widely used as bending strains are in reverse proportional to thickness. In principle, any material could become flexible when it is thin enough. Si ribbons with thicknesses of 100 nm become flexible and withstand bend radii of 1 cm where peak strain is 0.0005%. The decrease in bending rigidity eventually benefits conformal contact which is helpful for signal recording.[132] By using thin Au serpentine (50 nm thick) or PIN diodes on nanoscale silicon membranes (320 nm thick), a skin-like sensor/actuator was achieved which is conformal to epidermis and allows the accurate, continuous thermal mapping (Figure 5b).[133] An ultrathin electronic tattoo based on piezoelectric polymer with 28 μm thickness realizes the synchronous electrocardiogram and seismocardiography measurements.[134-135] Interfacial conformal attachment to the skin mainly is based

on van der Waals forces which indicates this film can be easily peeled off. Another advantage for matching young's modulus is users' attach-and-forget experience as these devices are mechanically invisible.[133] Despite the improvement in conformability, handling the ultrathin film is quite difficult due to the tendency of curling to decrease surface energy. Moreover, it is impractical to fabricate arrays or conduct systematic integration on ultrathin geometries as thin films (<10 μm) are not sufficiently self-supporting.

Natural biomaterials exhibit natural abundance, biocompatibility, biodegradability, bioresorbability, and being light-weight, which provide inspiration as building blocks towards next-generation flexible, biocompatible, biosustainable electronic devices as well as biological-related applications, e.g. epidermal sensors, diagnostics and therapy, prosthesis, rehabitation, and brain–machine interfaces.[136-138] The high mechanical flexibility and robustness allow devices to harmoniously attach onto the curved and soft tissue surfaces for high-fidelity data readout. Moreover, their biocompatibility relieves allergic reaction or inflammatory responses as well as avoids noise caused by device-induced irritation of tissue.

Silk, as a typical natural polymer, has attracted increasing attention due to the aforementioned merits, as well as mild aqueous processing and facile chemical/biological functionalization.[139] Recent works have demonstrated silk film-based transistors and various photonic devices.[139-140] Based on the bioresorbablility of silk fibroin, when used as substrate for ultrathin electronics, silk will dissolve and resorb which initiates a spontaneous, conformal wrapping to tissue

surface driven by capillary forces (Figure 5c).[141] By controlling the plasticization by ambient hydration and calcium chloride ($CaCl_2$) amount, Young's modulus of silk protein is tunable from tens of GPa to 0.1–2 MPa and stretchability is from <20% to and >400%.[109] As revealed by molecular dynamics simulations, doped ions and H_2O weaken the strength of crystallite and enhance the extension ability of secondary structures of amorphous domain. By further evaporating Au on soft silk substrate, the achieved devices with good conform contact to epidermis enables the dynamic on-skin EMG signal recording with high-quality.[109]

Hydrogels represent an almost ideal candidate for mechanically compatible electrodes due to their inherent softness similar to tissue. The limitation here is the low conductivity of most hydrogels, especially for electrophysiological recording application.[62] Using poly(3,4-ethylenedioxythiophene) polystyrene sulfonate (PEDOT:PSS) modified with a highly conductive ionic liquid to improve the conductivity, conductive hydrogel electrodes with micropillar structure are achieved.[62] These hydrogel electrodes showed tissue-like Young's modulus, improved signal amplitude and SNR, compared with rigid iridium oxide micropillar electrodes of the same diameter, which provide an ideal mechanical microenvironment for fundamental cardiac and neural researches (Figure 5d).

3.2.2 Impedance reducing for high fidelity

During electrophysiological measurement, the signal is transduced from ionic conductor to electronic conductor in the tissue-electrode interface. For frequency-dependent electrophysiological signals, interfacial impedance that

comprises resistance and reactance is used to evaluate how effective the charges are transferred from the body to the electrode. By superposition of all concurrent activities of neurons, a quantitative description of local field potentials is obtained,[142] illustrating that reducing impedance helps to improve electrophysiological monitoring performance, which are widely validated by many works.[143-147] For individual neuron cellular testing scenario, tuning the electrode capacitive characterize improves the high-fidelity of recording and stimulation.[148] In addition, optimization of the external measurement setup (e.g. amplifier) benefits the signal fidelity, but this part is mainly focused on the strategies for improving interfacial capacitive and resistive characteristics.[143, 149]

Surface modification is effective to decrease impedance by using hydrophilic materials with high porosity and charge storage capacity, such as hydrophilic-modified graphene electrode,[150] poly(3,4-ethylenedioxythiophene) (PEDOT),[151] nanoporous gold multiple-electrode arrays,[152] iridium oxide modification with enhanced charge storage capacity[147], and Pt coating on Si with reduced access impedance for intracellular electrophysiological signal monitoring (Figure 5e).[153] Typically, carbon nanotubes have been reported to decrease impedance from 940 kΩ to 38 kΩ at the frequency of 1 kHz which means the augment of charge transfer by ~40-fold (Figure 5e) in such biological significant frequency.[154]

Conjugated polymers is another kind of candidate material with low impedance.[155] The conductivity of polymers relies on the delocalization of

electrons and the doping process along π-bonded conjugated backbone, which allows them to be both electronic and ionic conductor. Their high transconductance facilitates biosignal transduction from the cell to the recording electrode.[80, 156] Polypyrrole (PPy) nanowires/ PPy film electrode shows a lower impedance than bare Au or PPy/Au electrode, high stretchability (≈100%), and high interfacial adhesion (1.9 MPa) (Figure 6f).[45] The polymeric microelectrode arrays are successfully applied in differentiating a normal rat from epileptic rat by *in vivo* recording electrocorticograph (ECoG) signals and stimulating the rat ischiadic nerve.[45] Besides, polyaniline, polythiophene derivatives such as poly(3,4-ethylenedioxythiophene) doped with poly(styrenesulfonate) (PEDOT:PSS)[156] are also well-established for electreophysiological signals. One more thing to be considered is the toxic residual monomers or oligomer and stability of electroactive polymers which might be adverse for constructing biocompatible interfaces.[157]

For biointerfaces that are soft, wet and ionic conductive, ionic hydrogel has been widely used in signal transduction due to their similarity with tissues.[142, 158-159] Despite their advantages, pure ionic hydrogels exhibit slow ion movement, and thus a slow response time and high resistance, which limits their application in recording high-speed (> 1,000 Hz) signals and electrical stimulation.[160] Efforts have been made to enhance their electronic conductivity by combining CP in hydrogel via printing, coating, or *in situ* polymerization.[161-162] For example, an ion gel film with an interconnected PEDOT:PSS network shows electrical conductivity of 47.4 ± 1.2 S

cm^{-1}.[39] Electrode arrays comprised of aforementioned hydrogel exhibit a significantly reduce in interfacial impedance, a ~30 times higher current-injection density compared to that of Pt electrodes.[39] These features allow the electrical stimulation of the sciatic nerve in live mice at localized low-voltage (Figure 5g). The dehydration of hydrogel was another issue that causes hydrogel delamination and damages the stability. Using multilayer elastomer encapsulation is reported to suppress the dehydration and store for several months in the dry state, which should benefit long-term testing.[163]

To sum up, electrophysiological signals can be detected via biopotential electrodes which convert ionic currents to electric currents at the interface between biological systems and measurement instruments. Good conformal contact helps to enhance sensitivity which can be achieved via decreasing film thickness, developing soft materials, and tissue-like hydrogel strategies. Decreased interfacial impedance via modified metal electrodes, polymeric electrodes, and ion-conductive hydrogel are other powerful ways to obtain electrophysiological signals with high fidelity. Moreover, long-term monitoring of biopotential is meaningful to comprehensively understand the working bodily functions and disease pathologies. There is still plenty of room to improve the durability of biopotential electrodes when exposed to epidermal secretion, continuous stretching, and even scratching. In addition, depolarized Ag/AgCl is widely used in commercial applications and clinical diagnostics as it shows a much more stable potential than other polarized metal electrodes. Enhancing the compatibility of Ag/AgCl with the aforementioned

elastomer and hydrogel system is believed to further push the transformation of research outcome to reality.

4. Flexible and patchable biosensors for cyber biochemical interface

Besides biophysical signals, there are numerous biochemical signals such as metabolites, proteins and nucleotidse that provide a window to reflect our overall well-being including state of health, the environment, and food safety.[164-166] For instance, glucose for diabetes, chloride for cystic fibrosis, human chorionicgonadotropin (hCG) for pregnancy, carcinoembryonic antigen (CEA) and prostate-specific antigen (PSA) for cancers, breath ethanol for drunk driving, and volatile organic compounds (VOC) for indoor air quality.[167-172] It is noted that these indicators do not work independently and have huge interconnection with each other. Hence, building CPI platforms capable of measuring the biochemical indicators and revealing their correlations precisely (at the molecular scale) and in real-time (with dynamical changes) reflect not only our internal health and external safety but also provide guidance for detecting diseases early, developing healthy lifestyles and smart living environment. To build CPI platforms for biomarkers monitoring, there are three critical aspects: biomarker identification, sample collection, and target detection, discussed in details as follows (**Figure 6**).

4.1 Biomarker identification

Biomarker identification includes the correlation between biomarkers and diseases, the specificity of biomarkers to certain diseases, and general availability of biomarkers, all of which are prerequisites for building CPI. Generally, to obtain

these information, researchers rely on extensive sample testing via well-developed techniques such as gas chromatography or liquid chromatography linked with mass spectrometry to select characteristic peaks for component identification.[173] Based on the chemical structure analysis for different samples, data processing then provides the quantitative correlation of biomarkers for certain diseases.[174] Next, the most representative biomarkers will be clinically validated for their feasibility by comparing with other gold-standard indices (Figure 6).

Even though rich information exists in perspiration, saliva and tears, the useful biomarkers reported so far have been limited to metabolites (glucose, lactate, uric acid, ethanol) and ions (Na^+, K^+, H^+, NH^{4+}, Ca^{2+}, Cl^-).[175-176] Hormones, proteins, and peptides are rarely reported due to their trace amounts, but which could provide deeper physiological insight into homeostasis mechanisms and the body's overall state of health. For instance, Neuropeptide Y (NPY)[177] involved in the body's stress response and interleukin 6[178] in the immune system could be promising candidates for future detection for depression, and injury or infection, respectively.

On the other hand, the biomarkers at these sites are more susceptible to external changes and human activities compared to that in blood with a mesomeric state. Hence, dynamic changes of the biomarker, and individual variations in the specific applications can complicate the target identification process. Currently, the rapid development of data-mining techniques on large sets of sensor measurements provides new opportunities to identify correlations between sweat analytes and health status in such a complex context. By utilizing big-data approach, information such

as biomarker-disease correlation in sweat analytes can be reverse-engineered from amassed data without *a priori* knowledge of their biochemistry and metabolism.[179] CPI platforms combining sensing elements with data mining are expected to add value to conventional target identification procedures by fully incorporating these dynamic changes and individual variations.

4.2 Quantitative sample collection

Quantitative sample collection is directly related to the reliability of biochemical sensors due to uncertainty of sweat gland density, sweat rate, and potential sweat loss. Sample collection has to be continuous, precise, non/minimally invasive, and real-time (Figure 6). The standard protocol begins with sweating stimulation by pilocarpine iontophoresis, followed by sweat collection on a filter paper or gauze pad. The sample was then weighed, treated (filtration and elution) and analysed in the laboratory using various clinical analytical methods.[180] The sample transporting process inevitably leads to a high incidence of error due to potential sweat evaporation and component changes induced by bacterial degradation or chelation. The Macroduct sweat collection system is a common method where sweat is collected in a coil, making it possible to measure the total solute concentration on raw sweat samples *in-situ* by osmolarity or conductivity.[181-183] But this system is bulky and the procedures are uncomfortable. The development of soft materials and micro manufacturing technology has enabled conformal interfaces to the epidermis and facilitated ambulatory modes for real-time sweat extraction and analysis.

Recently years have witnessed the rapid development of epidermal microfluidic

technologies with thin and mechanically soft features which can robust, water-tight integrated with epidermis.[184-186] Specifically, these microfluidic systems can capture and store sweat of μL scale driven by natural perspiration and capillary force without using traditional pumping procedures.[187] Microchannel design through valves, mixers, reservoirs, channel geometry, and other components are helpful for quantitative detection of perspiration rate and spatiotemporal sampling process.[187] They enable the local sweat chemistry analysis, the sweat rates evaluation, and dehydration status monitoring with single-gland resolution.[184, 188]

Another issue is that the perspiration rate from 12 to 120 μL/(h cm^2) is highly depending on the physical activities and the mounting location on the body.[188] Sweat is inaccessible in sedentary individuals, hence it is difficult to leverage rich source of information, especially if large volumes (≥10 μL) of sweat are needed. To make this process easier, an electrochemically enhanced iontophoresis technology is proposed which could extract sufficient sweat in sedentary individuals for robust analysis.[189] This interface shows programmable extraction rate up to 100 nL/(min cm^2) via both continuous or periodically way. In order to further enhance the technique reliability based on perspiration, hyaluronic acid (HA) penetration was introduced in the iontophoresis process using electrochemical twin channels (Figure 7b).[190] It is reported that HA increases the osmotic pressure of interstitial fluid (ISF) which enhanced intravascular blood glucose refiltration and refrained the reabsorption at the arterial and venous ends, respectively. In this way, HA penetration leads to increased amount of glucose filtrated into the ISF which improves the correlation of

sweat glucose with blood glucose.[190]

4.3 Target detection

The collected samples are then subsequently used in benchtop equipment such as mass spectrometry, spectrophotometer, electrochemical measurement, chloridometry, or other analytical methods. Among them, electrochemical and colorimetric outputs are most feasible to be miniaturized into portable and wearable modality such as tattoo-based perspiration sensor,[191-193] wearable mask-based breath sensor,[168] contact lenses-based tear sensor,[194] mouth guard-based saliva sensor[195] and epidermal sensor integrated with therapy systems[196] (Figure 6).[197] Taking the glucose biosensor as an example, the catalytic oxidation of glucose by glucose oxidase in the presence of oxygen (electron mediator) produces H_2O_2 (oxidized mediator). The redox reactions of H_2O_2 on the electrode or with dyes then generate a readable current or colorimetric signal which is utilized for quantitative analysis (**Figure 7**a).[171-172] Even though these sensing mechanisms and techniques are well-known and even commercialized, there are still key challenges when tested on wearable prototypes due to unexpected deformations and environmental variations.

The bio/chemical sensing process relies on the biomolecules or functional ligands to recognize specific targets, such as glucose oxidase for glucose, lactate oxidase for lactate, and ion-selective ligands for ions. Hence, maintaining highly-active biomolecules or ligands is important for achieving highly-sensitive and stable biosensors. As the intrinsic activity of biomolecules is highly dependent on pH, temperature, ionic strength, and (protein) deformations, physical calibration is

generally required at epidermal application where the aforementioned parameters vary significantly (Figure 7c).[27, 198] The fully integrated wearable sensor arrays incorporating glucose and lactate sensors with pH and temperature calibration marked a milestone for wearable biosensors with physical calibration *in-situ*.[27] Based on the calibration platform, other sensing systems for uric acid, ascorbic acid, Zn^{2+}, Cd^{2+}, Ca^{2+}, and even sensing and therapy systems have been reported.[167, 196, 199]

Apart from biorecognition reactions, signal collection is also crucial for a stable biosensing interface (Figure 7c). For electrochemical sensing, a potential is applied on the system and the current or potential output is detected, based on a three-electrode or simplified two-electrode device design. Hence, the potential shift directly influences the output signals by affecting the reaction thermodynamics according to Nernst equation. For on-skin application, human activities inevitably cause strains to the connectors, leading to resistance increases which alters the potential applied on the reaction interfaces and eventually leads to performance variations.[198] Screen printing of conducting inks with serpentine structure combines intrinsic and geometry-induced stretchability, which could sustain stable electrochemical interface after repeated mechanical deformations (500% strain).[200-201] This method was successfully applied to stretchable biosensors for perspiration glucose, ethanol, caffeine, etc. with potentials in both healthcare and chemically sensitive robotic skin.[202-203]

On the other hand, as the reference electrode (RF) potential is highly dependent on chloride concentration, to avoid potential shift, an optimized salt bridge has been

proposed to minimize equilibration between RF and the solutions.[204] Taking the advantages of salt bridge, reliable Cl^- testing (<40 mM) during 1 h continuous exercise was realized compare to rapid increase in Cl^- detected by traditional devices without using a salt bridge.[204] In addition, the salt bridge that is helpful for maintaining a stable RF potential is also meaningful for the stability of other metabolite electrochemical biosensors.

For colorimetric sensing, the signals rely on target-induced color changes of biosensing pattern which is susceptible to many factors that influence pattern colorimetry. Reference color markers such as white and black are used for to white balance, to calibrate for environmental influences and eliminate the variations caused by lighting conditions (e.g. daylight, shadows, and ambient light sources).[188]

To summarize, stable biosensing interfaces are challenging considering the stability of recognitive biomolecules and variations of signal collection element such as potential shift (electrochemical) or environmental color changes (colorimetric). Non-enzyme glucose sensors such as $CoWO_4$/CNT[205] are proposed to compensate for inherent instability issue of biomolecules and strain adverse effect. They are promising alternatives after enhancing the anti-inference properties, sensitivity and biocompatibility of alkaline testing condition. Moreover, developing novel sensing principles are also desired such as electrochemical transistor-based biosensors that is capable of amplifying the input signal and eliminating the requirement of a reference electrode.[206]

5. System integration

5.1 Array integration

To understand the profile of target objects, a large-scale sensor array consisting of mechanical, chemical and/or biological sensor units is usually required. In addition, array configuration is vital to data storage and display in the system. The crossbar array where each functional unit is placed at the overlap junction between the row and column line (**Figure 8a**) is the most effective configuration for achieving low cost, high-density and large-area integration.[140, 207-210] However, most functional units (sensors, memory and display units) show approximately linear current-voltage characteristics, which cannot be directly integrated into the crossbar configuration without any amendments due to the crosstalk issue.[210] This crosstalk issue is derived from the sneak path currents from neighboring pixels in the crossbar array, which can lead to the readout or other errors (Figure 8a).[208, 211] To resolve this, an electronic switch, also known as access device, is often connected in series with a functional unit in each pixel of the crossbar array (Figure 8b).[208] The electronic switch should exhibit a nonlinear current-voltage response (Figure 8c) in order to alleviate the sneak path currents in the crossbar array.[210] Typically, flexible electronic switches include: 1) three-terminal devices, e.g. flexible organic transistors,[207, 212-219] and 2) two-terminal devices, e.g. flexible diodes,[133, 172, 220-226] tunneling barrier devices,[227-229] and threshold switches.[208, 230]

Figure 8d shows the typical circuit schematic of an integrated array when using three-terminal transistors as flexible electronic switches. The functional unit is

connected with the source (drain) terminal of a transistor and the corresponding drain (source) terminal is connected the column select. The third gate terminal serves as the row select to access each individual unit in the crossbar array.[214] Organic transistors usually offer good switch-on and switch-off characteristics with good mechanical bending ability (Figure 8e), and thus are the current mainstream solution for flexible array integration. In addition, it is easy to fabricate three-terminal electronic switches on ultrathin flexible substrates by using thin-film processing techniques. For example, Martin *et.al.* has demonstrated a tactile sensor array by adopting the organic transistor backbone.[231] In this work, the sensor array fabricated on ultrathin (1μm) polymer foils can conform to a model of the upper human jaw for healthcare monitoring with minimal patient discomfort.

The other configuration using two-terminal electronic switches is shown in Figure 8g. In each pixel, one functional unit is connected with one two-terminal electronic switch in series. Compared to three-terminal transistors, the two-terminal electronic switches offer promising advantages such as simple structure, low operation voltage, and high-density three-dimensional stacking for flexible array integration.[208, 229] Diodes are one of the most common two-terminal electronic switches for array integration. Recently, Webb et. al. demonstrated a conformal skin-like sensor patch for precise monitoring of the epidermal temperature mapping (Figure 8h) based on a nanomembrane diode-based sensor array.[133] Threshold switch device is another promising example, which was recently used to solve the crosstalk issue of an integrated flexible sensory array.[208] The two-terminal

bidirectional threshold switch shows a high nonlinearity of 10^{10}, good cycling behavior (Figure 8i), and decent mechanical flexibility with a minimum bending radius of 1 mm.

5.2 System-level integration

Apart from the sensory units/arrays at the core, the following components should also be incorporated into the flexible/stretchable sensor platform to achieve complete system-level integration: i) Signal processing circuits, including multiplexers, amplifications, filter circuits, demodulation circuits, A/D translation circuits, compensation circuit, etc. ii) Data transmission modules that provide control, computation, and communication functions. iii) Power sources. Generally, two strategies are applied to realize the flexible/stretchable system-level integration: 1) Flexible electronics based on innovative materials, mainly using organic materials that are intrinsically mechanically flexible or stretchable to construct various circuit components of functional circuits. 2) Flexible hybrid integration, by combining conventional silicon electronics and flexible/stretchable electronics into one system, known as flexible hybrid electronics (FHE).

5.2.1 Organic electronics for system-level integration

The most intuitive approach for flexible/stretchable system integration is to make each building block in the systems flexible or stretchable, connected by flexible or stretchable interconnect wires. Hence, organic electronics have attracted much attention in recent decades due to its desirable mechanical flexibility, the ability for

large-area fabrication, low-temperature processing and low cost.[232-235] Various processing technologies (e.g. thin-film process, printing process, and transfer process, etc.), organic semiconductor materials (e.g. pentacene[213, 236-239], phthalocyanine,[108, 233, 240-242], sexithiophene,[233, 241, 243] naphthalenes[236, 244-246], fullerenes,[247] bithiophene,[248] nanotubes,[249-251] etc.), and even stretchable organic semiconductor materials (semiconducting polymers[61, 252]) and stretchable dielectrics[253-256] have been developed for flexible/stretchable electronic circuits and components[257-260] (**Figure 9**). For example, Someya's group has demonstrated a series of flexible organic transistor circuits, such as complementary inverters, five-stage complementary ring oscillators, amplifiers, and printed microelectromechanical-system switches, which can continue to function when folded into a small radius.[216-217, 261-262] Furthermore, fully integrated flexible circuit systems have been developed.[263-266] For example, Street et.al. reported a fully printed temperature threshold sensor tag, which consisted of the printed thermistor sensor, the jet-printed transistor circuit and the gravure-printed nonvolatile memories.[263] The sensor tag is employed to monitor temperature changes, where the control circuit would be triggered if the thermistor temperature exceeds a preset threshold. To further improve the fidelity of signals acquired from the objects, stretchability is required at both the sensing device and peripheral circuitry to create intimate contacts between the system and the nonplanar objects.[37, 88, 252] Recently, Bao's group has reported circuit design strategies for improving the accuracy and robustness of sensing systems by using intrinsically stretchable sensing circuits

(Figure 9g).[267] In this work, the stretchable static and dynamic differential sensing circuits with sensitivities of −24.2 and −20.2 mV °C^{-1} have been achieved based on stretchable carbon nanotube transistors. Moreover, an intrinsically stretchable amplifier with the stable operation even under 100% strain was fabricated, which can interface directly with skins.[252]

To the best of our knowledge, the state-of-the-art organic circuits are still limited to small and simple functional modules, e.g. inverters, ring oscillators, amplifiers, radio-frequency (RF) identification tags, simple analog-to-digital converters, and energy harvesters (Figure 9). One of the most sophisticated challenges is the limitation of low/moderate device performance of current organic transistors.[232, 268] To endow the flexible/stretchable sensor systems with relatively complex processing functionality, the FHE strategy was recently proposed by heterogeneously embodying both the conventional silicon-based electronics and the emerging flexible/stretchable electronics.

5.2.2 FHE for system-level integration

In FHE, high performance circuit elements, e.g. high-precision amplifiers, complex filter and modulation circuits, analog switch circuits, communications, and precise passive components, are provided by the well-established silicon fabrication process. On the other hand, the uncomplicated circuit elements, e.g. sensors, interconnect wires, and low performance circuits, are fabricated by the flexible/stretchable process technology. Hence, FHE can feature both the functionality and reliability of

silicon-based integrated circuits (ICs), and the mechanical flexibility of flexible/stretchable electronics. The hard silicon and soft elements are merged via soft-hard material interconnections that create suitable interface conditions for process integration and system stability. According to the configuration of soft-hard interfaces, the strategies for FHE integration can be divided into two categories: plug-in integration and interconnected integration (**Figure 10**).

5.2.2.1 Plug-in integration

In the plug-in integration, sensory units/arrays are separated from the corresponding peripheral circuitry into two substrates with homogeneous/heterogeneous properties, which are connected via "plug-in" interconnect wires. In most cases, the sensory components require more flexibility mechanically than the peripheral circuitry. This is because the sensors must directly contact the deformable sensing surfaces, such as skins, muscles, viscera, cells and other plastic objects, while peripheral circuits do not.[27] Hence, sensory components are usually fabricated on plastic or stretchable substrates, such as polyethylene terephthalate (PET), polyimide (PI), polyethylene naphthalate (PEN), PDMS, SEBS and Ecoflex. These flexible or stretchable substrates can offer an intimate and conformable contact between the sensors and the target objects to improve the quality of collected data.[88] In the plug-in integration, the substrates of peripheral circuits can be different from that of sensor parts, which allows us to select respective materials accordingly. Sometimes, peripheral circuit components are assembled onto commercially available flexible printed circuit boards

(PCB), or even rigid PCBs in order to guarantee the reliability and functionality of systems.[27, 107, 189, 199, 205, 269]

For example, Gao et.al. recently developed a wearable flexible integrated sensing array (Figure 10a and b) to extract physiologically and metabolically multiplexed information (e.g. glucose, lactate, sodium ions, potassium ions, and skin temperature) available from sweat by using the plug-in FHE integration.[27] In this system, the complex signal processing circuitry including signal transduction, amplification, and filtering, calibration, and compensation) and wireless transmission are consolidated on a flexible PCB while the five different sensors are deposited on a mechanically flexible PET substrate. One more case, Imani et.al. designed a wearable hybrid multi-sensor system based on the FHE approach (Figure 10e), which could simultaneously monitor both biochemical and biophysical signals from user.[270] To be more specific, a three-electrode biosensor and a bipolar electrocardiogram sensor were used to detect the lactate and electrocardiogram signals, which are integrated onto a flexible sensor patch. The plug-in integration strategy can decouple the strict mechanical and electrical requirements at the sensor and peripheral circuitry level, respectively, by selecting suitable fabrication processes. Another noteworthy merit of the approach is the amenability for disposable applications as expensive peripheral circuitry components can be reused, which has demonstrated in food packaging and medical fields.[199, 271]

5.2.2.2 Interconnected integration

In the interconnected integration, sensory and silicon IC components can be intricately assembled together via printed or stretchable interconnect wires (Figure 10f). Flexible PET, PEN and PI substrates, and stretchable PDMS, SEBS and Ecoflex substrates are commonly used in interconnected integration. Each sensor unit could be placed close to the corresponding silicon ICs components, such as signal transduction conditioning modules and signal processing modules, which can potentially minimize external disturbance.

Printing electronics is a suitable approach to realize the interconnected integration, because sensor units and interconnect wires can be directly printed on flexible substrates. In particular, printing technology is compatible with the flexible PCB assembly process, simplifying the interconnect complexities.[272] Figure 10g shows a typical FHE example based on a printed flexible substrate.[272] The ECG (gold electrodes) and temperature (nickel oxide thermistor) sensors are printed on one side of the double-sided copper-circuitized substrate, and silicon IC elements (i.e. an analog front end circuit, a Bluetooth module, and other hard passive elements) are hosted on the opposite side of the frame. These two copper circuit layers are interconnected by plated-through holes, using standard flexible PCB process.

When stretchable substrates are used, a stretchable system can be achieved by using the interconnected integration approach. Fully stretchable systems can offer intimate covering for dynamic and nonplanar surfaces of target objects, which is vital to realize the precise monitoring of physiochemical signals from users.[37, 88] However, interfacing soft elements to hard silicon ICs is quite challenging because of

sophisticated bonding processes, stretchable interconnect, and alignment. Structural design is a promising way to achieve stretchable FHE integration at system level, which not only enhances the stretchability of soft components, but also bestows stretchability to rigid components. Classical structural design strategies such as wave[20, 82, 89, 273-275], island–bridge[37, 276-280], origami/kirigami[281-285] and textile[286-289] have been developed for realizing stretchable systems or modules, which are discussed as follows.

(1) Wave. It is one of the earliest structural design approaches to make rigid silicon-based circuits become stretchable (**Figure 11**a). While silicon wafers are rigid and brittle, silicon-based thin films with a thickness of less than 25 μm can yield good mechanical bendability and flexibility, which can be obtained by wafer thinning or exfoliation of silicon nanomembranes from a silicon-on-insulator (SOI) wafer.[290-291] Similar to stretchable electrode obtained by wavy structural design, these thin-film ICs and sensors are then bonded on the surface of a stretchable substrate that is prestretched under a tensile strain. When the substrate is released, the thin films of silicon ICs would generate the wave/wrinkle patterns to compensate the compressive strain from the substrate. A mass of silicon-based stretchable, such as logic gates, ring oscillators, differential amplifiers, inverters, have been demonstrated by using this strategy.[20, 275]

(2) Island–bridge. In this design, high-modulus, rigid, or flexible functional elements are assembled as islands which are interconnected by highly stretchable conductive bridges (Figure 11b). When an external strain is applied, the

conductive bridges can stretch and deform while the islands remain intact. Depending on the design of the conductive bridges (e.g. serpentine, selfsimilar, spiral, arc-shape, non-coplanar serpentine and helix), the integrated systems with different levels of stretchability can be achieved. The maximum stretchability of the integrated systems in the previous reports is up to 1600%.[292] Another advantage of this approach is that the selection of silicon ICs and sensors can be diversified (organic or inorganic, lab-made or commercial-off-the-shelf, thin films or chip-scale packages), not limited to silicon nanomembranes as in the wave structural design.[88] Hence, the island–bridge design has been considered as the most common approach for stretchable system-level integration, which has been widely used for implementing various flexible/stretchable sensor systems, and critical stretchable circuitry components, such as wireless transmittance system and ring oscillators.[37, 278-279, 293] Noted that Rogers's group recently utilized the island–bridge design to develop a wireless epidermal electronic system that can implement in-sensor analytics for neonatal intensive care.[279] This system can softly and noninvasively interface onto neonatal skin to implement the vital signs monitoring, which is also compatible with visual inspection and with medical imaging techniques used in neonatal intensive care. In the island–bridge approach, interconnecting and aligning issues are two key challenges that limit the scale of large-area hybrid systems. A detailed requirement of various components for large-scale hybrid integration has been discussed in reference.[294]

(3) Origami/kirigami. Origami/kirigami arts have recently inspired a popular

structural design for stretchable electronics (Figure 11c). In origami, a planar sheet is transformed into a crease structure with a periodic pattern of mountain and valley folds, which can be recovered to the planar state when stretched. In kirigami, a mass of patterned slits are generated into the planar sheet that can buckle out of plane to dissipate the tensile energy. Both origami and kirigami can provide high throughput and large deformability for the rigid silicon ICs[295], and do not involve elastomeric substrates that are usually incompatible with standard manufacturing processes. Therefore, the origami/kirigami design has been widely used in stretchable electronics, e.g. stretchable lithium-ion batteries, stretchable solar cells, stretchable transistors, stretchable photodetectors, and stretchable supercapacitors.[281-283, 296-300]

(4) Textile. Textiles are a category of flexible and stretchable materials formed by weaving, knitting, spreading, crocheting, felting, or braiding. Embedding sensor systems or components with the desired mechanical and electrical characteristics onto textiles is an effective strategy toward stretchable electronic applications. For example, Chen et.al. demonstrated a woven hybrid power textile fabricated by integrating the triboelectric energy harvesters and solar cells on fabrics for simultaneously harvesting mechanical and solar energies (Figure 11d).[289] In addition to energy harvesters, a myriad of wearable/stretchable electronics based on this design have been reported to realize various functionalities, such as logic multiplexers, light-emitting diodes (LEDs), driving ICs, supercapacitors, and sensors.[286-287, 301-303]

6. Machine learning and edging computing

Sensing technologies are continuing to generate more and more data from various applications, such as healthcare, food security, environmental monitoring, smart home and city management. The generated data, including physiological signals (heart rate, blood pressure, clinical imaging, ECG, EMG, EEG, etc.), biochemical signals (glucose, antigens, ions, etc.), chemical signals (formaldehyde, diethyl ether, etc.), weather conditions (temperature, humidity, wind, etc.), and environmental parameters (noise, light, etc.) are usually heterogeneous, sparse, irregular, temporal-dependent, and even highly-dimensional.[304-306] Understanding and utilizing these meaningful data will further improve quality of life. However, there remains a key challenge for gaining insights from these complicated sensing data, due to the lack of sufficient domain knowledge and effective algorithms.[306]

Artificial intelligence (AI) technologies with the cores of machine learning and big data, have paved a promising way to enable these intelligent applications and services.[304, 307-319] In machine learning algorithms, computers can automatically learn knowledge from historical experiences data and make prediction on unknown tasks. With the improvement of data acquisition and computing infrastructure, machine learning (especially emerging deep learning) has recently shown or even exceeded the capabilities of human experts in the tasks of image classification, speech recognition, and natural language processing.[308, 320-323] Deep learning uses multiple levels of nonlinear functions to learn high-level representation of input data

layer-by-layer for making decision. The learned representation, is often abstract and composite, which can serve as input for the latter layers.[324] Therefore, deep learning technologies possess the ability of automated feature learning and provide an end-to-end learning paradigm to obtain the desired knowledge from complex sensor data. A number of deep learning algorithms, such as deep neural networks, convolutional neural networks (CNN), deep belief networks, deep residual neural networks, recurrent neural networks (RNN), deep reinforcement learning, capsule networks, autoencoders and generative networks continue to emerge.[323, 325-338] Such algorithms with different network configurations are often sensitive to the type of processed data. Here, we focus on recent progress in data analysis from sensors mainly using emerging deep learning algorithms. According to data dimensionality, sensor data are generally classified into three categories: 1) discrete, 2) time-series, and 3) image data.

(1) Discrete data. For applications such as food security, environmental monitoring, toxicity detection, pressure detection and strain detection, one or several discrete data is often enough to evaluate the current status of a target object. Typical threshold evaluation, Euclidean distance, principal component analysis (PCA) and clustering methods are usually used to analyze these discrete sensor data.[339-345] For example, in discriminating a specific class of chemical analytes, PCA and agglomerative hierarchical clustering approach have been proposed to process these sensor data collected from a colorimetric sensor array.[340] The results of

PCA (**Figure 12**a) and clustering statistical analysis indicate that the colorimetric method shows high discrimination ability and reproducibility, even down to amine concentrations of 50 ppm.

(2) Time-series data. Healthcare, especially clinical diagnosis, typically requires the continuous monitoring of one or more physiochemical signals for a prolonged period of time so as to accurately assess one's state of health. The healthcare data such as EEG, ECG and EMG, is often difficult to mine effectively by using traditional data analysis approaches, due to the long-term time dependency, varying length, and irregular sampling of the sensor data.[346-348] Enabled by automated feature extraction and end-to-end learning, various deep learning algorithms have been developed to process the time-series sensor data (Figure 12b-f).[317, 346, 349-351] In particular, RNNs with varying length sequences and long-range dependencies on training data are good at extracting knowledge from time-series data. In a recent study, a long short-term memory (LSTM) neural network that is a subcategory of RNNs has been used to analyze the complex clinical data.[346] In this work, the LSTM model can classify 128 diagnoses with surprisingly high accuracy, when given 13 irregularly sampled time-series clinical data, such as diastolic and systolic blood pressure, heart rate, peripheral capillary refill rate, etc.

(3) Image data. Visual sensing and recognition is one of the most important abilities for the survival and development of human beings, which helps us to perceive, recognize, and change the world. The analysis of image data has been widely

used in medical diagnosis, autonomous driving, security, Industry 4.0, Internet of Things (IoT), and so on. Image data usually contains rich internal information of studied objects beyond our intuitive insights, due to its intrinsic property of spatial distribution and complex multidimensionality.[352] Deep CNN inspired by biological visual information processes has been employed to handle the complex image-based sensor data and produce promising results. One of the most popular frameworks is the implementation of CNNs on raw image data such as ocular images, epidermis images, computed tomography (CT), magnetic resonance imaging (MRI) and X-rays images, to diagnose potentially relevant diseases.[307-308] For example, Esteva et.al. demonstrated a dermatologist-level classification of skin cancer using the CNN algorithm.[308] In their research, there are 129,450 clinical images in total (consisting of 2,032 different diseases) that are directly used to train a classification model for the skin cancer diagnosis.

Although deep learning provides a promising approach in analyzing these complex sensor data, most current deep learning algorithms cannot run directly in the end of sensor devices.[306, 351] Instead, deep learning is usually implemented on high performance servers or personal computers, as there are thousands and millions internal parameters need to be adjusted in the model, which is difficult to run in the sensor end[315, 353]. In addition, the user-centric serves in the sensor end are usually distributed and delay-sensitive, which requires real-time data processing and feedback. Because of limited bandwidth and strict latency time, the mainstream cloud computing that is usually centralized alone cannot support such ubiquitously

user-centric applications.[354-355] In recent years, a multi-tier computing network architecture was proposed to address these challenges and enable these intelligent applications and services (**Figure 13**a).[356]

The multi-tier architecture divides the whole computing network into four hierarchical layers, including cloud, fog, edge and sea computing technologies.[356] In the hierarchy, cloud computing is at the very top, which is in possession of the most information sources, the maximum storage space and the strongest computing capabilities. In addition, cloud computing owns the highest authority in making crucial decisions. Hence, cloud computing is usually used to process the complicated, sophisticated and global tasks, such as cross-domain information extraction, new knowledge discovery and creation, and global strategies. The next level is fog computing which bridges the cloud and edge computing layers. Fog computing collaboratively handles the global tasks at regional level with the second-tier computing, communication, and storage abilities. Compared to cloud and fog computing, edge computing in the third level has the least resources and computing capabilities, but enough to implement advanced deep learning algorithms. Edge computing is very close to the sensor end and can directly interact with users in various perspectives. Hence, it can handle proficiently the delay-sensitive tasks for information and monitoring using AI algorithms. Sea computing means the data computing occurs at the sensor end, which is the closest end to data generation. In sea computing, individual sensor systems possess the limited capabilities of the data processing, communication, storage, and power management. Hence, sea computing

can only support local requests and demands, such as physicochemical signal sensing, environment monitoring, mobility control, feedback and other basic functions. The effective interaction and collaboration across different levels and units are vital to the intelligent collaborative computing architecture. The multi-tier computing network architecture provides a promising solution for future intelligent applications and services, such as smart transportation, smart home, smart people, smart health, smart sea monitoring, and smart meters (Figure 13b). [357]

7. Perspectives on CPI

Interfacial signal exchange takes place anywhere and anytime in living things, in the physical world and even the universe to maintain their perception, interconnection, adaptability and equilibrium of systems, such as tactile perception based on epidermal mechanical signal exchanges in human. This provides an opportunity to understand and communicate with any system by constructing reliable platforms (CPI) that are capable of extracting and analyzing complex physical and biochemical signals, and providing active feedbacks to users. To achieve this aim, the bottom-up architecture of CPI comprises biochemical/biophysical sensing interface, signal processing and transmission interface and intelligent computing interface. Molecular, geometry, and materials design are used throughout system construction to endow CPI with stretchability, conformability, adhesion, biorecognition, and durability features (Figure 14). Driven by a niche need in healthcare, smart robotics and CHS, CPI rapidly expands and evolves into an interdisciplinary field focusing on the multiple

physical and biochemical interfaces. Despite recent progress, there remain several challenges in terms of 1) novel materials for sensing units and high-performance circuit systems, 2) biosignals collection and their correlation to diseases, 3) power consumption, and 4) security in the CPI framework.

The first issue on materials forms the basis for device and system fabrication. Achievements have been made regarding stretchable, soft, conformable electrodes, but it is still infancy for the functional circuits and systems that possess matched mechanical and electrical properties. In addition, inadequate features still exist, including biocompatibility with acceptable biotoxicity by FDA approval, antifouling to avoid the interference of biosecretions, multi-functionality with specific recognition, and durability for long-term monitoring. Synthesis of block copolymer, supramolecular, and hybrid compounds with predesigned properties will contribute towards the growing material library for CPI.

The second issue is the lack of reliable non-invasive biosensing interface. For example, sample collection is now a bottleneck for non-invasive sensing. Currently a sweat-uptake layer and a waterproof film are commonly used, but it suffers from activity-dependent sweat collection inconsistencies. Wearable microfluidics provide a solution for quantitative sampling, though continuous sampling with automatic refresh procedures is still less than ideal. Also, there is much controversy on the correlation between epidermal biomarkers and specific diseases, which impedes the development of CPI. Additionally, the time lag between biomarkers in biofluids and in blood also needs further verification. Moreover, abundant information conveyed

by proteins and nuclei has not been encoded due to the lack of facile wearable sensing techniques.

Thirdly, power is the priority concern for system integration, which is used in sensing, data processing and communication. Conventionally, energy consumption by data communication accounts for a large proportion in the whole sensing system. Reducing power data transmission is very vital to render the CPI towards the real applications.[358-360] Typical wireless communication technologies such as infrared communication, broadcast radio, microwave communication, Bluetooth, and Zigbee still need much more efforts to achieve an energy-efficient data transmission manner for CPI. On the other hand, low power consumption is also necessary for continuous and prolonged monitoring which requires a trade-off between energy utilization and performance. For physiochemical signals that allow interval sampling, periodicity transmitting data offers an alternative way for long-time monitoring at the cost of losing partial sensing information. Other strategies include the search for other biocompatible batteries, green energy harvesting devices, or alternative energy storage system (e.g. solar cells, thermoelectric, biofuel cells, piezoelectric and triboelectric devices, supercapacitor, or a combination of these devices), and self-powered system powered by biofuel cells.[361] The last but not the least, to provide for the entire CPI system, the power element should be also flexible and facile to be integrated with the sensing and data processing elements.

For any cyber system, cyber security is a top priority. Access to CPI information for queries, changes and custom operations should be strictly limited to authorized

users because individuals' biomedical data compromise privacy and also involve life-threatening/serious health consequences. Hence, communications between CPI system and users should be under careful surveillance and protection by rules and regulations to ensure users' benefits. With this in mind, AI and data mining technologies can be fully utilized to obtain the underlying correlation between different biomarkers, the dependence of diseases on certain biomarkers, the effect of lifestyle on diseases or biomarkers, and also providing active feedback to users such as early disease detection, dietary suggestions, and customized exercise plans.

In short, it is desirable to conduct comprehensive collaboration between scientists and engineers from various disciplines of materials science, bioanalytics, mechanical engineering, electrical engineering, and computing science, for the development of CPI. However, current research progress is still hindered by the lack of an integral international ecological environment due to insufficient confidence among different fields. We hope to encourage and anticipate barrier-free cooperation with problem-orientated effort to address the above issues, by linking the electronic, communication and computing technology with materials, chemical and biological science. Such a "data centric" sensing approach will be developed as a platform for increasingly complex future wearables with on-board intelligence, especially in the foreseeable next-generation personal healthcare technologies, such as adaptive prosthetics and augmentation of human capabilities, smart sports technology, health and dietary care, etc. We can even envision future applications, bringing the impossible to possible, such as mind readers, plant communicators, and human

enhancement.

8. Summary

To elucidate the interfacial issues in signal exchange processes, we propose the perspective of cyber-physiolochemical interface with the ability to collect biophysical and biochemical signals and closely link them with cyber space. This review summarizes the scientific and technical progress in CPI and highlights the challengs as well as strategies in building stable interfaces, including (i) stretchable and conformal sensors for cyber biophysical interface, (ii) flexible and patchable biosensors for cyber biochemical interface; (iii) system integration such as sensor array integration and full-system integration with functional circuits, and (iv) machine learning and edging computing. We hope to put forward an unprecedented multi-disciplinary scientific collaboration towards CPI, for constructing stable signal exchanges across a broad range of dynamic applications in healthcare, fitness and wellness, rehabitation, and soft robotics. These technologies will provide a paradigm shift in the development of next-generation personal healthcare technology, such as adaptive prosthetics and augmentation of human capabilities, smart sports technology, and health and dietary care.

Acknowledgements

T. W. and M. W. contribute equally to this work. We thank the financial support from the National Research Foundation (NRF), Prime Minister's office, Singapore,

under its NRF Investigatorship (NRF2016NRF-NRF1001-21), Singapore Ministry of Education (MOE2017-T2-2-107), and the Agency for Science, Technology and Research (A*STAR) under its AME Programmatic Funding Scheme (Project #A18A1b0045).

References

[1] M. W. Schwartz, S. C. Woods, D. Porte, R. J. Seeley, D. G. Baskin, *Nature* **2000**, *404*, 661.

[2] I. J. Wright, P. B. Reich, M. Westoby, D. D. Ackerly, Z. Baruch, F. Bongers, J. Cavender-Bares, T. Chapin, J. H. C. Cornelissen, M. Diemer, J. Flexas, E. Garnier, P. K. Groom, J. Gulias, K. Hikosaka, B. B. Lamont, T. Lee, W. Lee, C. Lusk, J. J. Midgley, M.-L. Navas, Ü. Niinemets, J. Oleksyn, N. Osada, H. Poorter, P. Poot, L. Prior, V. I. Pyankov, C. Roumet, S. C. Thomas, M. G. Tjoelker, E. J. Veneklaas, R. Villar, *Nature* **2004**, *428*, 821.

[3] Y. H. Jung, B. Park, J. U. Kim, T.-i. Kim, *Adv. Mater.* **2019**, *31*, 1803637.

[4] N. G. Jablonski, *Annu. Rev. Anthropol.* **2004**, *33*, 585.

[5] V. J. Lumelsky, M. S. Shur, S. Wagner, *IEEE Sens. J.* **2001**, *1*, 41.

[6] J. G. White, E. Southgate, J. N. Thomson, S. Brenner, *Philos. Trans. R. Soc. Lond. B. Biol. Sci.* **1986**, *314*, 1.

[7] A. Schütze, N. Helwig, T. Schneider, *J. Sens. Sens. Syst.* **2018**, *7*, 359.

[8] V. T. Srikar, S. M. Spearing, *Exp. Mech.* **2003**, *43*, 238.

[9] J. W. Judy, *Smart Mater. Struct.* **2001**, *10*, 1115.

[10] S. C. Mannsfeld, B. C. Tee, R. M. Stoltenberg, C. V. H. Chen, S. Barman, B. V. Muir, A. N. Sokolov, C. Reese, Z. Bao, *Nat. Mater.* **2010**, *9*, 859.

[11] A. J. Bandodkar, I. Jeerapan, J. Wang, *ACS Sensors* **2016**, *1*, 464.

[12] Y. Khan, A. E. Ostfeld, C. M. Lochner, A. Pierre, A. C. Arias, *Adv. Mater.* **2016**, *28*, 4373.

[13] S. R. Krishnan, T. R. Ray, A. B. Ayer, Y. Ma, P. Gutruf, K. Lee, J. Y. Lee, C. Wei, X. Feng, B. Ng, Z. A. Abecassis, N. Murthy, I. Stankiewicz, J. Freudman, J. Stillman, N. Kim, G. Young, C. Goudeseune, J. Ciraldo, M. Tate, Y. Huang, M. Potts, J. A. Rogers, *Sci. Transl. Med.* **2018**, *10*, eaat8437.

[14] *Chapter 1 - The Birth of the Computers*, in *Studies in Computer Science and Artificial Intelligence*, A. Nijholt, Editor. 1988, North-Holland. p. 3.

[15] D. R. Hartree, *Nature* **1946**, *158*, 500.

[16] W. Aspray, *IEEE Ann. Hist. Comput.* **1997**, *19*, 4.

[17] Z. Bao, X. Chen, *Adv. Mater.* **2016**, *28*, 4177.

[18] T. Sekitani, Y. Noguchi, K. Hata, T. Fukushima, T. Aida, T. Someya, *Science* **2008**, *321*, 1468.

[19] M. Kaltenbrunner, T. Sekitani, J. Reeder, T. Yokota, K. Kuribara, T. Tokuhara, M. Drack, R. Schwödiauer, I. Graz, S. Bauer-Gogonea, S. Bauer, T. Someya, *Nature* **2013**, *499*, 458.

[20] D.-H. Kim, J.-H. Ahn, W. M. Choi, H.-S. Kim, T.-H. Kim, J. Song, Y. Y. Huang, Z. Liu, C. Lu, J. A. Rogers, *Science* **2008**, *320*, 507.

[21] M. L. Hammock, A. Chortos, B. C.-K. Tee, J. B.-H. Tok, Z. Bao, *Adv. Mater.*

2013, *25*, 5997.

[22] Y. Kim, A. Chortos, W. Xu, Y. Liu, J. Y. Oh, D. Son, J. Kang, A. M. Foudeh, C. Zhu, Y. Lee, S. Niu, J. Liu, R. Pfattner, Z. Bao, T.-W. Lee, *Science* **2018**, *360*, 998.

[23] J. A. Rogers, Z. Bao, K. Baldwin, A. Dodabalapur, B. Crone, V. R. Raju, V. Kuck, H. Katz, K. Amundson, J. Ewing, P. Drzaic, *Proc. Natl. Acad. Sci.* **2001**, *98*, 4835.

[24] W. Gao, H. Ota, D. Kiriya, K. Takei, A. Javey, *Acc. Chem. Res.* **2019**, *52*, 523.

[25] Y. Ma, Y. Zhang, S. Cai, Z. Han, X. Liu, F. Wang, Y. Cao, Z. Wang, H. Li, Y. Chen, X. Feng, *Adv. Mater.* **2019**, *0*, 1902062.

[26] A. Zhang, C. M. Lieber, *Chem. Rev.* **2015**, *116*, 215.

[27] W. Gao, S. Emaminejad, H. Y. Y. Nyein, S. Challa, K. Chen, A. Peck, H. M. Fahad, H. Ota, H. Shiraki, D. Kiriya, D.-H. Lien, G. A. Brooks, R. W. Davis, A. Javey, *Nature* **2016**, *529*, 509.

[28] R. Rajkumar, I. Lee, L. Sha, J. Stankovic. *Design Automation Conference*, IEEE, **2010**, 731.

[29] L. Sha, S. Gopalakrishnan, X. Liu, Q. Wang. *2008 IEEE International Conference on Sensor Networks, Ubiquitous, and Trustworthy Computing (sutc 2008)*, IEEE, **2008**, 1.

[30] R. Poovendran, *P. IEEE* **2010**, *98*, 1363.

[31] J. Lee, B. Bagheri, H.-A. Kao, *Manuf. Lett.* **2015**, *3*, 18.

[32] J. Gubbi, R. Buyya, S. Marusic, M. Palaniswami, *Future Gener. Comp. Sy.*

2013, *29*, 1645.

[33] F. Wang, *IEEE Intell. Syst.* **2010**, *25*, 85.

[34] M. Krugh, L. Mears, *Manuf. Lett.* **2018**, *15*, 89.

[35] R. Gravina, C. Ma, P. Pace, G. Aloi, W. Russo, W. Li, G. Fortino, *Future Gener. Comp. Sy.* **2017**, *75*, 158.

[36] P. Kumari, L. Mathew, P. Syal, *Biosens. Bioelectron.* **2017**, *90*, 298.

[37] D.-H. Kim, N. Lu, R. Ma, Y.-S. Kim, R.-H. Kim, S. Wang, J. Wu, S. M. Won, H. Tao, A. Islam, K. J. Yu, T.-i. Kim, R. Chowdhury, M. Ying, L. Xu, M. Li, H.-J. Chung, H. Keum, M. McCormick, P. Liu, Y.-W. Zhang, F. G. Omenetto, Y. Huang, T. Coleman, J. A. Rogers, *Science* **2011**, *333*, 838.

[38] R. Tong, G. Chen, D. Pan, H. Qi, R. a. Li, J. Tian, F. Lu, M. He, *Biomacromolecules* **2019**, *20*, 2096.

[39] Y. Liu, J. Liu, S. Chen, T. Lei, Y. Kim, S. Niu, H. Wang, X. Wang, A. M. Foudeh, J. B. H. Tok, Z. Bao, *Nat. Biomed. Eng.* **2019**, *3*, 58.

[40] Y. Liu, A. F. McGuire, H.-Y. Lou, T. L. Li, J. B.-H. Tok, B. Cui, Z. Bao, *Proc. Natl. Acad. Sci.* **2018**, *115*, 11718.

[41] A. Blau, *Curr. Opin. Colloid Interface Sci.* **2013**, *18*, 481.

[42] D. E. Discher, P. Janmey, Y.-l. Wang, *Science* **2005**, *310*, 1139.

[43] I. R. Minev, P. Musienko, A. Hirsch, Q. Barraud, N. Wenger, E. M. Moraud, J. Gandar, M. Capogrosso, T. Milekovic, L. Asboth, R. F. Torres, N. Vachicouras, Q. Liu, N. Pavlova, S. Duis, A. Larmagnac, J. Vörös, S. Micera, Z. Suo, G. Courtine, S. P. Lacour, *Science* **2015**, *347*, 159.

[44] X. Chen, *Small Methods* **2017**, *1*, 1600029.

[45] D. Qi, Z. Liu, Y. Liu, Y. Jiang, W. R. Leow, M. Pal, S. Pan, H. Yang, Y. Wang, X. Zhang, J. Yu, B. Li, Z. Yu, W. Wang, X. Chen, *Adv. Mater.* **2017**, *29*, 1702800.

[46] S. Budday, R. Nay, R. de Rooij, P. Steinmann, T. Wyrobek, T. C. Ovaert, E. Kuhl, *J. Mech. Behav. Biomed. Mater.* **2015**, *46*, 318.

[47] Y. Liu, M. Pharr, G. A. Salvatore, *ACS Nano* **2017**, *11*, 9614.

[48] H. Yang, D. Qi, Z. Liu, B. K. Chandran, T. Wang, J. Yu, X. Chen, *Adv. Mater.* **2016**, *28*, 9175.

[49] H. Ghapanchizadeh, S. A. Ahmad, A. J. Ishak, M. S. Al-quraishi, *Biomed. Res.* **2017**, *28*.

[50] D. Bruen, C. Delaney, L. Florea, D. Diamond, *Sensors* **2017**, *17*, 1866.

[51] J. A. Rogers, T. Someya, Y. Huang, *Science* **2010**, *327*, 1603.

[52] S. Yao, Y. Zhu, *Adv. Mater.* **2015**, *27*, 1480.

[53] G. Chen, Y. Cui, X. Chen, *Chem. Soc. Rev.* **2019**, *48*, 1434.

[54] J. Wang, M.-F. Lin, S. Park, P. S. Lee, *Mater. Today* **2018**, *21*, 508.

[55] K. Xu, Y. Lu, K. Takei, *Adv. Mater. Technol.* **2019**, *4*, 1800628.

[56] A. M. Kushner, J. D. Vossler, G. A. Williams, Z. Guan, *J. Am. Chem. Soc.* **2009**, *131*, 8766.

[57] Y. Liu, Z. Tang, S. Wu, B. Guo, *ACS Macro Lett.* **2019**, *8*, 193.

[58] T. T. Myllymaki, L. Lemetti, O. Ikkala, *ACS Macro Lett.* **2017**, *6*, 210.

[59] P. B. J. St. Onge, M. U. Ocheje, M. Selivanova, S. Rondeau-Gagné, *Chem.*

Rec. **2019**, *19*, 1008.

[60] K. Zhang, S. Kong, Y. Li, M. Lu, D. Kong, *Lab Chip* **2019**, *19*, 2709.

[61] J. Y. Oh, S. Rondeau-Gagné, Y.-C. Chiu, A. Chortos, F. Lissel, G.-J. N. Wang, B. C. Schroeder, T. Kurosawa, J. Lopez, T. Katsumata, J. Xu, C. Zhu, X. Gu, W.-G. Bae, Y. Kim, L. Jin, J. W. Chung, J. B. H. Tok, Z. Bao, *Nature* **2016**, *539*, 411.

[62] X. Yan, Z. Liu, Q. Zhang, J. Lopez, H. Wang, H.-C. Wu, S. Niu, H. Yan, S. Wang, T. Lei, J. Li, D. Qi, P. Huang, J. Huang, Y. Zhang, Y. Wang, G. Li, J. B. H. Tok, X. Chen, Z. Bao, *J. Am. Chem. Soc.* **2018**, *140*, 5280.

[63] M. D. Dickey, *Adv. Mater.* **2017**, *29*, 1606425.

[64] E. Palleau, S. Reece, S. C. Desai, M. E. Smith, M. D. Dickey, *Adv. Mater.* **2013**, *25*, 1589.

[65] Y. Lu, Q. Hu, Y. Lin, D. B. Pacardo, C. Wang, W. Sun, F. S. Ligler, M. D. Dickey, Z. Gu, *Nat. Commun.* **2015**, *6*, 10066.

[66] M. D. Dickey, *ACS Appl. Mater. Interfaces* **2014**, *6*, 18369.

[67] B. Y. Ahn, E. B. Duoss, M. J. Motala, X. Guo, S.-I. Park, Y. Xiong, J. Yoon, R. G. Nuzzo, J. A. Rogers, J. A. Lewis, *Science* **2009**, *323*, 1590.

[68] F. Xu, Y. Zhu, *Adv. Mater.* **2012**, *24*, 5117.

[69] B. Tian, C. M. Lieber, *Chem. Rev.* **2019**, *119*, 9136.

[70] Y. Wang, J. Wang, S. Cao, D. Kong, *J. Mater. Chem. C* **2019**, *7*, 9748.

[71] K. S. Kim, Y. Zhao, H. Jang, S. Y. Lee, J. M. Kim, K. S. Kim, J.-H. Ahn, P. Kim, J.-Y. Choi, B. H. Hong, *Nature* **2009**, *457*, 706.

[72] N. Liu, A. Chortos, T. Lei, L. Jin, T. R. Kim, W.-G. Bae, C. Zhu, S. Wang, R. Pfattner, X. Chen, R. Sinclair, Z. Bao, *Sci. Adv.* **2017**, *3*, e1700159.

[73] J. Liang, L. Li, K. Tong, Z. Ren, W. Hu, X. Niu, Y. Chen, Q. Pei, *ACS Nano* **2014**, *8*, 1590.

[74] K.-Y. Chun, Y. Oh, J. Rho, J.-H. Ahn, Y.-J. Kim, H. R. Choi, S. Baik, *Nat. Nanotechnol.* **2010**, *5*, 853.

[75] N. Matsuhisa, D. Inoue, P. Zalar, H. Jin, Y. Matsuba, A. Itoh, T. Yokota, D. Hashizume, T. Someya, *Nat. Mater.* **2017**, *16*, 834.

[76] L. Xiao, Z. Chen, C. Feng, L. Liu, Z.-Q. Bai, Y. Wang, L. Qian, Y. Zhang, Q. Li, K. Jiang, *Nano Lett.* **2008**, *8*, 4539.

[77] P. Lee, J. Lee, H. Lee, J. Yeo, S. Hong, K. H. Nam, D. Lee, S. S. Lee, S. H. Ko, *Adv. Mater.* **2012**, *24*, 3326.

[78] J. Ge, H.-B. Yao, X. Wang, Y.-D. Ye, J.-L. Wang, Z.-Y. Wu, J.-W. Liu, F.-J. Fan, H.-L. Gao, C.-L. Zhang, S.-H. Yu, *Angew. Chem. Int. Ed.* **2013**, *125*, 1698.

[79] S. Han, S. Hong, J. Ham, J. Yeo, J. Lee, B. Kang, P. Lee, J. Kwon, S. S. Lee, M.-Y. Yang, S. H. Ko, *Adv. Mater.* **2014**, *26*, 5808.

[80] S. Inal, J. Rivnay, A.-O. Suiu, G. G. Malliaras, I. McCulloch, *Acc. Chem. Res.* **2018**, *51*, 1368.

[81] D. Qi, Z. Liu, M. Yu, Y. Liu, Y. Tang, J. Lv, Y. Li, J. Wei, B. Liedberg, Z. Yu, X. Chen, *Adv. Mater.* **2015**, *27*, 3145.

[82] D.-Y. Khang, H. Jiang, Y. Huang, J. A. Rogers, *Science* **2006**, *311*, 208.

[83] L. Wang, N. Lu, *J. Appl. Mech.* **2016**, *83*.

[84] M. S. White, M. Kaltenbrunner, E. D. Głowacki, K. Gutnichenko, G. Kettlgruber, I. Graz, S. Aazou, C. Ulbricht, D. A. M. Egbe, M. C. Miron, Z. Major, M. C. Scharber, T. Sekitani, T. Someya, S. Bauer, N. S. Sariciftci, *Nat. Photonics* **2013**, *7*, 811.

[85] M. Kaltenbrunner, M. S. White, E. D. Głowacki, T. Sekitani, T. Someya, N. S. Sariciftci, S. Bauer, *Nat. Commun.* **2012**, *3*, 770.

[86] T. Li, Z. Huang, Z. Suo, S. P. Lacour, S. Wagner, *Appl. Phys. Lett.* **2004**, *85*, 3435.

[87] S. P. Lacour, J. Jones, Z. Suo, S. Wagner, *IEEE Electron Device Lett.* **2004**, *25*, 179.

[88] C. Wang, C. Wang, Z. Huang, S. Xu, *Adv. Mater.* **2018**, *30*, 1801368.

[89] Y. Sun, W. M. Choi, H. Jiang, Y. Y. Huang, J. A. Rogers, *Nat. Nanotechnol.* **2006**, *1*, 201.

[90] S. P. Lacour, S. Wagner, Z. Huang, Z. Suo, *Appl. Phys. Lett.* **2003**, *82*, 2404.

[91] Z. Lv, W. Li, L. Yang, X. J. Loh, X. Chen, *ACS Energy Lett.* **2019**, *4*, 606.

[92] S. P. Lacour, D. Chan, S. Wagner, T. Li, Z. Suo, *Appl. Phys. Lett.* **2006**, *88*, 204103.

[93] Z. Liu, M. Yu, J. Lv, Y. Li, Z. Yu, *ACS Appl. Mater. Interfaces* **2014**, *6*, 13487.

[94] C. F. Guo, T. Sun, Q. Liu, Z. Suo, Z. Ren, *Nat. Commun.* **2014**, *5*, 3121.

[95] A. Miyamoto, S. Lee, N. F. Cooray, S. Lee, M. Mori, N. Matsuhisa, H. Jin, L. Yoda, T. Yokota, A. Itoh, M. Sekino, H. Kawasaki, T. Ebihara, M. Amagai, T.

Someya, *Nat. Nanotechnol.* **2017**, *12*, 907.

[96] C. Keplinger, J.-Y. Sun, C. C. Foo, P. Rothemund, G. M. Whitesides, Z. Suo, *Science* **2013**, *341*, 984.

[97] J.-Y. Sun, X. Zhao, W. R. Illeperuma, O. Chaudhuri, K. H. Oh, D. J. Mooney, J. J. Vlassak, Z. Suo, *Nature* **2012**, *489*, 133.

[98] D. J. Lipomi, M. Vosgueritchian, B. C. K. Tee, S. L. Hellstrom, J. A. Lee, C. H. Fox, Z. Bao, *Nat. Nanotechnol.* **2011**, *6*, 788.

[99] B. Zhu, Z. Niu, H. Wang, W. R. Leow, H. Wang, Y. Li, L. Zheng, J. Wei, F. Huo, X. Chen, *Small* **2014**, *10*, 3625.

[100] C.-L. Choong, M.-B. Shim, B.-S. Lee, S. Jeon, D.-S. Ko, T.-H. Kang, J. Bae, S. H. Lee, K.-E. Byun, J. Im, Y. J. Jeong, C. E. Park, J.-J. Park, U.-I. Chung, *Adv. Mater.* **2014**, *26*, 3451.

[101] B. C. K. Tee, A. Chortos, R. R. Dunn, G. Schwartz, E. Eason, Z. Bao, *Adv. Funct. Mater.* **2014**, *24*, 5427.

[102] T. Q. Trung, N. E. Lee, *Adv. Mater.* **2016**, *28*, 4338.

[103] C. Wang, D. Hwang, Z. Yu, K. Takei, J. Park, T. Chen, B. Ma, A. Javey, *Nat. Mater.* **2013**, *12*, 899.

[104] Z. Liu, D. Qi, P. Guo, Y. Liu, B. Zhu, H. Yang, Y. Liu, B. Li, C. Zhang, J. Yu, *Adv. Mater.* **2015**, *27*, 6230.

[105] Y. Jiang, Z. Liu, C. Wang, X. Chen, *Acc. Chem. Res.* **2018**, *52*, 82.

[106] S. Pan, Z. Liu, M. Wang, Y. Jiang, Y. Luo, C. Wan, D. Qi, C. Wang, X. Ge, X. Chen, *Adv. Mater.* **2019**, *0*, 1903130.

[107] Z. Liu, D. Qi, G. Hu, H. Wang, Y. Jiang, G. Chen, Y. Luo, X. J. Loh, B. Liedberg, X. Chen, *Adv. Mater.* **2018**, *30*, 1704229.

[108] Y. Jiang, Z. Liu, N. Matsuhisa, D. Qi, W. R. Leow, H. Yang, J. Yu, G. Chen, Y. Liu, C. Wan, Z. Liu, X. Chen, *Adv. Mater.* **2018**, *30*, 1706589.

[109] Z. Liu, D. Qi, W. R. Leow, J. Yu, M. Xiloyannnis, L. Cappello, Y. Liu, B. Zhu, Y. Jiang, G. Chen, L. Masia, B. Liedberg, X. Chen, *Adv. Mater.* **2018**, *30*, 1707285.

[110] T. Yamada, Y. Hayamizu, Y. Yamamoto, Y. Yomogida, A. Izadi-Najafabadi, D. N. Futaba, K. Hata, *Nat. Nanotechnol.* **2011**, *6*, 296.

[111] C. Pang, J. H. Koo, A. Nguyen, J. M. Caves, M. G. Kim, A. Chortos, K. Kim, P. J. Wang, J. B. H. Tok, Z. Bao, *Adv. Mater.* **2015**, *27*, 634.

[112] D. M. Drotlef, M. Amjadi, M. Yunusa, M. Sitti, *Adv. Mater.* **2017**, *29*, 1701353.

[113] N. Matsuhisa, M. Kaltenbrunner, T. Yokota, H. Jinno, K. Kuribara, T. Sekitani, T. Someya, *Nat. Commun.* **2015**, *6*, 7461.

[114] Z. Liu, X. Wang, D. Qi, C. Xu, J. Yu, Y. Liu, Y. Jiang, B. Liedberg, X. Chen, *Adv. Mater.* **2017**, *29*, 1603382.

[115] C. Wang, X. Li, H. Hu, L. Zhang, Z. Huang, M. Lin, Z. Zhang, Z. Yin, B. Huang, H. Gong, S. Bhaskaran, Y. Gu, M. Makihata, Y. Guo, Y. Lei, Y. Chen, C. Wang, Y. Li, T. Zhang, Z. Chen, A. P. Pisano, L. Zhang, Q. Zhou, S. Xu, *Nat. Biomed. Eng.* **2018**, *2*, 687.

[116] D. Son, J. Lee, S. Qiao, R. Ghaffari, J. Kim, J. E. Lee, C. Song, S. J. Kim, D. J.

Lee, S. W. Jun, S. Yang, M. Park, J. Shin, K. Do, M. Lee, K. Kang, C. S. Hwang, N. Lu, T. Hyeon, D.-H. Kim, *Nat. Nanotechnol.* **2014**, *9*, 397.

[117] S. Yao, Y. Zhu, *JOM* **2016**, *68*, 1145.

[118] P. Campisi, D. La Rocca, G. Scarano, *Computer* **2012**, *45*, 87.

[119] P. Rai, S. Oh, P. Shyamkumar, M. Ramasamy, R. E. Harbaugh, V. K. Varadan, *J. Electrochem. Soc.* **2014**, *161*, B3116.

[120] S. P. Lacour, G. Courtine, J. Guck, *Nat. Rev. Mater.* **2016**, *1*, 16063.

[121] R. Chen, A. Canales, P. Anikeeva, *Nat. Rev. Mater.* **2017**, *2*, 16093.

[122] Q. Li, K. Nan, P. Le Floch, Z. Lin, H. Sheng, T. S. Blum, J. Liu, *Nano Lett.* **2019**, *19*, 5781.

[123] W. Lee, D. Kim, N. Matsuhisa, M. Nagase, M. Sekino, G. G. Malliaras, T. Yokota, T. Someya, *Proc. Natl. Acad. Sci.* **2017**, *114*, 10554.

[124] D. Khodagholy, T. Doublet, P. Quilichini, M. Gurfinkel, P. Leleux, A. Ghestem, E. Ismailova, T. Hervé, S. Sanaur, C. Bernard, G. G. Malliaras, *Nat. Commun.* **2013**, *4*, 1575.

[125] L. M. Ferrari, S. Sudha, S. Tarantino, R. Esposti, F. Bolzoni, P. Cavallari, C. Cipriani, V. Mattoli, F. Greco, *Adv. Sci.* **2018**, *5*, 1700771.

[126] G. Hong, T.-M. Fu, M. Qiao, R. D. Viveros, X. Yang, T. Zhou, J. M. Lee, H.-G. Park, J. R. Sanes, C. M. Lieber, *Science* **2018**, *360*, 1447.

[127] G. Schiavone, S. P. Lacour, *Sci. Transl. Med.* **2019**, *11*, eaaw5858.

[128] H. Acarón Ledesma, X. Li, J. L. Carvalho-de-Souza, W. Wei, F. Bezanilla, B. Tian, *Nat. Nanotechnol.* **2019**, *14*, 645.

[129] Y. Fang, B. Tian, *Nat. Nanotechnol.* **2019**, *14*, 733.

[130] X. Yang, T. Zhou, T. J. Zwang, G. Hong, Y. Zhao, R. D. Viveros, T.-M. Fu, T. Gao, C. M. Lieber, *Nat. Mater.* **2019**, *18*, 510.

[131] Y. Fang, Y. Jiang, H. Acaron Ledesma, J. Yi, X. Gao, D. E. Weiss, F. Shi, B. Tian, *Nano Lett.* **2018**, *18*, 4487.

[132] J. J. S. Norton, D. S. Lee, J. W. Lee, W. Lee, O. Kwon, P. Won, S.-Y. Jung, H. Cheng, J.-W. Jeong, A. Akce, S. Umunna, I. Na, Y. H. Kwon, X.-Q. Wang, Z. Liu, U. Paik, Y. Huang, T. Bretl, W.-H. Yeo, J. A. Rogers, *Proc. Natl. Acad. Sci.* **2015**, *112*, 3920.

[133] R. C. Webb, A. P. Bonifas, A. Behnaz, Y. Zhang, K. J. Yu, H. Cheng, M. Shi, Z. Bian, Z. Liu, Y.-S. Kim, W.-H. Yeo, J. S. Park, J. Song, Y. Li, Y. Huang, A. M. Gorbach, J. A. Rogers, *Nat. Mater.* **2013**, *12*, 938.

[134] T. Ha, J. Tran, S. Liu, H. Jang, H. Jeong, R. Mitbander, H. Huh, Y. Qiu, J. Duong, R. L. Wang, P. Wang, A. Tandon, J. Sirohi, N. Lu, *Adv. Sci.* **2019**, *6*, 1900290.

[135] Y. Wang, Y. Qiu, S. K. Ameri, H. Jang, Z. Dai, Y. Huang, N. Lu, *NPJ Flexible Electronics* **2018**, *2*, 6.

[136] C. J. Bettinger, Z. Bao, *Adv. Mater.* **2010**, *22*, 651.

[137] M. Nogi, H. Yano, *Adv. Mater.* **2008**, *20*, 1849.

[138] M. C. Barr, J. A. Rowehl, R. R. Lunt, J. Xu, A. Wang, C. M. Boyce, S. G. Im, V. Bulović, K. K. Gleason, *Adv. Mater.* **2011**, *23*, 3500.

[139] B. Zhu, H. Wang, W. R. Leow, Y. Cai, X. J. Loh, M. Y. Han, X. Chen, *Adv.*

Mater. **2016**, *28*, 4250.

[140] H. Wang, B. Zhu, H. Wang, X. Ma, Y. Hao, X. Chen, *Small* **2016**, *12*, 3360.

[141] D.-H. Kim, J. Viventi, J. J. Amsden, J. Xiao, L. Vigeland, Y.-S. Kim, J. A. Blanco, B. Panilaitis, E. S. Frechette, D. Contreras, D. L. Kaplan, F. G. Omenetto, Y. Huang, K.-C. Hwang, M. R. Zakin, B. Litt, J. A. Rogers, *Nat. Mater.* **2010**, *9*, 511.

[142] H. Yuk, B. Lu, X. Zhao, *Chem. Soc. Rev.* **2019**, *48*, 1642.

[143] E. S. Kappenman, S. J. Luck, *Psychophysiology* **2010**, *47*, 888.

[144] S. J. Kim, K. W. Cho, H. R. Cho, L. Wang, S. Y. Park, S. E. Lee, T. Hyeon, N. Lu, S. H. Choi, D.-H. Kim, *Adv. Funct. Mater.* **2016**, *26*, 3207.

[145] E. Huigen, A. Peper, C. Grimbergen, *Med. Biol. Eng. Comput.* **2002**, *40*, 332.

[146] C. Gondran, E. Siebert, S. Yacoub, E. Novakov, *Med. Biol. Eng. Comput.* **1996**, *34*, 460.

[147] Z. C. Lin, C. Xie, Y. Osakada, Y. Cui, B. Cui, *Nat. Commun.* **2014**, *5*, 3206.

[148] R. Feiner, T. Dvir, *Nat. Rev. Mater.* **2017**, *3*, 17076.

[149] M. Nishizawa, *Bull. Chem. Soc. Jpn.* **2018**, *91*, 1141.

[150] C.-H. Chen, C.-T. Lin, W.-L. Hsu, Y.-C. Chang, S.-R. Yeh, L.-J. Li, D.-J. Yao, *Nanomedicine: NBM* **2013**, *9*, 600.

[151] V. Castagnola, E. Descamps, A. Lecestre, L. Dahan, J. Remaud, L. G. Nowak, C. Bergaud, *Biosens. Bioelectron.* **2015**, *67*, 450.

[152] E. Seker, Y. Berdichevsky, M. R. Begley, M. L. Reed, K. J. Staley, M. L. Yarmush, *Nanotechnology* **2010**, *21*, 125504.

[153] J. Abbott, T. Ye, L. Qin, M. Jorgolli, R. S. Gertner, D. Ham, H. Park, *Nat. Nanotechnol.* **2017**, *12*, 460.

[154] E. W. Keefer, B. R. Botterman, M. I. Romero, A. F. Rossi, G. W. Gross, *Nat. Nanotechnol.* **2008**, *3*, 434.

[155] P. M. C. Inácio, A. L. G. Mestre, M. d. C. R. d. Medeiros, S. Asgarifar, Y. Elamine, J. Canudo, J. M. A. Santos, J. Bragança, J. Morgado, F. Biscarini, H. L. Gomes, *IEEE Sens. J.* **2017**, *17*, 3961.

[156] E. Bihar, T. Roberts, E. Ismailova, M. Saadaoui, M. Isik, A. Sanchez-Sanchez, D. Mecerreyes, T. Hervé, J. B. De Graaf, G. G. Malliaras, *Adv. Mater. Technol.* **2017**, *2*, 1600251.

[157] K. Woeppel, Q. Yang, X. T. Cui, *Current Opin. Biomed. Eng,* **2017**, *4*, 21.

[158] C. Yang, Z. Suo, *Nat. Rev. Mater.* **2018**, *3*, 125.

[159] C. Wan, K. Xiao, A. Angelin, M. Antonietti, X. Chen, *Advanced Intelligent Systems*, *0*, 1900073.

[160] A. Guiseppi-Elie, *Biomaterials* **2010**, *31*, 2701.

[161] S. Sekine, Y. Ido, T. Miyake, K. Nagamine, M. Nishizawa, *J. Am. Chem. Soc.* **2010**, *132*, 13174.

[162] V. R. Feig, H. Tran, M. Lee, Z. Bao, *Nat. Commun.* **2018**, *9*, 2740.

[163] J. Macron, A. P. Gerratt, S. P. Lacour, *Adv. Mater. Technol.* **2019**, *4*, 1900331.

[164] Y. Yang, W. Gao, *Chem. Soc. Rev.* **2019**, *48*, 1465.

[165] T. Wang, Y. Guo, P. Wan, H. Zhang, X. Chen, X. Sun, *Small* **2016**, *12*, 3748.

[166] T. Wang, Y. Guo, P. Wan, X. Sun, H. Zhang, Z. Yu, X. Chen, *Nanoscale* **2017**,

9, 869.

[167] M. Bariya, H. Y. Y. Nyein, A. Javey, *Nat. Electron.* **2018**, *1*, 160.

[168] S.-J. Kim, S.-J. Choi, J.-S. Jang, H.-J. Cho, I.-D. Kim, *Acc. Chem. Res.* **2017**, *50*, 1587.

[169] T. Wang, H. Yang, D. Qi, Z. Liu, P. Cai, H. Zhang, X. Chen, *Small* **2018**, *14*, 1702933.

[170] T. Wang, D. Qi, H. Yang, Z. Liu, M. Wang, W. R. Leow, G. Chen, J. Yu, K. He, H. Cheng, Y.-L. Wu, H. Zhang, X. Chen, *Adv. Mater.* **2019**, *31*, 1803883.

[171] T. Wang, Y. Fu, L. Chai, L. Chao, L. Bu, Y. Meng, C. Chen, M. Ma, Q. Xie, S. Yao, *Chem.-Eur. J.* **2014**, *20*, 2623.

[172] T. Wang, Y. Fu, L. Bu, C. Qin, Y. Meng, C. Chen, M. Ma, Q. Xie, S. Yao, *J. Phys. Chem. C* **2012**, *116*, 20908.

[173] M. Schenone, V. Dančík, B. K. Wagner, P. A. Clemons, *Nat. Chem. Biol.* **2013**, *9*, 232.

[174] K. Hooton, L. Li, *Anal. Chem.* **2017**, *89*, 7847.

[175] H. Y. Y. Nyein, W. Gao, Z. Shahpar, S. Emaminejad, S. Challa, K. Chen, H. M. Fahad, L.-C. Tai, H. Ota, R. W. Davis, A. Javey, *ACS Nano* **2016**, *10*, 7216.

[176] W. Gao, H. Y. Y. Nyein, Z. Shahpar, H. M. Fahad, K. Chen, S. Emaminejad, Y. Gao, L.-C. Tai, H. Ota, E. Wu, J. Bullock, Y. Zeng, D.-H. Lien, A. Javey, *ACS Sensors* **2016**, *1*, 866.

[177] G. Cizza, A. H. Marques, F. Eskandari, I. C. Christie, S. Torvik, M. N. Silverman, T. M. Phillips, E. M. Sternberg, P. S. Group, *Biol. Psychiatry* **2008**,

64, 907.

[178] M. M. Raiszadeh, M. M. Ross, P. S. Russo, M. A. Schaepper, W. Zhou, J. Deng, D. Ng, A. Dickson, C. Dickson, M. Strom, C. Osorio, T. Soeprono, J. D. Wulfkuhle, E. F. Petricoin, L. A. Liotta, W. M. Kirsch, *J. Proteome Res.* **2012**, *11*, 2127.

[179] A. Zhavoronkov, *Mol. Pharmaceut.* **2018**, *15*, 4311.

[180] D. Wing, M. R. Prausnitz, M. J. Buono, *Clin. Physiol. Funct. Imaging* **2013**, *33*, 436.

[181] G. Mastella, G. Di Cesare, A. Borruso, L. Menin, L. Zanolla, *Acta Paediatr.* **2000**, *89*, 933.

[182] A. V.-v. Langen, E. Dompeling, J.-B. Yntema, B. Arets, H. Tiddens, G. Loeber, J. Dankert-Roelse, *Eur. J. Pediatr.* **2015**, *174*, 1025.

[183] A. Mena-Bravo, M. D. Luque de Castro, *J. Pharm. Biomed. Anal.* **2014**, *90*, 139.

[184] J. Choi, R. Ghaffari, L. B. Baker, J. A. Rogers, *Sci. Adv.* **2018**, *4*, eaar3921.

[185] T. R. Ray, J. Choi, A. J. Bandodkar, S. Krishnan, P. Gutruf, L. Tian, R. Ghaffari, J. A. Rogers, *Chem. Rev.* **2019**, *119*, 5461.

[186] A. J. Bandodkar, W. J. Jeang, R. Ghaffari, J. A. Rogers, *Annu. Rev. Anal. Chem.* **2019**, *12*, 1.

[187] J. Choi, D. Kang, S. Han, S. B. Kim, J. A. Rogers, *Adv. Healthc. Mater.* **2017**, *6*, 1601355.

[188] A. Koh, D. Kang, Y. Xue, S. Lee, R. M. Pielak, J. Kim, T. Hwang, S. Min, A.

Banks, P. Bastien, M. C. Manco, L. Wang, K. R. Ammann, K.-I. Jang, P. Won, S. Han, R. Ghaffari, U. Paik, M. J. Slepian, G. Balooch, Y. Huang, J. A. Rogers, *Sci. Transl. Med.* **2016**, *8*, 366ra165.

[189] S. Emaminejad, W. Gao, E. Wu, Z. A. Davies, H. Yin Yin Nyein, S. Challa, S. P. Ryan, H. M. Fahad, K. Chen, Z. Shahpar, S. Talebi, C. Milla, A. Javey, R. W. Davis, *Proc. Natl. Acad. Sci.* **2017**, *114*, 4625.

[190] Y. Chen, S. Lu, S. Zhang, Y. Li, Z. Qu, Y. Chen, B. Lu, X. Wang, X. Feng, *Sci. Adv.* **2017**, *3*, e1701629.

[191] A. J. Bandodkar, W. Jia, C. Yardımcı, X. Wang, J. Ramirez, J. Wang, *Anal. Chem.* **2014**, *87*, 394.

[192] W. Gao, H. Y. Nyein, Z. Shahpar, L.-C. Tai, E. Wu, M. Bariya, H. Ota, H. M. Fahad, K. Chen, A. Javey. *2016 IEEE International Electron Devices Meeting (IEDM)*, IEEE, **2016**, 6.6. 1.

[193] A. J. Bandodkar, W. Jia, J. Wang, *Electroanal.* **2015**, *27*, 562.

[194] J. Park, J. Kim, S.-Y. Kim, W. H. Cheong, J. Jang, Y.-G. Park, K. Na, Y.-T. Kim, J. H. Heo, C. Y. Lee, J. H. Lee, F. Bien, J.-U. Park, *Sci. Adv.* **2018**, *4*, eaap9841.

[195] M. S. Mannoor, H. Tao, J. D. Clayton, A. Sengupta, D. L. Kaplan, R. R. Naik, N. Verma, F. G. Omenetto, M. C. McAlpine, *Nat. Commun.* **2012**, *3*, 763.

[196] H. Lee, T. K. Choi, Y. B. Lee, H. R. Cho, R. Ghaffari, L. Wang, H. J. Choi, T. D. Chung, N. Lu, T. Hyeon, S. H. Choi, D.-H. Kim, *Nat. Nanotechnol.* **2016**, *11*, 566.

[197] J. Kim, A. S. Campbell, B. E.-F. de Ávila, J. Wang, *Nat. Biotechnol.* **2019**, 1.

[198] Q. Zhai, S. Gong, Y. Wang, Q. Lyu, Y. Liu, Y. Ling, J. Wang, G. P. Simon, W. Cheng, *ACS Appl. Mater. Interfaces* **2019**, *11*, 9724.

[199] H. Lee, C. Song, Y. S. Hong, M. S. Kim, H. R. Cho, T. Kang, K. Shin, S. H. Choi, T. Hyeon, D.-H. Kim, *Sci. Adv.* **2017**, *3*, e1601314.

[200] A. J. Bandodkar, I. Jeerapan, J.-M. You, R. Nuñez-Flores, J. Wang, *Nano Lett.* **2016**, *16*, 721.

[201] A. J. Bandodkar, R. Nuñez-Flores, W. Jia, J. Wang, *Adv. Mater.* **2015**, *27*, 3060.

[202] A. Abellán-Llobregat, I. Jeerapan, A. Bandodkar, L. Vidal, A. Canals, J. Wang, E. Morallón, *Biosens. Bioelectron.* **2017**, *91*, 885.

[203] B. Ciui, A. Martin, R. K. Mishra, T. Nakagawa, T. J. Dawkins, M. Lyu, C. Cristea, R. Sandulescu, J. Wang, *ACS Sensors* **2018**, *3*, 2375.

[204] D.-H. Choi, J. S. Kim, G. R. Cutting, P. C. Searson, *Anal. Chem.* **2016**, *88*, 12241.

[205] S. Y. Oh, S. Y. Hong, Y. R. Jeong, J. Yun, H. Park, S. W. Jin, G. Lee, J. H. Oh, H. Lee, S.-S. Lee, J. S. Ha, *ACS Appl. Mater. Interfaces* **2018**, *10*, 13729.

[206] A. M. Pappa, D. Ohayon, A. Giovannitti, I. P. Maria, A. Savva, I. Uguz, J. Rivnay, I. McCulloch, R. M. Owens, S. Inal, *Sci. Adv.* **2018**, *4*, eaat0911.

[207] T. Someya, T. Sekitani, S. Iba, Y. Kato, H. Kawaguchi, T. Sakurai, *Proc. Natl. Acad. Sci.* **2004**, *101*, 9966.

[208] M. Wang, W. Wang, W. R. Leow, C. Wan, G. Chen, Y. Zeng, J. Yu, Y. Liu, P.

Cai, H. Wang, D. Ielmini, X. Chen, *Adv. Mater.* **2018**, *30*, 1802516.

[209] B. Comiskey, J. D. Albert, H. Yoshizawa, J. Jacobson, *Nature* **1998**, *394*, 253.

[210] A. Sobel, *Nat. Mater.* **2003**, *2*, 643.

[211] K. Zhang, S. Long, Q. Liu, H. Lü, Y. Li, Y. Wang, W. Lian, M. Wang, S. Zhang, M. Liu, *Sci. China Technol. Sc.* **2011**, *54*, 811.

[212] K. Takei, T. Takahashi, J. C. Ho, H. Ko, A. G. Gillies, P. W. Leu, R. S. Fearing, A. Javey, *Nat. Mater.* **2010**, *9*, 821.

[213] G. H. Gelinck, H. E. A. Huitema, E. van Veenendaal, E. Cantatore, L. Schrijnemakers, J. B. P. H. van der Putten, T. C. T. Geuns, M. Beenhakkers, J. B. Giesbers, B.-H. Huisman, E. J. Meijer, E. M. Benito, F. J. Touwslager, A. W. Marsman, B. J. E. van Rens, D. M. de Leeuw, *Nat. Mater.* **2004**, *3*, 106.

[214] C. Yeom, K. Chen, D. Kiriya, Z. Yu, G. Cho, A. Javey, *Adv. Mater.* **2015**, *27*, 1561.

[215] T. Sekitani, T. Yokota, U. Zschieschang, H. Klauk, S. Bauer, K. Takeuchi, M. Takamiya, T. Sakurai, T. Someya, *Science* **2009**, *326*, 1516.

[216] T. Sekitani, T. Yokota, K. Kuribara, M. Kaltenbrunner, T. Fukushima, Y. Inoue, M. Sekino, T. Isoyama, Y. Abe, H. Onodera, T. Someya, *Nat. Commun.* **2016**, *7*, 11425.

[217] T. Sekitani, U. Zschieschang, H. Klauk, T. Someya, *Nat. Mater.* **2010**, *9*, 1015.

[218] T. Someya, Y. Kato, T. Sekitani, S. Iba, Y. Noguchi, Y. Murase, H. Kawaguchi, T. Sakurai, *Proc. Natl. Acad. Sci.* **2005**, *102*, 12321.

[219] I. Graz, M. Krause, S. Bauer-Gogonea, S. Bauer, S. P. Lacour, B. Ploss, M.

Zirkl, B. Stadlober, S. Wagner, *J. Appl. Phys.* **2009**, *106*, 034503.

[220] N. Matsuhisa, H. Sakamoto, T. Yokota, P. Zalar, A. Reuveny, S. Lee, T. Someya, *Adv. Electron. Mater.* **2016**, *2*, 1600259.

[221] J.-J. Huang, T.-H. Hou, C.-W. Hsu, Y.-M. Tseng, W.-H. Chang, W.-Y. Jang, C.-H. Lin, *Jpn. J. Appl. Phys.* **2012**, *51*, 04DD09.

[222] J. Zhang, Y. Li, B. Zhang, H. Wang, Q. Xin, A. Song, *Nat. Commun.* **2015**, *6*, 7561.

[223] X. Zhang, J. Zhai, X. Yu, L. Ding, W. Zhang, *Thin Solid Films* **2013**, *548*, 623.

[224] D. H. Lee, K. Nomura, T. Kamiya, H. Hosono, *IEEE Electron Device Lett.* **2011**, *32*, 1695.

[225] Y. Ji, D. F. Zeigler, D. S. Lee, H. Choi, A. K.-Y. Jen, H. C. Ko, T.-W. Kim, *Nat. Commun.* **2013**, *4*, 2707.

[226] C.-Y. Lin, C.-H. Tsai, H.-T. Lin, L.-C. Chang, Y.-H. Yeh, Z. Pei, Y.-R. Peng, C.-C. Wu, *Org. Electron.* **2011**, *12*, 1777.

[227] S. Kim, J. H. Son, S. H. Lee, B. K. You, K. I. Park, H. K. Lee, M. Byun, K. J. Lee, *Adv. Mater.* **2014**, *26*, 7480.

[228] M. Wang, J. Zhou, Y. Yang, S. Gaba, M. Liu, W. D. Lu, *Nanoscale* **2015**, *7*, 4964.

[229] B. J. Choi, J. Zhang, K. Norris, G. Gibson, K. M. Kim, W. Jackson, M. X. M. Zhang, Z. Li, J. J. Yang, R. S. Williams, *Adv. Mater.* **2016**, *28*, 356.

[230] Y. Park, U. B. Han, M. K. Kim, J. S. Lee, *Adv. Electron. Mater.* **2018**, *4*, 1700521.

[231] M. Kaltenbrunner, T. Sekitani, J. Reeder, T. Yokota, K. Kuribara, T. Tokuhara, M. Drack, R. Schwödiauer, I. Graz, S. Bauer-Gogonea, S. Bauer, T. Someya, *Nature* **2013**, *499*, 458.

[232] R. H. Reuss, G. B. Raupp, B. E. Gnade, *P. IEEE* **2015**, *103*, 491.

[233] B. Crone, A. Dodabalapur, Y.-Y. Lin, R. Filas, Z. Bao, A. LaDuca, R. Sarpeshkar, H. Katz, W. Li, *Nature* **2000**, *403*, 521.

[234] C. D. Dimitrakopoulos, D. J. Mascaro, *IBM J. RES. DEV.* **2001**, *45*, 11.

[235] K. Torikai, R. Furlan de Oliveira, D. H. Starnini de Camargo, C. C. Bof Bufon, *Nano Lett.* **2018**, *18*, 5552.

[236] J. Kwon, S. Kyung, S. Yoon, J. J. Kim, S. Jung, *Adv. Sci.* **2016**, *3*, 1500439.

[237] H. Klauk, M. Halik, U. Zschieschang, F. Eder, G. Schmid, C. Dehm, *Appl. Phys. Lett.* **2003**, *82*, 4175.

[238] S. K. Park, J. E. Anthony, T. N. Jackson, *IEEE Electron Device Lett.* **2007**, *28*, 877.

[239] H. Klauk, U. Zschieschang, J. Pflaum, M. Halik, *Nature* **2007**, *445*, 745.

[240] O. A. Melville, B. H. Lessard, T. P. Bender, *ACS Appl. Mater. Interfaces* **2015**, *7*, 13105.

[241] B. Crone, A. Dodabalapur, R. Sarpeshkar, A. Gelperin, H. Katz, Z. Bao, *J. Appl. Phys.* **2002**, *91*, 10140.

[242] K. Eguchi, M. M. Matsushita, K. Awaga, *J. Phys. Chem. C* **2018**, *122*, 26054.

[243] K. Kobashi, R. Hayakawa, T. Chikyow, Y. Wakayama, *Nano Lett.* **2018**, *18*, 4355.

[244] J. G. Laquindanum, H. E. Katz, A. Dodabalapur, A. J. Lovinger, *J. Am. Chem. Soc.* **1996**, *118*, 11331.

[245] A. Dodabalapur, J. Laquindanum, H. Katz, Z. Bao, *Appl. Phys. Lett.* **1996**, *69*, 4227.

[246] Y. H. Ha, J. G. Oh, S. Park, S.-K. Kwon, T. K. An, J. Jang, Y.-H. Kim, *Org. Electron.* **2018**, *63*, 250.

[247] A. Dodabalapur, H. Katz, L. Torsi, R. Haddon, *Appl. Phys. Lett.* **1996**, *68*, 1108.

[248] M. Irimia-Vladu, P. A. Troshin, M. Reisinger, L. Shmygleva, Y. Kanbur, G. Schwabegger, M. Bodea, R. Schwödiauer, A. Mumyatov, J. W. Fergus, V. F. Razumov, H. Sitter, N. S. Sariciftci, S. Bauer, *Adv. Funct. Mater.* **2010**, *20*, 4069.

[249] M. F. De Volder, S. H. Tawfick, R. H. Baughman, A. J. Hart, *Science* **2013**, *339*, 535.

[250] E. Snow, P. Campbell, M. Ancona, J. Novak, *Appl. Phys. Lett.* **2005**, *86*, 033105.

[251] T. Lei, I. Pochorovski, Z. Bao, *Acc. Chem. Res.* **2017**, *50*, 1096.

[252] S. Wang, J. Xu, W. Wang, G.-J. N. Wang, R. Rastak, F. Molina-Lopez, J. W. Chung, S. Niu, V. R. Feig, J. Lopez, T. Lei, S.-K. Kwon, Y. Kim, A. M. Foudeh, A. Ehrlich, A. Gasperini, Y. Yun, B. Murmann, J. B. H. Tok, Z. Bao, *Nature* **2018**, *555*, 83.

[253] F. Carpi, S. Bauer, D. De Rossi, *Science* **2010**, *330*, 1759.

[254] R. Pelrine, R. Kornbluh, Q. Pei, J. Joseph, *Science* **2000**, *287*, 836.

[255] C. Keplinger, T. Li, R. Baumgartner, Z. Suo, S. Bauer, *Soft Matter* **2012**, *8*, 285.

[256] S. Bauer, S. Bauer-Gogonea, I. Graz, M. Kaltenbrunner, C. Keplinger, R. Schwödiauer, *Adv. Mater.* **2014**, *26*, 149.

[257] R. Cheng, S. Jiang, Y. Chen, Y. Liu, N. Weiss, H.-C. Cheng, H. Wu, Y. Huang, X. Duan, *Nat. Commun.* **2014**, *5*, 5143.

[258] J. Chang, X. Zhang, T. Ge, J. Zhou, *Org. Electron.* **2014**, *15*, 701.

[259] A. C. Hübler, G. C. Schmidt, H. Kempa, K. Reuter, M. Hambsch, M. Bellmann, *Org. Electron.* **2011**, *12*, 419.

[260] M. Allen, C. Lee, B. Ahn, T. Kololuoma, K. Shin, S. Ko, *Microelectron. Eng.* **2011**, *88*, 3293.

[261] T. Yokota, T. Kajitani, R. Shidachi, T. Tokuhara, M. Kaltenbrunner, Y. Shoji, F. Ishiwari, T. Sekitani, T. Fukushima, T. Someya, *Nat. Nanotechnol.* **2018**, *13*, 139.

[262] T. Sekitani, M. Takamiya, Y. Noguchi, S. Nakano, Y. Kato, T. Sakurai, T. Someya, *Nat. Mater.* **2007**, *6*, 413.

[263] R. A. Street, T. Ng, D. E. Schwartz, G. L. Whiting, J. Lu, R. Bringans, J. Veres, *P. IEEE* **2015**, *103*, 607.

[264] M. Jung, J. Kim, J. Noh, N. Lim, C. Lim, G. Lee, J. Kim, H. Kang, K. Jung, A. D. Leonard, *IEEE T. Electron Dev.* **2010**, *57*, 571.

[265] H. Kang, H. Park, Y. Park, M. Jung, B. C. Kim, G. Wallace, G. Cho, *Sci. Rep.*

2014, *4*, 5387.

[266] K. Myny, S. Smout, M. Rockelé, A. Bhoolokam, T. H. Ke, S. Steudel, B. Cobb, A. Gulati, F. G. Rodriguez, K. Obata, M. Marinkovic, D.-V. Pham, A. Hoppe, G. H. Gelinck, J. Genoe, W. Dehaene, P. Heremans, *Sci. Rep.* **2014**, *4*, 7398.

[267] C. Zhu, A. Chortos, Y. Wang, R. Pfattner, T. Lei, A. C. Hinckley, I. Pochorovski, X. Yan, J. W. F. To, J. Y. Oh, J. B. H. Tok, Z. Bao, B. Murmann, *Nat. Electron.* **2018**, *1*, 183.

[268] G. Tong, Z. Jia, J. Chang. *2018 IEEE International Symposium on Circuits and Systems (ISCAS)*, IEEE, **2018**, 1.

[269] S. Nakata, M. Shiomi, Y. Fujita, T. Arie, S. Akita, K. Takei, *Nat. Electron.* **2018**, *1*, 596.

[270] S. Imani, A. J. Bandodkar, A. M. V. Mohan, R. Kumar, S. Yu, J. Wang, P. P. Mercier, *Nat. Commun.* **2016**, *7*, 11650.

[271] K. Chen, W. Gao, S. Emaminejad, D. Kiriya, H. Ota, H. Y. Y. Nyein, K. Takei, A. Javey, *Adv. Mater.* **2016**, *28*, 4397.

[272] Y. Khan, M. Garg, Q. Gui, M. Schadt, A. Gaikwad, D. Han, N. A. D. Yamamoto, P. Hart, R. Welte, W. Wilson, S. Czarnecki, M. Poliks, Z. Jin, K. Ghose, F. Egitto, J. Turner, A. C. Arias, *Adv. Funct. Mater.* **2016**, *26*, 8764.

[273] H. Jiang, D.-Y. Khang, J. Song, Y. Sun, Y. Huang, J. A. Rogers, *Proc. Natl. Acad. Sci.* **2007**, *104*, 15607.

[274] W. M. Choi, J. Song, D.-Y. Khang, H. Jiang, Y. Y. Huang, J. A. Rogers, *Nano Lett.* **2007**, *7*, 1655.

[275] G. Cantarella, C. Vogt, R. Hopf, N. Münzenrieder, P. Andrianakis, L. Petti, A. Daus, S. Knobelspies, L. Büthe, G. Tröster, G. A. Salvatore, *ACS Appl. Mater. Interfaces* **2017**, *9*, 28750.

[276] D.-H. Kim, J. Song, W. M. Choi, H.-S. Kim, R.-H. Kim, Z. Liu, Y. Y. Huang, K.-C. Hwang, Y.-w. Zhang, J. A. Rogers, *Proc. Natl. Acad. Sci.* **2008**, *105*, 18675.

[277] S. Xu, Y. Zhang, L. Jia, K. E. Mathewson, K.-I. Jang, J. Kim, H. Fu, X. Huang, P. Chava, R. Wang, S. Bhole, L. Wang, Y. J. Na, Y. Guan, M. Flavin, Z. Han, Y. Huang, J. A. Rogers, *Science* **2014**, *344*, 70.

[278] K.-I. Jang, K. Li, H. U. Chung, S. Xu, H. N. Jung, Y. Yang, J. W. Kwak, H. H. Jung, J. Song, C. Yang, A. Wang, Z. Liu, J. Y. Lee, B. H. Kim, J.-H. Kim, J. Lee, Y. Yu, B. J. Kim, H. Jang, K. J. Yu, J. Kim, J. W. Lee, J.-W. Jeong, Y. M. Song, Y. Huang, Y. Zhang, J. A. Rogers, *Nat. Commun.* **2017**, *8*, 15894.

[279] H. U. Chung, B. H. Kim, J. Y. Lee, J. Lee, Z. Xie, E. M. Ibler, K. Lee, A. Banks, J. Y. Jeong, J. Kim, C. Ogle, D. Grande, Y. Yu, H. Jang, P. Assem, D. Ryu, J. W. Kwak, M. Namkoong, J. B. Park, Y. Lee, D. H. Kim, A. Ryu, J. Jeong, K. You, B. Ji, Z. Liu, Q. Huo, X. Feng, Y. Deng, Y. Xu, K.-I. Jang, J. Kim, Y. Zhang, R. Ghaffari, C. M. Rand, M. Schau, A. Hamvas, D. E. Weese-Mayer, Y. Huang, S. M. Lee, C. H. Lee, N. R. Shanbhag, A. S. Paller, S. Xu, J. A. Rogers, *Science* **2019**, *363*, eaau0780.

[280] Z. Huang, Y. Hao, Y. Li, H. Hu, C. Wang, A. Nomoto, T. Pan, Y. Gu, Y. Chen, T. Zhang, W. Li, Y. Lei, N. Kim, C. Wang, L. Zhang, J. W. Ward, A. Maralani,

X. Li, M. F. Durstock, A. Pisano, Y. Lin, S. Xu, *Nat. Electron.* **2018**, *1*, 473.

[281] Y. Zhang, Z. Yan, K. Nan, D. Xiao, Y. Liu, H. Luan, H. Fu, X. Wang, Q. Yang, J. Wang, *Proc. Natl. Acad. Sci.* **2015**, *112*, 11757.

[282] M. Humood, Y. Shi, M. Han, J. Lefebvre, Z. Yan, M. Pharr, Y. Zhang, Y. Huang, J. A. Rogers, A. A. Polycarpou, *Small* **2018**, *14*, 1870045.

[283] M. K. Blees, A. W. Barnard, P. A. Rose, S. P. Roberts, K. L. McGill, P. Y. Huang, A. R. Ruyack, J. W. Kevek, B. Kobrin, D. A. Muller, *Nature* **2015**, *524*, 204.

[284] A. Lamoureux, K. Lee, M. Shlian, S. R. Forrest, M. Shtein, *Nat. Commun.* **2015**, *6*, 8092.

[285] S. J. P. Callens, A. A. Zadpoor, *Mater. Today* **2018**, *21*, 241.

[286] M. Hamedi, R. Forchheimer, O. Inganäs, *Nat. Mater.* **2007**, *6*, 357.

[287] M. von Krshiwoblozki, T. Linz, A. Neudeck, C. Kallmayer, *Adv. Sci. Technol.* **2013**, *85*, 1.

[288] P. Shyamkumar, P. Rai, S. Oh, M. Ramasamy, R. Harbaugh, V. Varadan, *Electronics* **2014**, *3*, 504.

[289] J. Chen, Y. Huang, N. Zhang, H. Zou, R. Liu, C. Tao, X. Fan, Z. L. Wang, *Nat. Energy* **2016**, *1*, 16138.

[290] J. N. Burghartz, W. Appel, C. Harendt, H. Rempp, H. Richter, M. Zimmermann, *Solid-State Electron.* **2010**, *54*, 818.

[291] R. Herbert, J.-H. Kim, Y. Kim, H. Lee, W.-H. Yeo, *Materials* **2018**, *11*, 187.

[292] G. Lanzara, J. Feng, F. Chang, *Smart Mater. Struct.* **2010**, *19*, 045013.

[293] T. Moy, L. Huang, W. Rieutort-Louis, C. Wu, P. Cuff, S. Wagner, J. C. Sturm, N. Verma, *IEEE J. Solid-State Circuits* **2017**, *52*, 309.

[294] W. S. A. Rieutort-Louis, J. Sanz-Robinson, T. Moy, L. Huang, Y. Hu, Y. Afsar, J. C. Sturm, N. Verma, S. Wagner, *IEEE T. Compon. Pack. T.* **2015**, *5*, 1219.

[295] J. Rogers, Y. Huang, O. G. Schmidt, D. H. Gracias, *MRS Bull.* **2016**, *41*, 123.

[296] Q. Cheng, Z. Song, T. Ma, B. B. Smith, R. Tang, H. Yu, H. Jiang, C. K. Chan, *Nano Lett.* **2013**, *13*, 4969.

[297] Z. Song, T. Ma, R. Tang, Q. Cheng, X. Wang, D. Krishnaraju, R. Panat, C. K. Chan, H. Yu, H. Jiang, *Nat. Commun.* **2014**, *5*, 3140.

[298] Z. Lv, Y. Luo, Y. Tang, J. Wei, Z. Zhu, X. Zhou, W. Li, Y. Zeng, W. Zhang, Y. Zhang, D. Qi, S. Pan, X. J. Loh, X. Chen, *Adv. Mater.* **2018**, *30*, 1704531.

[299] Z. Lv, Y. Tang, Z. Zhu, J. Wei, W. Li, H. Xia, Y. Jiang, Z. Liu, Y. Luo, X. Ge, Y. Zhang, R. Wang, W. Zhang, X. J. Loh, X. Chen, *Adv. Mater.* **2018**, *30*, 1805468.

[300] K. Zhang, Y. H. Jung, S. Mikael, J.-H. Seo, M. Kim, H. Mi, H. Zhou, Z. Xia, W. Zhou, S. Gong, Z. Ma, *Nat. Commun.* **2017**, *8*, 1782.

[301] S. Kwon, H. Kim, S. Choi, E. G. Jeong, D. Kim, S. Lee, H. S. Lee, Y. C. Seo, K. C. Choi, *Nano Lett.* **2017**, *18*, 347.

[302] K. Jost, D. P. Durkin, L. M. Haverhals, E. K. Brown, M. Langenstein, H. C. De Long, P. C. Trulove, Y. Gogotsi, G. Dion, *Adv. Energy Mater.* **2015**, *5*, 1401286.

[303] J. Lee, H. Kwon, J. Seo, S. Shin, J. H. Koo, C. Pang, S. Son, J. H. Kim, Y. H.

Jang, D. E. Kim, T. Lee, *Adv. Mater.* **2015**, *27*, 2433.

[304] S. J. Mooney, V. Pejaver, *Annu. Rev. Public Health* **2018**, *39*, 95.

[305] P. B. Jensen, L. J. Jensen, S. Brunak, *Nat. Rev. Genet.* **2012**, *13*, 395.

[306] R. Miotto, F. Wang, S. Wang, X. Jiang, J. T. Dudley, *Brief. Bioinform.* **2017**, *19*, 1236.

[307] E. Long, H. Lin, Z. Liu, X. Wu, L. Wang, J. Jiang, Y. An, Z. Lin, X. Li, J. Chen, *Nat. Biomed. Eng.* **2017**, *1*, 0024.

[308] A. Esteva, B. Kuprel, R. A. Novoa, J. Ko, S. M. Swetter, H. M. Blau, S. Thrun, *Nature* **2017**, *542*, 115.

[309] M. M. Al Rahhal, Y. Bazi, H. AlHichri, N. Alajlan, F. Melgani, R. R. Yager, *Inf. Sci.* **2016**, *345*, 340.

[310] U. R. Acharya, S. L. Oh, Y. Hagiwara, J. H. Tan, M. Adam, A. Gertych, R. San Tan, *Comput. Biol. Med.* **2017**, *89*, 389.

[311] B. Pourbabaee, M. J. Roshtkhari, K. Khorasani, *IEEE T. Syst. Man Cy-S.* **2017**, 1.

[312] S. Kiranyaz, T. Ince, M. Gabbouj, *IEEE Trans. Biomed. Eng.* **2015**, *63*, 664.

[313] O. Faust, Y. Hagiwara, T. J. Hong, O. S. Lih, U. R. Acharya, *Comput. Methods Programs Biomed.* **2018**, *161*, 1.

[314] M. Längkvist, L. Karlsson, A. Loutfi, *Adv. Artif. Neu. Sys.* **2012**, *2012*, 107046.

[315] Q. Zhang, L. T. Yang, Z. Chen, P. Li, *Inform. Fusion.* **2018**, *42*, 146.

[316] D. Capper, D. T. W. Jones, M. Sill, V. Hovestadt, D. Schrimpf, D. Sturm, C.

Koelsche, F. Sahm, L. Chavez, D. E. Reuss, A. Kratz, A. K. Wefers, K. Huang, K. W. Pajtler, L. Schweizer, D. Stichel, A. Olar, N. W. Engel, K. Lindenberg, P. N. Harter, A. K. Braczynski, K. H. Plate, H. Dohmen, B. K. Garvalov, R. Coras, A. Hölsken, E. Hewer, M. Bewerunge-Hudler, M. Schick, R. Fischer, R. Beschorner, J. Schittenhelm, O. Staszewski, K. Wani, P. Varlet, M. Pages, P. Temming, D. Lohmann, F. Selt, H. Witt, T. Milde, O. Witt, E. Aronica, F. Giangaspero, E. Rushing, W. Scheurlen, C. Geisenberger, F. J. Rodriguez, A. Becker, M. Preusser, C. Haberler, R. Bjerkvig, J. Cryan, M. Farrell, M. Deckert, J. Hench, S. Frank, J. Serrano, K. Kannan, A. Tsirigos, W. Brück, S. Hofer, S. Brehmer, M. Seiz-Rosenhagen, D. Hänggi, V. Hans, S. Rozsnoki, J. R. Hansford, P. Kohlhof, B. W. Kristensen, M. Lechner, B. Lopes, C. Mawrin, R. Ketter, A. Kulozik, Z. Khatib, F. Heppner, A. Koch, A. Jouvet, C. Keohane, H. Mühleisen, W. Mueller, U. Pohl, M. Prinz, A. Benner, M. Zapatka, N. G. Gottardo, P. H. Driever, C. M. Kramm, H. L. Müller, S. Rutkowski, K. von Hoff, M. C. Frühwald, A. Gnekow, G. Fleischhack, S. Tippelt, G. Calaminus, C.-M. Monoranu, A. Perry, C. Jones, T. S. Jacques, B. Radlwimmer, M. Gessi, T. Pietsch, J. Schramm, G. Schackert, M. Westphal, G. Reifenberger, P. Wesseling, M. Weller, V. P. Collins, I. Blümcke, M. Bendszus, J. Debus, A. Huang, N. Jabado, P. A. Northcott, W. Paulus, A. Gajjar, G. W. Robinson, M. D. Taylor, Z. Jaunmuktane, M. Ryzhova, M. Platten, A. Unterberg, W. Wick, M. A. Karajannis, M. Mittelbronn, T. Acker, C. Hartmann, K. Aldape, U. Schüller, R. Buslei, P. Lichter, M. Kool, C. Herold-Mende, D. W. Ellison, M.

Hasselblatt, M. Snuderl, S. Brandner, A. Korshunov, A. von Deimling, S. M. Pfister, *Nature* **2018**, *555*, 469.

[317] A. Y. Hannun, P. Rajpurkar, M. Haghpanahi, G. H. Tison, C. Bourn, M. P. Turakhia, A. Y. Ng, *Nat. Med.* **2019**, *25*, 65.

[318] M. Veta, Y. J. Heng, N. Stathonikos, B. E. Bejnordi, F. Beca, T. Wollmann, K. Rohr, M. A. Shah, D. Wang, M. Rousson, M. Hedlund, D. Tellez, F. Ciompi, E. Zerhouni, D. Lanyi, M. Viana, V. Kovalev, V. Liauchuk, H. A. Phoulady, T. Qaiser, S. Graham, N. Rajpoot, E. Sjöblom, J. Molin, K. Paeng, S. Hwang, S. Park, Z. Jia, E. I. C. Chang, Y. Xu, A. H. Beck, P. J. van Diest, J. P. W. Pluim, *Med. Image Anal.* **2019**, *54*, 111.

[319] K.-H. Yu, A. L. Beam, I. S. Kohane, *Nat. Biomed. Eng.* **2018**, *2*, 719.

[320] Y. LeCun, Y. Bengio, G. Hinton, *Nature* **2015**, *521*, 436.

[321] D. Silver, A. Huang, C. J. Maddison, A. Guez, L. Sifre, G. van den Driessche, J. Schrittwieser, I. Antonoglou, V. Panneershelvam, M. Lanctot, S. Dieleman, D. Grewe, J. Nham, N. Kalchbrenner, I. Sutskever, T. Lillicrap, M. Leach, K. Kavukcuoglu, T. Graepel, D. Hassabis, *Nature* **2016**, *529*, 484.

[322] D. Silver, J. Schrittwieser, K. Simonyan, I. Antonoglou, A. Huang, A. Guez, T. Hubert, L. Baker, M. Lai, A. Bolton, Y. Chen, T. Lillicrap, F. Hui, L. Sifre, G. van den Driessche, T. Graepel, D. Hassabis, *Nature* **2017**, *550*, 354.

[323] A. Krizhevsky, I. Sutskever, G. E. Hinton. *Adv. Neural Inf. Process. Syst.*, Neural Information Processing Systems Foundation, Inc., Lake Tahoe, USA, **2012**, 1097.

[324] M. Wang, T. Wang, P. Cai, X. Chen, *Small Methods* **2019**, 1900025.

[325] K. He, X. Zhang, S. Ren, J. Sun. *Proc. IEEE Conf. Comput. Vis. Pattern Recognit.*, IEEE, **2016**, 770.

[326] H. Van Hasselt, A. Guez, D. Silver. *Thirtieth AAAI Conference on Artificial Intelligence*, AAAI Press, Palo Alto, CA, **2016**, 2094.

[327] V. Mnih, K. Kavukcuoglu, D. Silver, A. A. Rusu, J. Veness, M. G. Bellemare, A. Graves, M. Riedmiller, A. K. Fidjeland, G. Ostrovski, S. Petersen, C. Beattie, A. Sadik, I. Antonoglou, H. King, D. Kumaran, D. Wierstra, S. Legg, D. Hassabis, *Nature* **2015**, *518*, 529.

[328] A. Krizhevsky, G. E. Hinton. *Proceedings of the 19th European Symposium on Artificial Neural Networks (ESANN)*, **2011**,

[329] J. Nagi, F. Ducatelle, G. A. Di Caro, D. Cireşan, U. Meier, A. Giusti, F. Nagi, J. Schmidhuber, L. M. Gambardella. *2011 IEEE International Conference on Signal and Image Processing Applications (ICSIPA)*, IEEE, **2011**, 342.

[330] S. Sabour, N. Frosst, G. E. Hinton. *Adv. Neural Inf. Process. Syst.*, Neural Information Processing Systems Foundation, Inc., Lake Tahoe, USA, **2017**, 3856.

[331] K. Simonyan, A. Zisserman, *arXiv preprint arXiv:1409.1556* **2014**.

[332] C. Szegedy, V. Vanhoucke, S. Ioffe, J. Shlens, Z. Wojna. *Proc. IEEE Conf. Comput. Vis. Pattern Recognit.*, IEEE, **2016**, 2818.

[333] S. Xie, R. Girshick, P. Dollár, Z. Tu, K. He. *Proc. IEEE Conf. Comput. Vis. Pattern Recognit.*, IEEE, **2017**, 1492.

[334] S. Ren, K. He, R. Girshick, J. Sun. *Adv. Neural Inf. Process. Syst.*, Neural Information Processing Systems Foundation, Inc., Lake Tahoe, USA, **2015**, 91.

[335] J. Redmon, S. Divvala, R. Girshick, A. Farhadi. *Proc. IEEE Conf. Comput. Vis. Pattern Recognit.*, IEEE, **2016**, 779.

[336] V. Badrinarayanan, A. Kendall, R. Cipolla, *IEEE T. Pattern Anal.* **2017**, *39*, 2481.

[337] I. Goodfellow, J. Pouget-Abadie, M. Mirza, B. Xu, D. Warde-Farley, S. Ozair, A. Courville, Y. Bengio. *Adv. Neural Inf. Process. Syst.*, Neural Information Processing Systems Foundation, Inc., Lake Tahoe, USA, **2014**, 2672.

[338] B. Wu, F. Iandola, P. H. Jin, K. Keutzer. *Proc. IEEE Conf. Comput. Vis. Pattern Recognit. workshops*, IEEE, **2017**, 129.

[339] S. H. Lim, L. Feng, J. W. Kemling, C. J. Musto, K. S. Suslick, *Nat. Chem.* **2009**, *1*, 562.

[340] T. Soga, Y. Jimbo, K. Suzuki, D. Citterio, *Anal. Chem.* **2013**, *85*, 8973.

[341] H. Li, Q. Chen, J. Zhao, Q. Ouyang, *Anal. Methods* **2014**, *6*, 6271.

[342] Z. Xiaobo, H. Xiaowei, M. Povey, *Analyst* **2016**, *141*, 1587.

[343] Z. Li, H. Li, M. K. LaGasse, K. S. Suslick, *Anal. Chem.* **2016**, *88*, 5615.

[344] Z. Li, K. S. Suslick, *ACS Sensors* **2016**, *1*, 1330.

[345] M. J. Kangas, R. M. Burks, J. Atwater, R. M. Lukowicz, B. Garver, A. E. Holmes, *J. Chemom.* **2018**, *32*, e2961.

[346] Z. C. Lipton, D. C. Kale, C. Elkan, R. Wetzel, *arXiv preprint*

arXiv:1511.03677 **2015**.

[347] B. M. Marlin, D. C. Kale, R. G. Khemani, R. C. Wetzel. *Proceedings of the 2nd ACM SIGHIT international health informatics symposium*, ACM, **2012**, 389.

[348] M. Längkvist, L. Karlsson, A. Loutfi, *Pattern Recognit. Lett.* **2014**, *42*, 11.

[349] E. Nurse, B. S. Mashford, A. J. Yepes, I. Kiral-Kornek, S. Harrer, D. R. Freestone. *Proceedings of the ACM International Conference on Computing Frontiers*, ACM, **2016**, 259.

[350] A. Sathyanarayana, S. Joty, L. Fernandez-Luque, F. Ofli, J. Srivastava, A. Elmagarmid, T. Arora, S. Taheri, *JMIR mHealth and uHealth* **2016**, *4*, e129.

[351] D. Ravi, C. Wong, B. Lo, G.-Z. Yang, *IEEE J. Biomed. Health* **2017**, *21*, 56.

[352] S. V. Kalinin, B. G. Sumpter, R. K. Archibald, *Nat. Mater.* **2015**, *14*, 973.

[353] X.-W. Chen, X. Lin, *IEEE Access* **2014**, *2*, 514.

[354] M. Satyanarayanan, *Nat. Electron.* **2019**, *2*, 42.

[355] M. Satyanarayanan, P. Bahl, R. Caceres, N. Davies, *IEEE Pervas. Comput.* **2009**, 14.

[356] Y. Yang, *Nat. Electron.* **2019**, *2*, 4.

[357] W. Z. Khan, E. Ahmed, S. Hakak, I. Yaqoob, A. Ahmed, *Future Gener. Comp. Sy.* **2019**, *97*, 219.

[358] D. C. Daly, P. P. Mercier, M. Bhardwaj, A. L. Stone, Z. N. Aldworth, T. L. Daniel, J. Voldman, J. G. Hildebrand, A. P. Chandrakasan, *IEEE J. Solid-State Circuits* **2010**, *45*, 153.

[359] S. Bandyopadhyay, P. P. Mercier, A. C. Lysaght, K. M. Stankovic, A. P. Chandrakasan, *IEEE J. Solid-State Circuits* **2014**, *49*, 2812.

[360] P. P. Mercier, S. Bandyopadhyay, A. C. Lysaght, K. M. Stankovic, A. P. Chandrakasan, *IEEE J. Solid-State Circuits* **2014**, *49*, 1463.

[361] S. Stauss, I. Honma, *Bull. Chem. Soc. Jpn.* **2018**, *91*, 492.

[362] C. E. Parker, C. H. Borchers, *Mol. Oncol.* **2014**, *8*, 840.

[363] J. Choi, Y. Xue, W. Xia, T. R. Ray, J. T. Reeder, A. J. Bandodkar, D. Kang, S. Xu, Y. Huang, J. A. Rogers, *Lab Chip* **2017**, *17*, 2572.

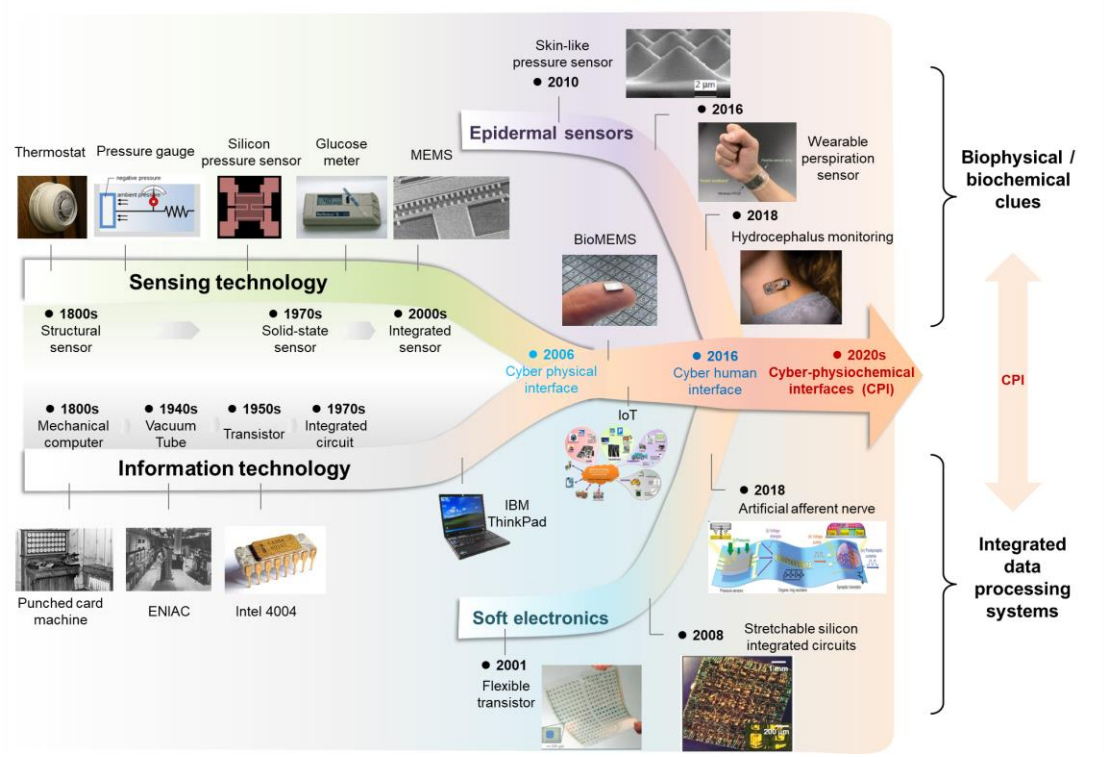

Figure 1. Timelines for the convergence of sensing and information technologies. The initial convergence brings about a cyber physical system with typical examples such as Internet of Things (IoT). The rapid development of soft electronics and epidermal sensing technology propels forward the cyber human system. By merging these technologies, future cyber physiochemical interfaces aim to link the electronic and computing technology (cyber) with biophysical and biochemical signal output by addressing the interfacial issues. Thermostat, Glucose meter, Intel 4004 images are downloaded from Wikipedia; Micrograph of MEMS (Courtesy of E Lau and C. V. Thompson, MIT.),[8] BioMEMS Image Credit: Internet of Things Agenda. Pressure gauge. Reproduced with permission.[7] Copyright 2018, the authors, Copernicus GmbH. Skin-like pressure sensor. Reproduced with permission.[10] Copyright 2010, Nature Publishing Group. Wearable perspiration sensor. Reproduced with permission.[27] Copyright 2016, Nature Publishing Group. Hydrocephalus

monitoring. Reproduced with permission,[13] Copyright 2018. American Association for the Advancement of Science (AAAS). Punched card machine image credited to IBM. ENIAC, Reproduced with permission.[15] Copyright 1946, Nature Publishing Group. Laptop image credited to Lenovo ThinkPad. IoT. Reproduced with permission.[32] Copyright 2013, Elsevier Ltd. Flexible Transistor. Reproduced with permission,[23] Copyright 2001, National Academy of Sciences, U.S.A. Stretchable silicon integrated circuits. Reproduced with permission,[20] Copyright 2008, American Association for the Advancement of Science (AAAS). Artificial afferent nerve. Reproduced with permission,[22] Copyright 2018, American Association for the Advancement of Science (AAAS).

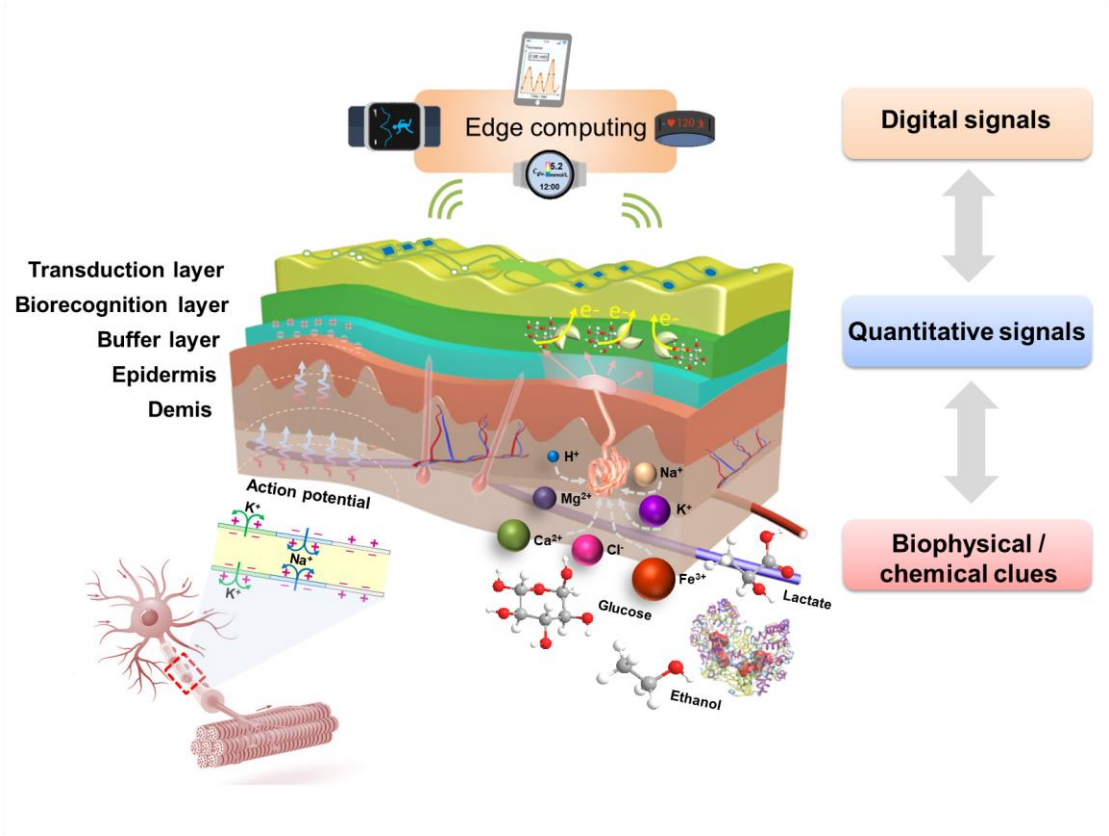

Figure 2. Schematic illustration of a typical example of CPI. It reliably extracts biophysical/chemical clues of human beings such as electrophysiological signals and metabolites, transfers them to quantitative electrical signals, converts them to digital signals, and eventually provides correlation and feedback via edge computing. This forms the basis for stable cyber-human systems.

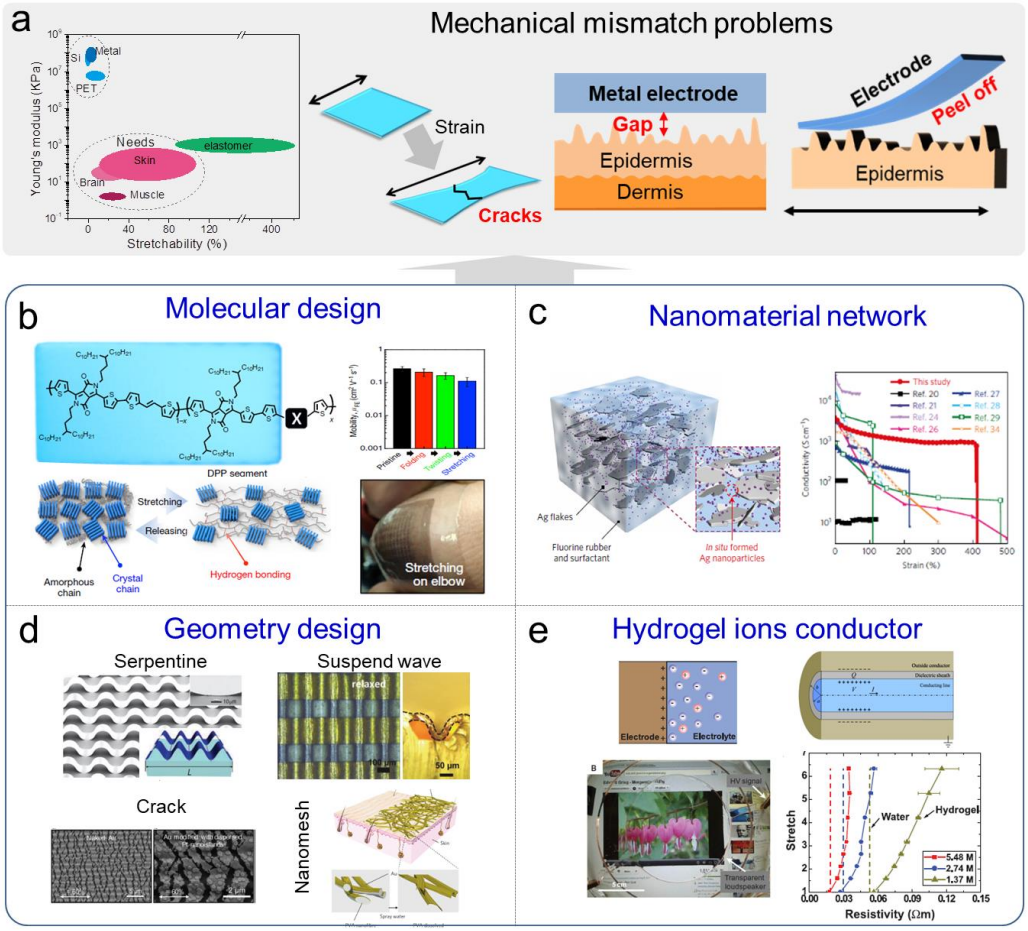

Figure 3. a) Device malfunction due to interfacial mechanical mismatch and incompatibility in terms of Young's modulus and stretchability. To overcome these mechanical mismatch issues, strategies include b) molecular design that comprise both elastic and rigid elements, c) Nanomaterial network such as silver nanoparticles elastic conductor, d) Geometry design such as serpentine, suspend waves, cracks, nanomesh, and e) hydrogel based electrodes with intrinsic stretchability and ionic conductivity. Molecular design. Reproduced with permission,[61] Copyright 2016, Nature Publishing Group. Nanomaterial network, Reproduced with permission.[75] Copyright 2017, Nature Publishing Group. Serpentine. Reproduced with permission.[89] Copyright 2006, Nature Publishing Group. Suspend waves.

Reproduced with permission.[81] Copyright 2015, Wiley-VCH. Cracks. Reproduced with permission.[93] Copyright 2014, American Chemical Society. Nanomesh. Reproduced with permission.[95] Copyright 2017, Nature Publishing Group. Hydrogel. Reproduced with permission.[96] Copyright 2013, American Association for the Advancement of Science (AAAS).

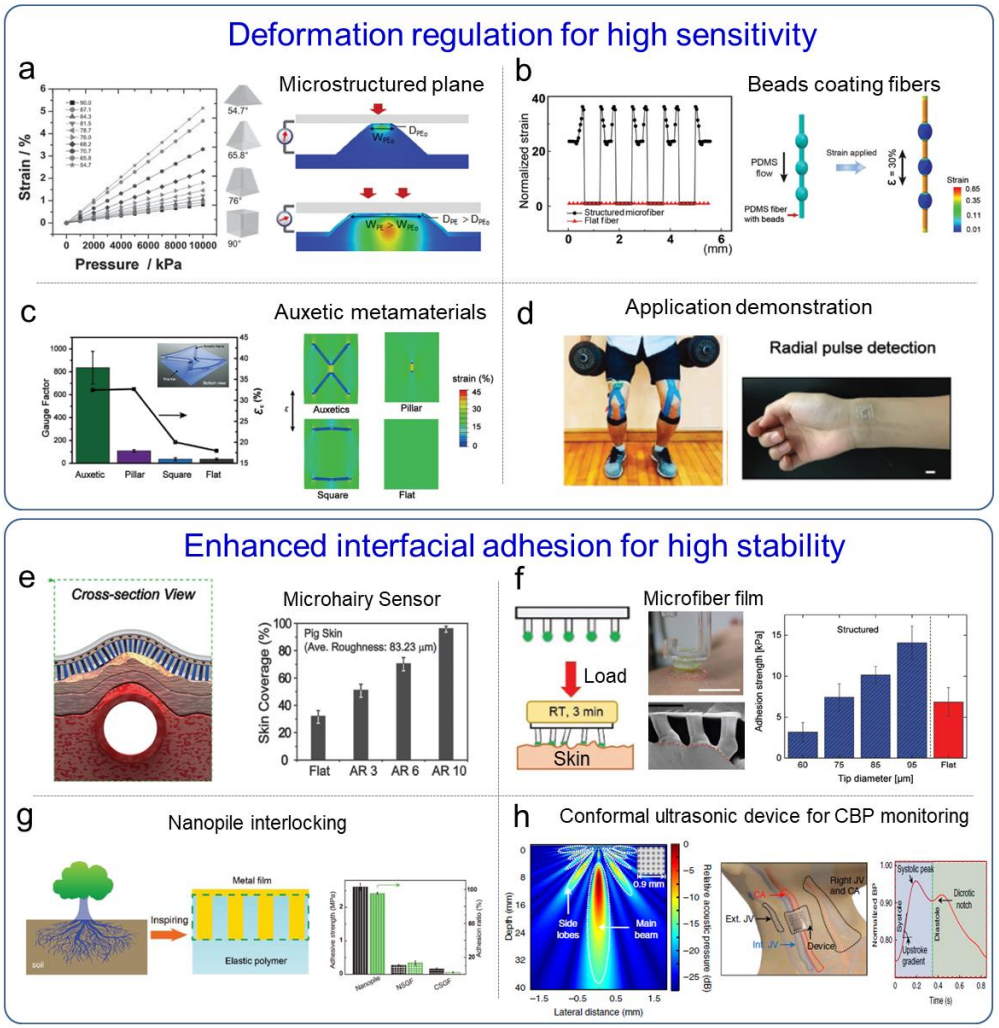

Figure 4. Two categories of solutions to improve the performance of mechanical sensors. One is deformation or strain regulation for high sensitivity pressure or strain sensors. a) micropyramidal structures with optimized sidewall angle, Reproduced with permission.[101] Copyright 2014, Wiley-VCH. Reproduced with permission.[100] Copyright 2014, Wiley-VCH. b) Microbeads-distributed fiber-shaped stretchable strain sensors, Reproduced with permission.[107] Copyright 2018, Wiley-VCH. c) Auxetic mechanical metamaterials with bidirectional expansion. Reproduced with permission.[108] Copyright 2018, Wiley-VCH. d) Application demonstration. Reproduced with permission.[107-108] Copyright 2018,

Wiley-VCH. Another is enhancing interfacial adhesion for high stability sensing by following strategies. e) Microhair structures. Reproduced with permission.[111] Copyright 2015, Wiley-VCH. f) Surface modification, interlocking strategy with increased electrode and elastomer adhesion. Reproduced with permission,[112] Copyright 2017, Wiley-VCH. g) Interlocking strategy with increased electrode and elastomer adhesion. Reproduced with permission.[114] Copyright 2017, Wiley-VCH. h) Conformal ultrasonic sensor for blood pressure measurement and typical pulse waveform at the carotid artery correlated to the left atrial and ventricular events. Reproduced with permission.[115] Copyright 2018, Nature Publishing Group.

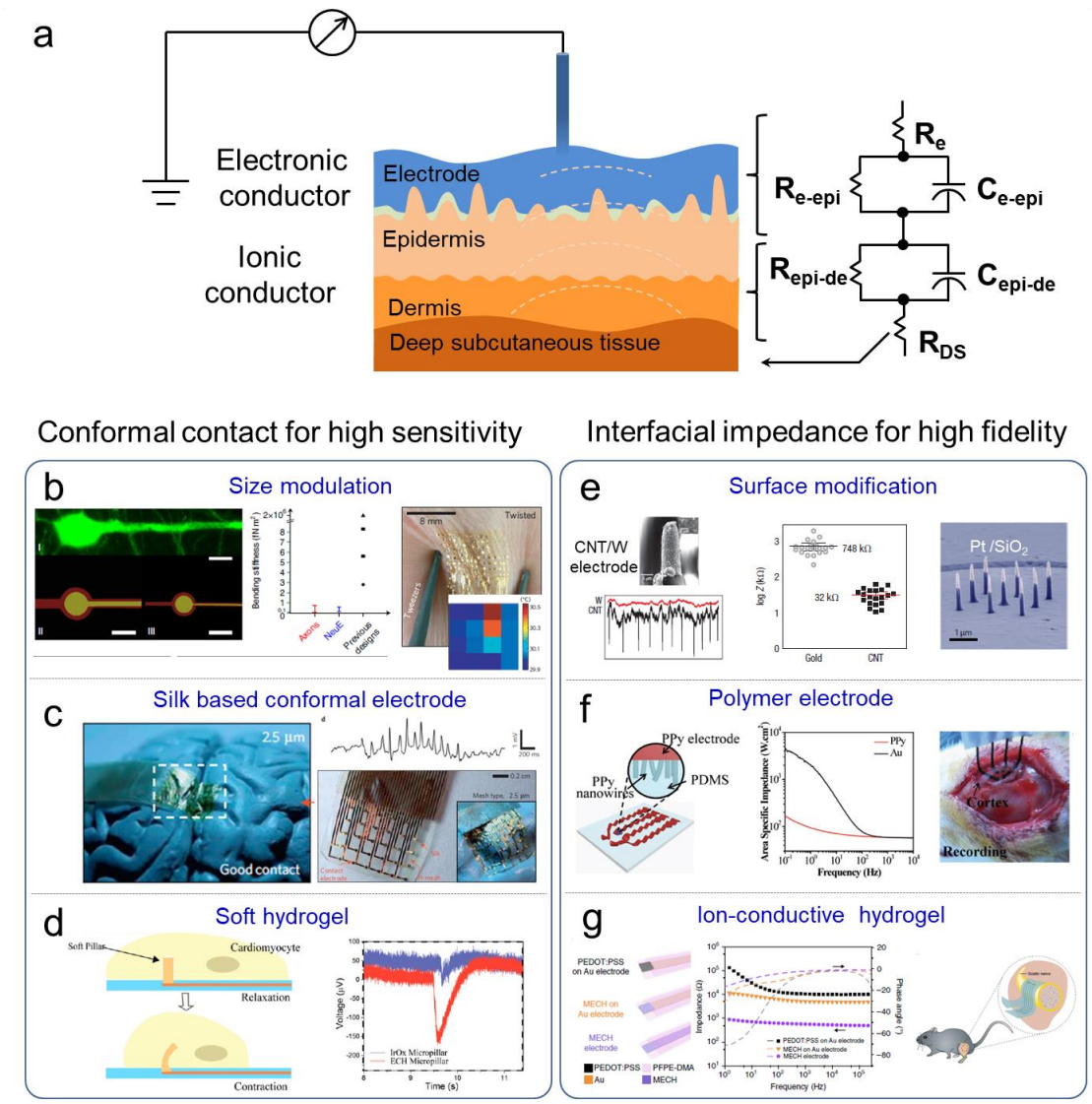

Figure 5. a) An electrophysiological sensing interface which involves biosignal transfer between epidermal ionic and electronic conductors. Both good conformal contact and decreased interfacial impedance are expected to enhance the selectivity and fidelity of sensors. The conformal contact can be achieved by using b) size modulation for matched mechanicals including decreasing diameter and thickness, c) natural polymer based soft film, and d) soft hydrogel. Ways to decrease interfacial impedance include e) surface modification such as CNT modified tungsten electrode and Pt modified Si electrode array, f) polymer-based, and g) ion-conductive electrode.

Size modulation. Reproduced with permission.[130] Copyright 2019, Nature Publishing Group. Reproduced with permission.[133] Copyright 2013, Nature Publishing Group. Silk-based conformal electrode. Reproduced with permission.[141] Copyright 2010, Nature Publishing Group. Soft hydrogel. Reproduced with permission.[40] Copyright 2018, National Academy of Sciences of the United States of America. CNT/W electrode, Reproduced with permission.[154] Copyright 2008, Nature Publishing Group. Pt/Si electrode, Reproduced with permission.[153] Copyright 2017, Nature Publishing Group. Polymer electrode. Reproduced with permission.[45] Copyright 2017, Wiley-VCH. Ion-conductive hydrogel. Reproduced with permission,[39] Copyright 2019, Nature Publishing Group.

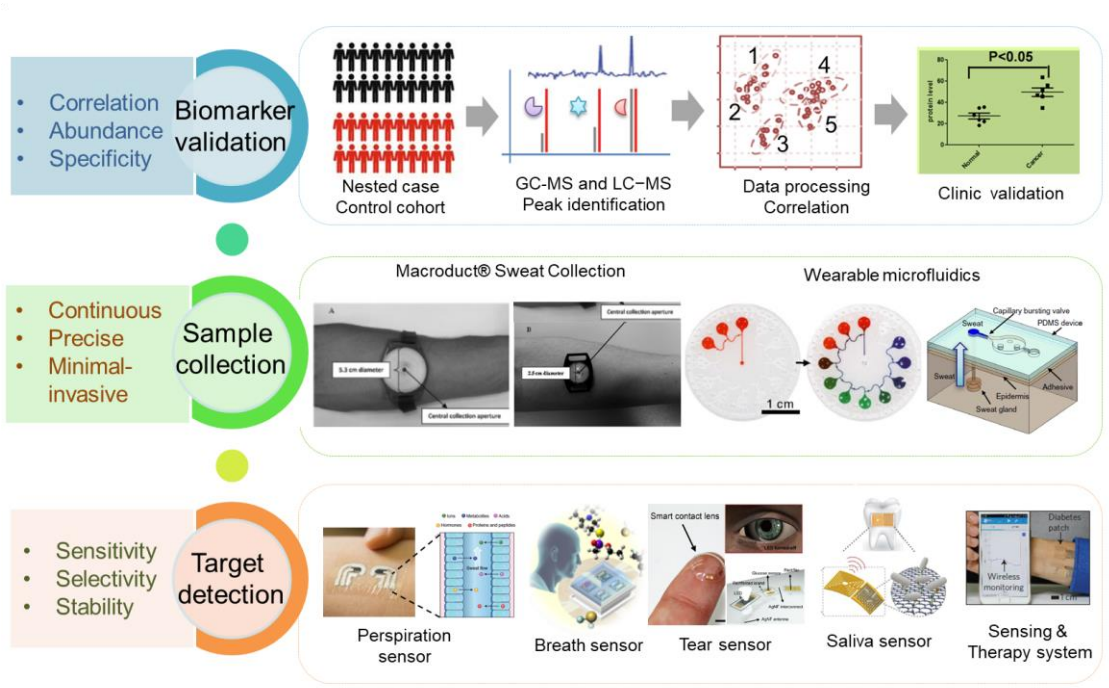

Figure 6. Three critical aspects for epidermal biochemical sensors including biomarker validation, sample collection, and target detection. The flowchart of biomarker validation includes target screening via standard methods, data processing to get correlation information, and clinic validation to test the feasibility.[173, 362] Based on identified biomarkers, sample collections via continuous, precise, and minimal or non-invasive way are desired. One promising way is wearable microfluidics. Macrduct@Sweat collection. Reproduced with permission,[183] Copyright 2013 Elsevier. Wearable microfluidics. Reproduced with permission.[187] Copyright 2017, Wiley-VCH. Reproduced from Ref [363] with permission from The Royal Society of Chemistry. Target detection technologies with sensitivity, selectivity, stability were applied in perspiration, breath, tear, saliva sensing as well as sensing and therapy systems. Perspiration sensor. Reproduced with permission.[191] Copyright 2014, American Chemical Society. Reproduced with permission, [167] Copyright 2018, Nature Publishing Group. Breath sensor. Reproduced with

permission.[168] Copyright 2017, American Chemical Society. Tear sensor. Reproduced with permission.[194] Copyright 2018, the Authors, American Association for the Advancement of Science (AAAS). Saliva sensor. Reproduced with permission.[195] Copyright 2012, the Authors, Nature Publishing Group. Sensing and therapy system. Reproduced with permission.[196] Copyright 2016, Nature Publishing Group.

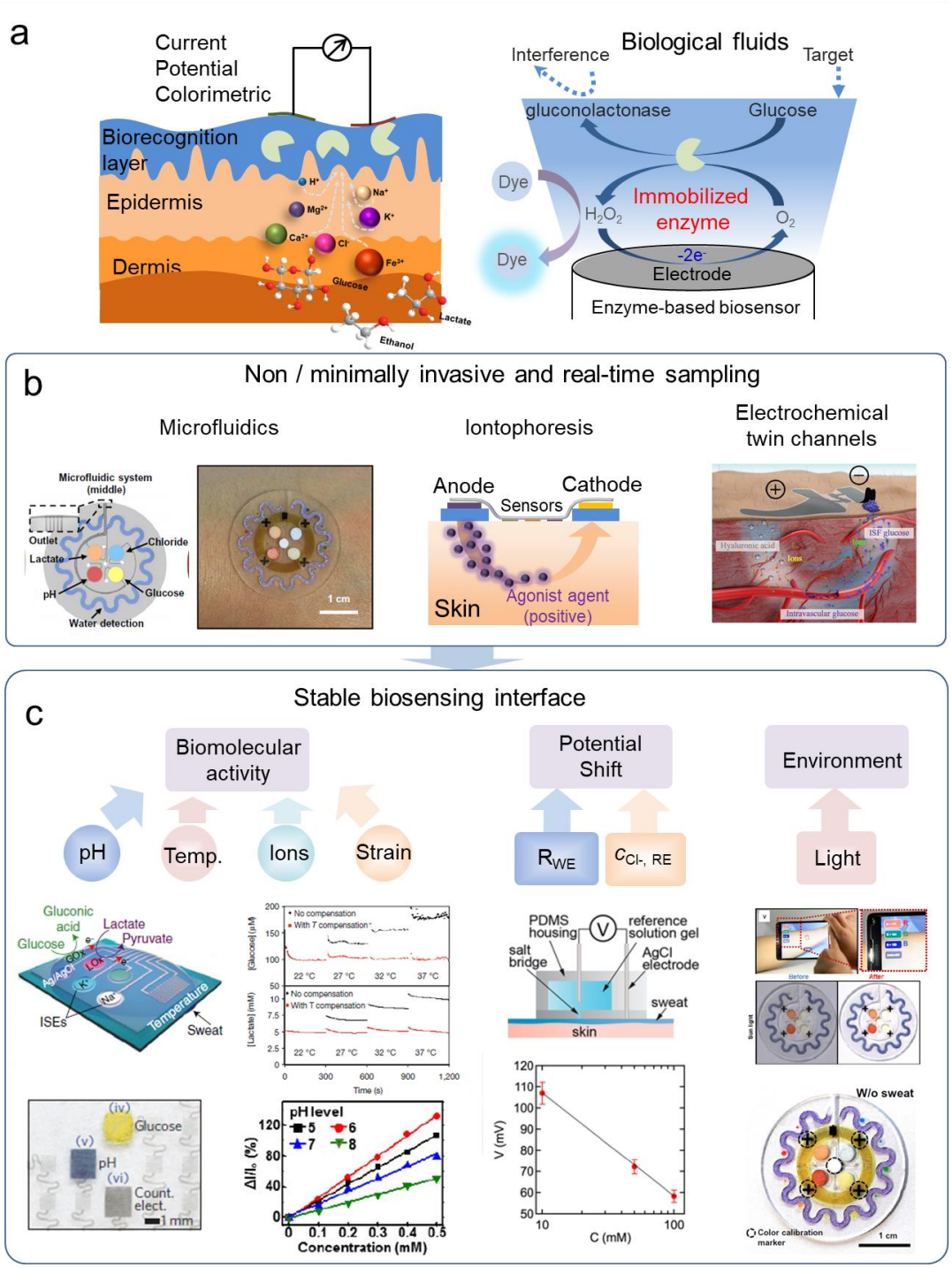

Figure 7. a) Scheme of epidermal biosensors and a biosensing mechanism, based on a specific biorecognition reaction coupled with the release of electrical or colorimetric signals. b) Three sampling strategies, namely, microfluidics, iontophoresis, and electrochemical twin channels are capable of in-situ collection of sweat. c) Stable

biosensing interface achieved by calibrating the biomolecule activity based on pH, temperature, ions, and strain parameters, potential shift (electrochemical), and ambient light (colorimetric). Microfluidics. Reproduced with permission.[188] Copyright 2016, American Association for the Advancement of Science (AAAS), Iontophoresis. Reproduced with permission.[189] Copyright 2017, the authors, National Academy of Sciences. U. S. A.. Electrochemical twin channels. Reproduced with permission.[190] Copyright 2017, the Authors, American Association for the Advancement of Science (AAAS). Multiplex biosensor and temperature-induced sensor variations. Reproduced with permission.[27] Copyright 2016, Nature Publishing Group. Stretchable biosensor and pH-induced sensor variations. Reproduced with permission. [196] Copyright 2016, Nature Publishing Group. Potential shift. Reproduced with permission.[204] Copyright 2014, American Chemical Society. Ambient light calibration. Reproduced with permission.[188] Copyright 2016, American Association for the Advancement of Science (AAAS).

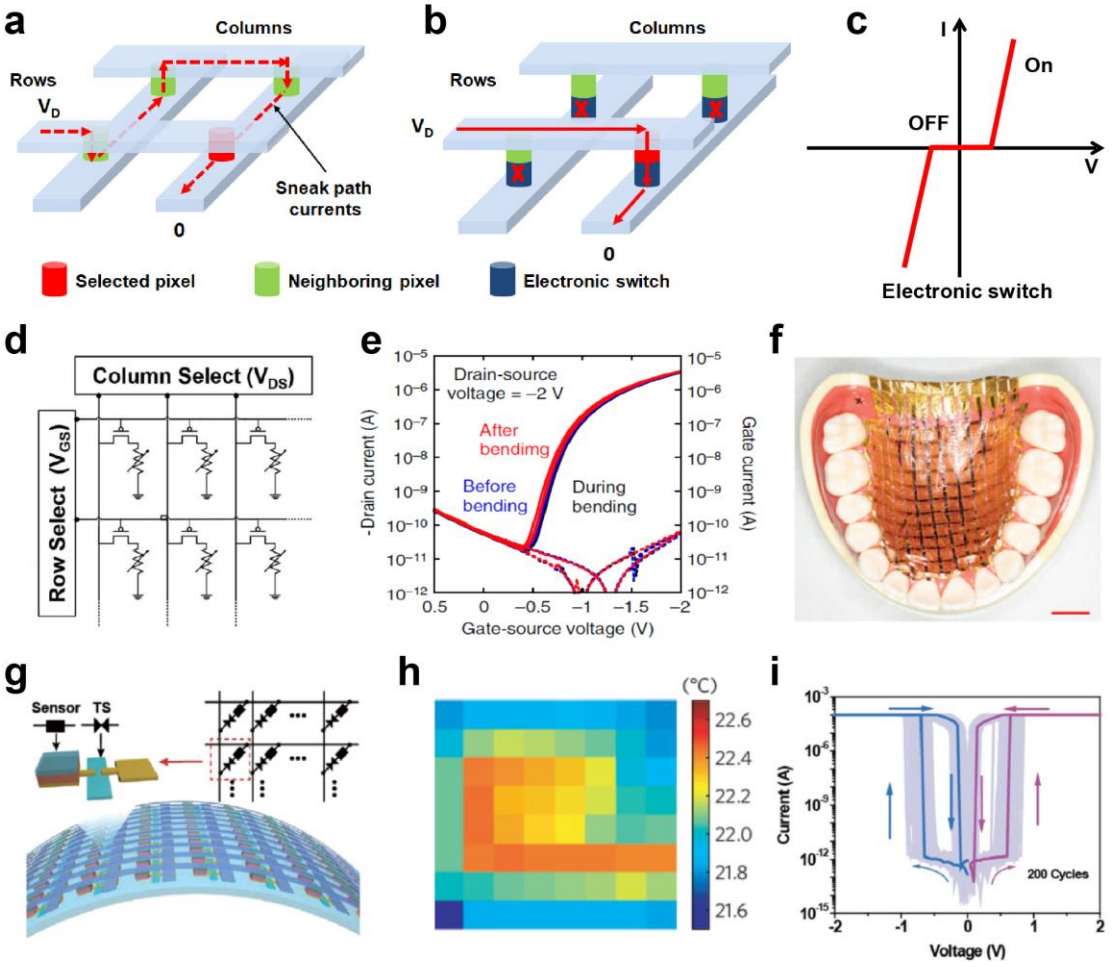

Figure 8. Array integration. a)-b) Crosstalk issue and solutions for array integration. c) Ideal electronic switch exhibiting a nonlinear current-voltage response. d) Typical circuit schematic of array integration using three-terminal transistors. Reproduced with permission.[214] Copyright 2015, Wiley-VCH. e) Typical current-voltage curves of flexible organic transistors. Reproduced with permission.[216] Copyright 2016, the Authors, Nature Publishing Group. f) Tactile sensor array conforming to a model of the human upper jaw. Scale bar, 1 cm. Reproduced with permission.[231] Copyright 2013, Nature Publishing Group. g)

Configuration of array integration using two-terminal electronic switches. Reproduced with permission.[208] Copyright 2018, Wiley-VCH. h) Measured distribution of temperature by using a nanomembrane diode sensor array. Reproduced with permission.[133] Copyright 2013, Nature Publishing Group. i) Current-voltage curves of a two-terminal, flexible, and bidirectional threshold switch. Reproduced with permission.[208] Copyright 2018, Wiley-VCH.

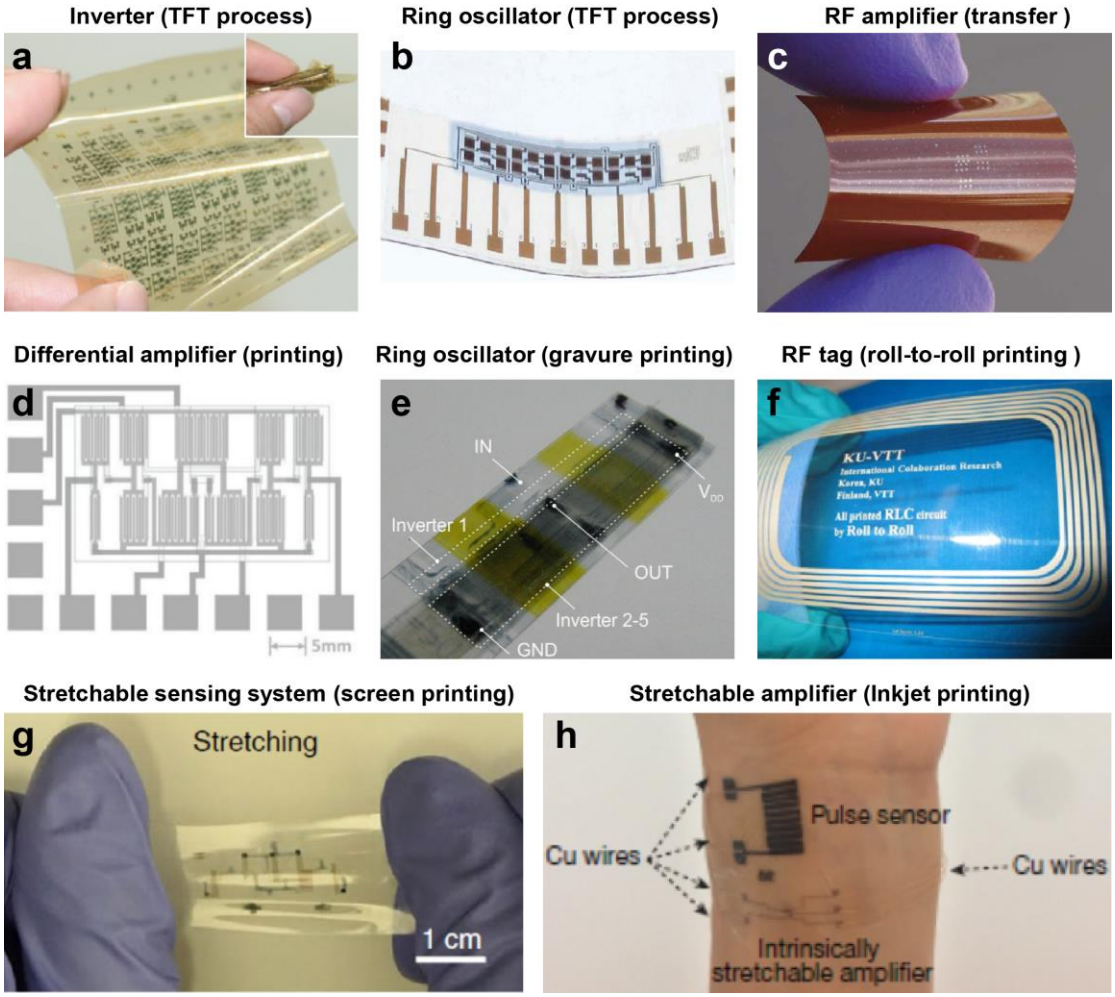

Figure 9. Organic circuit components and systems. a) Ultraflexible organic complementary inverter circuits on a polyimide substrate. Reproduced with permission.[217] Copyright 2010, Nature Publishing Group. b) Organic ring oscillator based on pseudo–complementary metal-oxide semiconductor (CMOS) process. Reproduced with permission.[22] Copyright 2018, American Association for the Advancement of Science (AAAS). c) Flexible MoS_2 transistors-based-radio frequency (RF) amplifier. Reproduced with permission.[257] Copyright 2014, the Authors, Nature Publishing Group. d) Fully printed differential amplifier.[258] Reproduced with permission. Copyright 2014, Elsevier. e) Ring oscillator using exclusively gravure and flexographic printing. Reproduced with permission.[259]

Copyright 2011, Elsevier. f) Printed RF resonant tag based on roll-to-roll printing. Reproduced with permission.[260] Copyright 2011, Elsevier. g) Stretchable temperature sensor stretching with 25% uniaxial strain. Reproduced with permission.[267] Copyright 2018, Nature Publishing Group. h) Intrinsically stretchable amplifier. Reproduced with permission.[252] Copyright 2018, Nature Publishing Group.

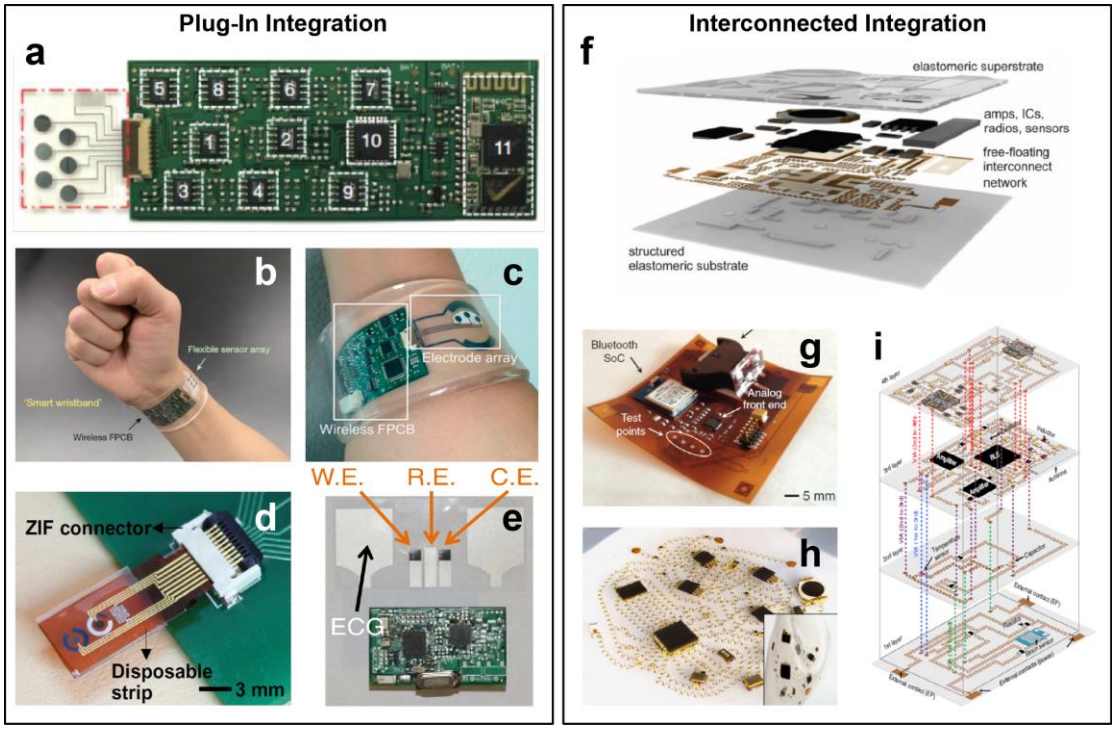

Figure 10. Approaches of flexible hybrid integration (FHE): Plug-in integration a)-e), and interconnected integration f)-i). a)-b) Fully integrated wearable sensor arrays for perspiration analysis. Reproduced with permission.[27] Copyright 2018, Nature Publishing Group. c) Autonomous sweat extraction and sensing platform. Reproduced with permission.[189] Copyright 2017, National Academy of Sciences of the United States of America, d) Wearable/disposable sweat-based glucose monitoring devices. Reproduced with permission.[199] Copyright 2017, the Authors, American Association for the Advancement of Science (AAAS). e) Wearable chemical–electrophysiological hybrid sensor patch. Reproduced with permission.[270] Copyright 2015, the Authors, Nature Publishing Group. f) Soft microfluidic assemblies. Reproduced with permission.[277] Copyright 2014, American Association for the Advancement of Science (AAAS). g) Kapton PI-based wearable sensor patch (WSP). Reproduced with permission.[272] Copyright 2016, Wiley-VCH. h) Helical

microcoils for soft electronics. Reproduced with permission.[278] Copyright 2017, the Authors, Nature Publishing Group. i) Three-dimensional integrated stretchable electronics. Reproduced with permission.[280] Copyright 2018, Nature Publishing Group.

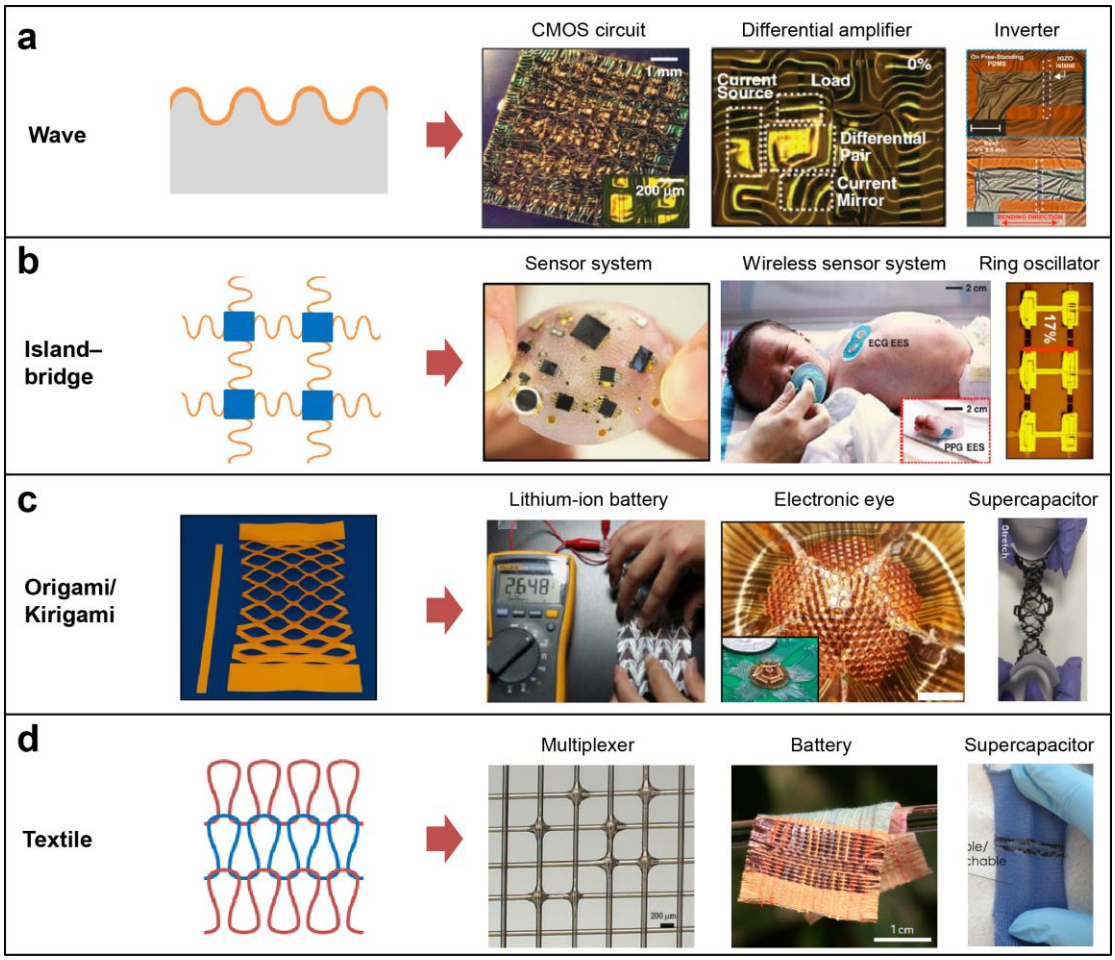

Figure 11. Structural designs for stretchable FHE integration. a) Wave strategy used in examples of a COMS circuit, differential amplifier, and inverter. b) Island–bridge strategy used in examples of a sensor system, wireless sensor system and ring oscillator. c) Origami/kirigami strategy used in examples of a lithium-ion battery, electronic eye, and supercapacitor. d) Textile strategy. Used in examples of a multiplexer, battery, and supercapacitor. COMS circuit. Reproduced with permission.[20] Copyright 2008, American Association for the Advancement of Science (AAAS). Differential amplifier, Reproduced with permission.[20] Copyright 2008, American Association for the Advancement of Science (AAAS). Inverter. Reproduced with permission.[275] Copyright 2017, American Chemical Society. Sensor system. Reproduced with permission.[278] Copyright 2017, the Authors, Nature

Publishing Group. Wireless sensor system. Reproduced with permission.[279] Copyright 2019, the Authors, American Association for the Advancement of Science (AAAS). Ring oscillator. Reproduced with permission.[276] Copyright 2008, National Academy of Sciences, U. S. A. Origami/kirigami strategy. Reproduced with permission.[285] Copyright 2018, Elsevier. Lithium-ion battery. Reproduced with permission.[297] Copyright 2014, the Authors, Nature Publishing Group. Electronic eye. Reproduced with permission.[300] Copyright 2017, the Authors, Nature Publishing Group. Supercapacitor. Reproduced with permission.[298] Copyright 2018, Wiley-VCH. d) Multiplexer. Reproduced with permission.[286] Copyright 2007, Nature Publishing Group. Battery. Reproduced with permission.[289] Copyright 2016, Nature Publishing Group. Supercapacitor. Reproduced with permission.[302] Copyright 2015, Wiley-VCH.

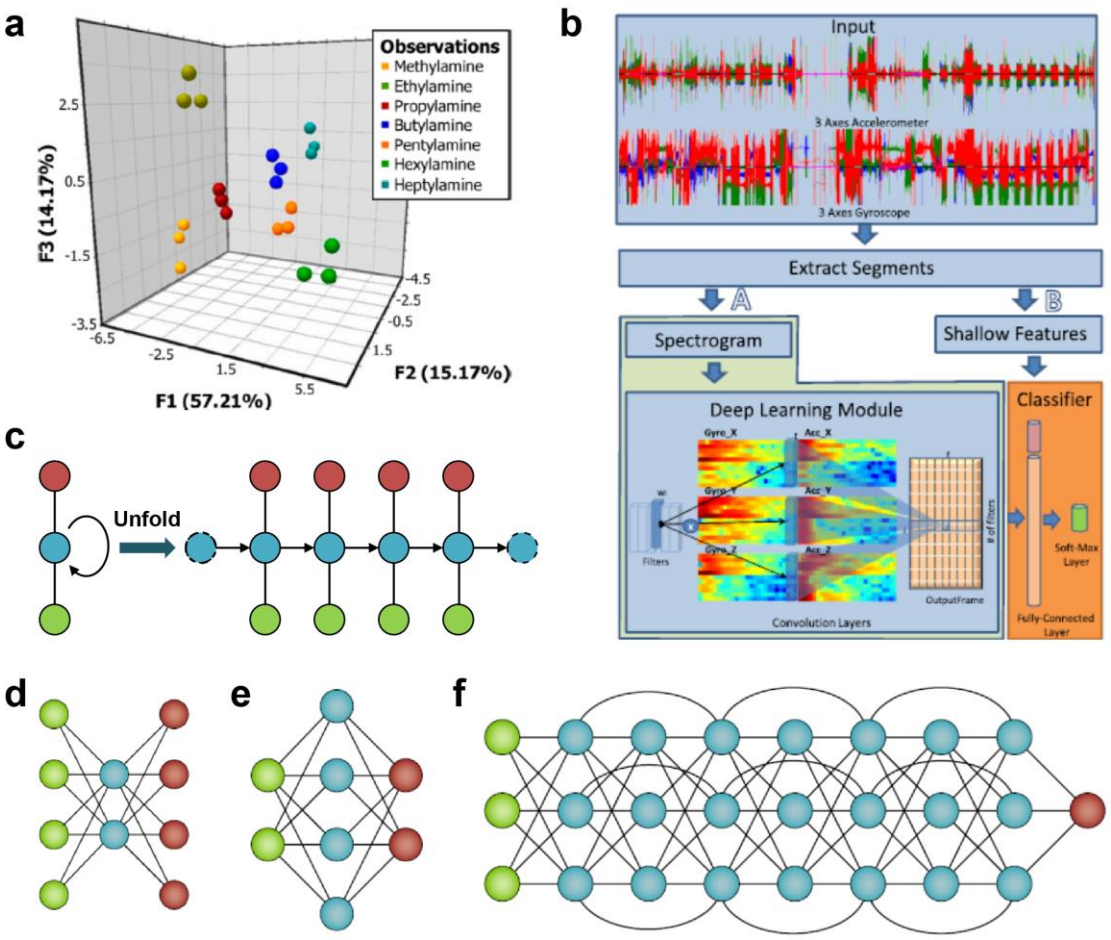

Figure 12. Recent progress of machine learning in sensor data analysis. a) PCA result for the discrimination of volatile amines. Reproduced with permission.[340] Copyright 2013, American Chemical Society. b) Schematic workflow of deep learning for time-series data. Reproduced with permission.[351] Copyright 2017, the Authors, IEEE. c) RNN architecture. The architecture of d) an autoencoder, e) a sparse autoencoder, and f) a deep residual neural network. Reproduced with permission.[319] Copyright 2018, Nature Publishing Group.

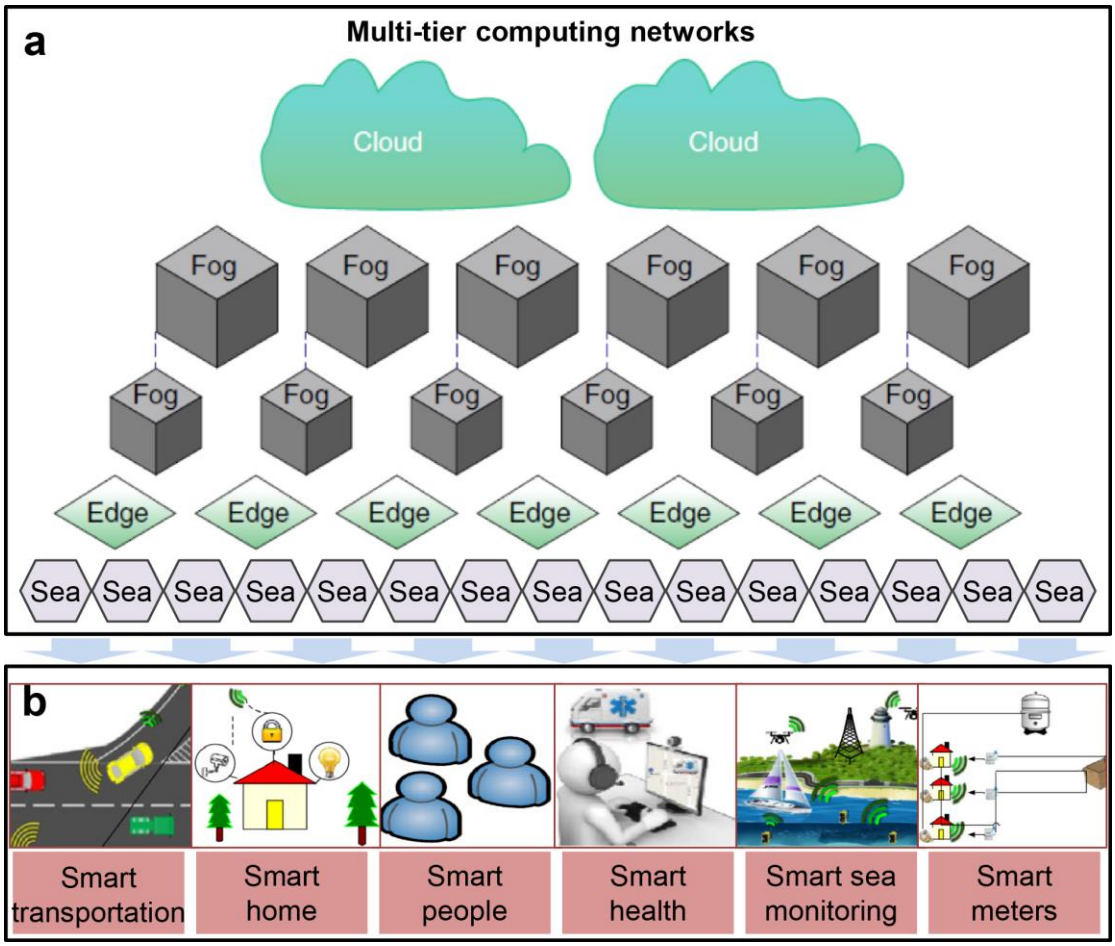

Figure 13. Multi-tier computing networks for intelligent applications and services. a) Multi-tier computing network architecture with hierarchical layers, consisting of cloud, fog, edge and sea computing. Reproduced with permission.[356] Copyright 2019, Nature Publishing Group. b) Intelligent applications and services, such as smart transportation, smart home, smart people, smart health, smart sea monitoring, and smart meters. Reproduced with permission.[357] Copyright 2019, Elsevier.

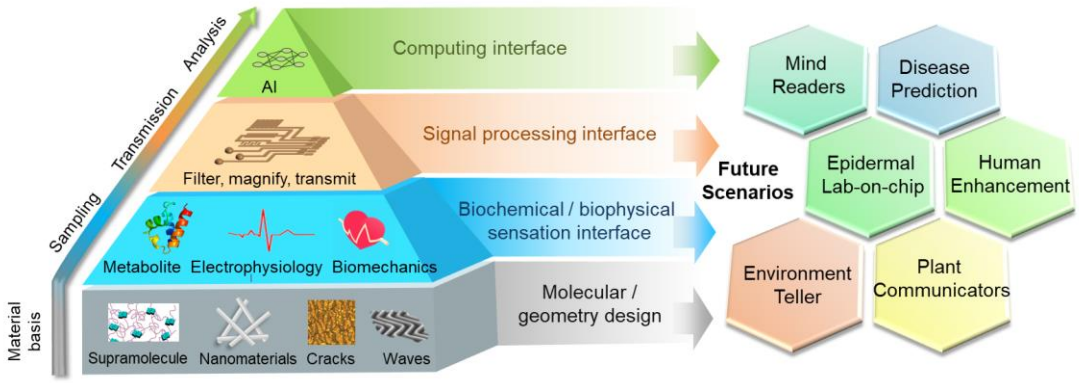

Figure 14. Perspectives of CPI in a pyramidal hierarchical structure. The bottom-up architecture of CPI comprises biochemical/biophysical sensation interface, signal processing interface, and edge computing interface based on molecular or geometry design to endow stretchability, conformability and adhesion, biorecognition, and durability features. Based on the pyramidal hierarchy of CPI, future applications can involve any process that releases physical/chemical/bio signals. We can envision futuristic applications such as mind readers, disease prediction by epidermal lab-on-chip, human enhancement, environment tellers, and plant communicators.

The table of contents entry

Cyber-Physiochemical Interfaces are presented to elucidate interfacial issues including material basis, sensor development, system-level integration, and signal processing techniques, for achieving the capability of extracting biophysical and biochemical signals, and closely relating them to electronic and computing technology (cyber).

Physiochemical interfaces, cyber information, stretchable sensors, healthcare, artificial intelligence

Ting Wang, Ming Wang, Le Yang, Zhuyun Li, Xian Jun Loh,* and Xiaodong Chen*

Cyber-Physiochemical Interfaces